JOURNAL
OF
PHYSICS OF THE EARTH

Volume II July 1954 Number 1

CONTENTS

PUBLISHED BY
THE SEISMOLOGICAL SOCIETY OF JAPAN

The object of the publication of JOURNAL OF PHYSICS OF THE EARTH is to provide an international medium for the publication of original contributions in the field of geophysical science, more particularly concerning with physical properties and conditions of and phenomena occurring in the solid part of the earth.

The JOURNAL is open to any one who wishes to contribute his (or her) article. But the authors are, in principle, requested to pay page charges necessary for publishing their respective articles. The authors receive 100 copies of reprints free of charge.

In order to serve the purposes for which this JOURNAL is published, all contributions should be written in widely understandable languages, such as English, French and German, etc. Contributions should be sent to the Editor or to one of the Associate Editors.

For the time being, this JOURNAL will be issued at variable prices and at irregular intervals, three or four times a year. The price of this issue is 200 yen inside Japan and $1.00 for foreign countries, the latter including postage.

*Temperature Distributions within the Earth.**

By

Haruo MIKI

Geophysical Institute, Faculty of Science, Kyoto University, Kyoto, Japan.

Abstract

Several features of the temperature distribution within the earth's interior were derived from the modern theory of solids. The main results are as follows: (1) GRÜNEISEN's parameter in the B-layer (33–413 km.) must be greater than 1.5. (2) Temperature in the D-layer (1000–2898 km.) increases almost linearly with increasing depth and its gradient depends on the mean atomic weight rather than on GRÜNEISEN's parameter. For instance, the gradient is 1.79°/km. for $A=20$ and 3.74°/km. for $A=40$. (4) The temperature gradient in the B-layer decreases with increasing depth.

Notations. P: Pressure, r: Distance from the earth's center, g: Acceleration of gravity, ρ: Density, T: Temperature, K_T: Isothermal bulk modulus, K_S: Adiabatic bulk modulus, α: Coefficient of thermal expansion, C_P: Specific heat at constant pressure, C_V: Specific heat at constant volume, $\phi=K_S/\rho$, A: Mean atomic weight, V: Molar volume, γ_G: GRÜNEISEN's parameter, ν_m: DEBYE's maximum frequency, N_L: LOSCHMIDT's number, v_P: Velocity of longitudinal elastic wave, v_S: Velocity of transversal elastic wave.

Theory If we assume that the condition of hydrostatic equilibrium is satisfied within the earth, that is, $dP=-g\rho dr$, then the variation in density with depth is expressed by the following equation

$$\frac{d\rho}{dr}=\left(\frac{\partial\rho}{\partial P}\right)_T\frac{dP}{dr}+\left(\frac{\partial\rho}{\partial T}\right)_P\frac{dT}{dr}$$
$$=-\frac{g\rho^2}{K_T}-\frac{dT}{dr}\rho\alpha. \tag{1}$$

Let the radial temperature gradient be expressed as follows,

$$\frac{dT}{dr}=\frac{T\alpha}{\rho C_P}\frac{dP}{dr}-\tau=-\frac{T\alpha g}{C_P}-\tau \tag{2}$$

where τ denotes the difference between the actual gradient of temperature and the adiabatic gradient, $-T\alpha g/C_P$. In virtue of the thermodynamical relation between isothermal and adiabatic bulk moduli,

$$K_T/K_S=1-T\alpha^2K_T/\rho C_P,$$

the equation for the density variation with depth may be written as follows (BIRCH, 1952):

$$\frac{d\rho}{dr}=\frac{g\rho^2}{K_T}\left(1-\frac{T\alpha^2K_T}{\rho C_P}\right)+\alpha\rho\tau=-\frac{g\rho^2}{K_S}+\alpha\rho\tau. \tag{3}$$

Let the earth be divided into thin spherical shells, the inner and outer radii being r_1 and r_2. We use the suffixes 1 and 2 also to distinguish the physical quantities of the materials existing at r_1 and r_2. Then (3) can be approximated by the following equation (MIKI, 1952):

$$\frac{\rho_1-\rho_2}{r_1-r_2}=-\frac{g}{\phi}\frac{\rho_1+\rho_2}{2}+\alpha\tau\frac{\rho_1+\rho_2}{2},$$

which can be transformed as follows:

$$\frac{1}{r_1-r_2}\left(\frac{A}{V_1}-\frac{A}{V_2}\right)$$
$$=-\frac{1}{2}\frac{g}{\phi}\left(\frac{A}{V_1}+\frac{A}{V_2}\right)+\frac{1}{2}\alpha\tau\left(\frac{A}{V_1}+\frac{A}{V_2}\right)$$

or

$$\frac{1}{r_1-r_2}\left(1-\frac{V_1}{V_2}\right)=\frac{1}{2}\left(1+\frac{V_1}{V_2}\right)\left(\alpha\tau-\frac{g}{\phi}\right).$$

Therefore, we get

* Contribution to Geophysical Papers dedicated to Prof. M. HASEGAWA on his sixtieth birthday.

$$\alpha\tau=\frac{\frac{1}{r_1-r_2}\left(1-\frac{V_1}{V_2}\right)}{\frac{1}{2}\left(1+\frac{V_1}{V_2}\right)}+\frac{g}{\phi}. \tag{4}$$

The ratio of molar volumes V_1/V_2 can be derived from the definition of Grüneisen's parameter, thus

$$\left(\frac{V_1}{V_2}\right)^{3\gamma_G-1}=\frac{\left(\frac{1}{v_P{}^3}+\frac{2}{v_S{}^3}\right)_1}{\left(\frac{1}{v_P{}^3}+\frac{2}{v_S{}^3}\right)_2}, \tag{5}$$

where

$$\gamma_G=-\frac{d\log\nu_m}{d\log V},\quad\text{and}\quad \nu_m=\left(\frac{9}{4\pi}\frac{N_L}{V}\frac{1}{\frac{1}{v_P{}^3}+\frac{2}{v_S{}^3}}\right)^{\frac{1}{3}}.$$

Since v_P and v_S are quantities which can be known from observations of seismic waves, V_1/V_2 can be calculated from (5) taking γ_G as a parameter. Then $\alpha\tau$ can be estimated from equation (4), since ϕ is a known quantity and g is nearly constant within the earth's mantle (about 10^3 cm. sec.$^{-2}$).

On the other hand, in virtue of the following relations:

$$\frac{\alpha}{C_P}=\frac{\alpha}{C_V(1+T\alpha\gamma_G)}, \tag{6}$$

and

$$\gamma_G=\frac{K_S\alpha A}{\rho C_P}, \tag{7}$$

the temperature can be expressed as follows:

$$T=\frac{1}{\gamma_G}\left(\frac{K_S}{\rho}\frac{A}{\gamma_G C_V}-\frac{1}{\alpha}\right). \tag{8}$$

We have known the value of $\alpha\tau$ at each depth, that is, we have known α's as a function of τ at various depths. From this functional relation and equation (8), the corresponding values of T and τ can be known. In other words, we can know τ as a function of T. Thus we can find the distribution of temperature in the earth by numerical integration of equation (2) after substituting the above functional relation between T and τ. The first term of the right-hand-side in equation (2) is the adiabatic temperature gradient and it can be transformed into $-\frac{\rho\gamma_G}{K_S A}T_g$ by (7), and the coefficient of T can be calculated from experimental values. C_V at high temperature is 2.49432×10^8 erg. deg.$^{-1}$ mol.$^{-1}$ by Dulong-Petit's law. The results of calculations are given in Table I.

Results

Table I Absolute Temperatures within the Earth

		Mean atomic weight 20						Mean atomic weight 40					
	Depth (km.)	$\gamma_G=1.5$			$\gamma_G=2.0$			$\gamma_G=1.5$			$\gamma_G=2.0$		
	33	1000*			1000*			1000*			1000*		
B	100	982			1058			960			1122		
	200	933			1139			855			1292		
	300	819			1190			616			1397		
	413												
C	600												
	800												
	1000	2000*	2500*	3000*	2000*	2500*	3000*	2000*	2500*	3000*	2000*	2500*	3000*
	1200	2256	2752	3248	2340	2825	3318	2525	3021	3516	2721	3210	3698
	1400	2590	3081	3572	2714	3188	3669	3211	3701	4191	3511	3988	4464
	1600	2952	3438	3923	3097	3560	4030	3954	4439	4923	4318	4782	5247
	1800	3348	3828	4308	3492	3944	4404	4766	5244	5722	5147	5601	6055
D	2000	3711	4187	4662	3868	4311	4761	5507	5981	6454	5933	6376	6820
	2200	4136	4606	5076	4270	4703	5143	6376	6843	7311	6770	7204	7637
	2400	4439	4905	5372	4616	5041	5473	6990	7454	7918	7487	7912	8338
	2600	4813	5275	5737	4988	5405	5829	7751	8210	8669	8257	8674	9091
	2800	5198	5656	6113	5322	5770	6186	8533	8987	9442	9028	9437	9846
	2898												

* assumed values

C-layer (413–1000 km.) was not considered in the above calculations.

If GRÜNEISEN's parameter is taken as 1.5, the temperature decreases with increasing depth in the B-layer. This in an inconceivable conclusion. Therefore the value of GRÜNEISEN's parameter must be greater than 1.5 in the B-layer.

We see that the temperature increases approximately linearly with increasing depth in the D-layer. The mean temperature gradient in this layer is as in Table II.

Table II. Temperature gradient in the D-layer (°/km.)

Mean atomic weight	Total mean	$\gamma_G=1.5$			$\gamma_G=2.0$		
		$T_{1000}=2000$	2500	3000	2000	2500	3000
20	1.79	1.79	1.75	1.73	1.87	1.82	1.77
40	3.73	3.63	3.60	3.58	3.90	3.85	3.80

Table II shows that the temperature gradient depends mainly on the mean atomic weight rather than on GRÜNEISEN's parameter.

The temperature gradient in the B-layer is as in Table III.

Table III. Temperature gradient in the B-layer (°/km.)

Depth (km.)	Mean atomic weight 20	Mean atomic weight 40
33		
100	0.864	1.761
200	0.661	1.375
300	0.321	0.638

Table III shows that the temperature gradient in the B-layer decreases with increasing depth.

References

1) BIRCH, Francis:
1952: Journ. Geophys. Res., **57**, 227.
2) MIKI, Haruo:
1952: Journ. Phys. Earth, **1**, 19.

On a Self-Exciting Process in Magneto-Hydrodynamics (III).

By
Hitoshi TAKEUCHI and Yasuo SHIMAZU.
Geophysical Institute, Faculty of Science, Tokyo University, Tokyo.

Abstract

In our recent papers (referred to as Paper I and II), it has been shown that a self-exciting process is possible by which the earth's main magnetic field may be produced and maintained.

In these papers, however, a kind of theoretical "cut off" has been made, and only the magnetic fields of comparatively lower harmonics have been taken into acount in the discussions. In the present paper, the relative importance of the magnetic fields of higher harmonics in driving the self-exciting dynamo is estimated. It is shown that the results in Paper I and II remain true even if we include the magnetic fields of higher harmonics in our dynamo model.

§ 1. In a recent paper, E. C. BULLARD and H. GELLMAN (1952) have made comments on our first paper (1952) on a self-exciting process in magneto-hydrodynamics (which will be referred to hereafter as Paper I) and stated as follows: "The existence of such eigen-values does not establish the existence of dynamo solutions of Maxwell's equations, since in Figure 1 (in our Paper I) all harmonics beyond the second have been omitted ....though naturally the existence of solutions of the simpler equations makes it more likely that the complete set also has solutions". In order to make the matter clearer, we shall reconsider the way of reasoning taken in Paper I. In Paper I, the existence of velocity fields (relative to the earth's mantle) of T_1^0– and S_2^{2C}–types in the earth's core was assumed *a priori*. Owing to the inductive action due to these velocity field, groups of magnetic fields may be caused and maintained in the earth's core. In these groups, there may exist one which contains a dipole (S_1^0–type) magnetic field as its constituent. It is this group that we studied in details in Paper I and in our more recent paper (1952) (which will be referred to as Paper II). In the model earth adopted in our study, the earth's core is assumed to be surrounded by an insulating mantle. In the mantle, only the magnetic field of dipole type is assumed to exist. In Paper I, we investigated under what condition the group of magnetic fields considered above can exist. The problem is reduced to an eigen-value problem for κ (conductivity of the earth's core) times V (absolute value of the velocity). The eigen-value problem is solved in Paper I and II. In view of the results obtained in these papers, we may expect that the group of magnetic fields considered above can exist in the earth's core. In the course of the analyses, however, we have made a theoretical "cut off". BULLARD and GELLMAN's remark above referred to is on this point, and may be stated as follows.

There are infinite numbers of magnetic fields which are coupled with the dipole magnetic field by the inductive action of the above fluid motions. These fields are labelled with the suffixes n and m, which are the degree and order of the surface spherical harmonics belonging to the fields respectively. These fields are caused and maintained in a self-exciting way. From the physical point of view, the self-exciting dynamo may be considered to be driven by the magnetic fields of comparatively lower harmonics. In fact, in our Paper I, only the magnetic fields of $n, m \leqq 2$ were taken into account. It is, however, not self-evident from the beginning

that the magnetic fields of higher harmonics play no important roles in the self-exciting dynamo. In this meaning, BULLARD and GELLMAN's remark is to the point. It is the object of the present paper to estimate the relative importance of the magnetic fields of higher harmonics in driving our self-exciting dynamo.

§ 2. In order to investigate the general theory of magneto-hydrodynamical couplings, we shall make use of the following expressions for the (r, θ, ϕ)-components of magnetic fields.

S-type (Poloidal type) magnetic field

$$H_S=\begin{cases} -n(n+1)S_n^m(r)r^{n-1}Y_n^m, \\ -\left[r\dfrac{dS_n^m}{dr}+(n+1)S_n^m\right]r^{n-1}\dfrac{\partial Y_n^m}{\partial\theta}, \\ -\left[\qquad \text{〃} \qquad\right]r^{n-1}\dfrac{\partial Y_n^m}{\sin\theta\partial\phi}, \end{cases}$$

$$\text{curl } H_S=\begin{cases} 0, \\ \left[r\dfrac{d^2S_n^m}{dr^2}+2(n+1)\dfrac{dS_n^m}{dr}\right]r^{n-1}\dfrac{\partial Y_n^m}{\sin\theta\partial\phi}, \\ -\left[\qquad \text{〃} \qquad\right]r^{n-1}\dfrac{\partial Y_n^m}{\partial\theta}, \end{cases}$$

$$\nabla^2 H_S=\begin{cases} -n(n+1)\left[\dfrac{d^2S_n^m}{dr^2}+\dfrac{2(n+1)}{r}\dfrac{dS_n^m}{dr}\right]r^{n-1}Y_n^m, \\ -\left[r\dfrac{d^3S_n^m}{dr^3}+3(n+1)\dfrac{d^2S_n^m}{dr^2}+2n(n+1)\dfrac{1}{r}\dfrac{dS_n^m}{dr}\right]r^{n-1}\dfrac{\partial Y_n^m}{\partial\theta}, \\ -\left[\qquad \text{〃} \qquad\right]r^{n-1}\dfrac{\partial Y_n^m}{\sin\theta\partial\phi}. \end{cases} \qquad \cdots\cdots (2.1)$$

T-type (Toroidal type) magnetic field

$$H_T=\begin{cases} 0, \\ -T_n^m(r)r^n\dfrac{\partial Y_n^m}{\sin\theta\partial\phi}, \\ T_n^m(r)r^n\dfrac{\partial Y_n^m}{\partial\theta}, \end{cases}$$

$$\text{curl } H_T=\begin{cases} -n(n+1)T_n^m r^{n-1}Y_n^m, \\ -\left[r\dfrac{dT_n^m}{dr}+(n+1)T_n^m\right]r^{n-1}\dfrac{\partial Y_n^m}{\partial\theta}, \\ -\left[\qquad \text{〃} \qquad\right]r^{n-1}\dfrac{\partial Y_n^m}{\sin\theta\partial\phi}, \end{cases}$$

$$\nabla^2 H_T=\begin{cases} 0, \\ -\left[\dfrac{d^2T_n^m}{dr^2}+\dfrac{2(n+1)}{r}\dfrac{dT_n^m}{dr}\right]r^n\dfrac{\partial Y_n^m}{\sin\theta\partial\phi}, \\ \left[\qquad \text{〃} \qquad\right]r^n\dfrac{\partial Y_n^m}{\partial\phi}. \end{cases} \qquad \cdots\cdots (2.2)$$

The velocity field in the earth's core is assumed, as in Papers I and II, to be expressed as an arbitrary linear combination of the following two fields.

S-type velocity field

$$V_S=\begin{cases} -n(n+1)V_{S,n}^m(r)r^{n-1}Y_n^m, \\ -\left[r\dfrac{dV_{S,n}^m}{dr}+(n+1)V_{S,n}^m\right]r^{n-1}\dfrac{\partial Y_n^m}{\partial\theta}, \\ -\left[\qquad \text{〃} \qquad\right]r^{n-1}\dfrac{\partial Y_n^m}{\sin\theta\partial\phi}, \end{cases} \qquad \cdots\cdots (2.3)$$

with $n=2$ and $m=2c$ ($2c$ means $\cos 2\phi$ in the expression of (2.5).

T-type velocity field

$$V_T=\begin{cases} 0, \\ -V_{T,n}^{\ m}(r)r^n\dfrac{\partial Y_n^{\ m}}{\sin\theta\partial\phi}, \\ V_{T,n}^{\ m}(r)r^n\dfrac{\partial Y_n^{\ m}}{\partial\theta}, \end{cases} \qquad \ldots\ldots (2.4)$$

with $n=1$ and $m=0$. In (2.1)–(2.4), Y_n^m is a surface spherical harmonic with degree n and order m,

$$Y_n^{\ m}=P_n^{\ m}(\cos\theta)\frac{\cos}{\sin}m\phi. \qquad (2.5)$$

The expressions for the magneto-hydrodynamical couplings of general (poloidal and toroidal) magnetic fields with general (poloidal and toroidal) velocity fields will be given as follows.

With the suffixes

α: primary (inducing) magnetic field,

β: velocity field,

γ: secondary (induced) magnetic field,

the orthogonal condition for the MAXWELL's equation ((3.6) in Paper I) is expressed by

$$\int_0^a\int_0^\pi\int_0^{2\pi}\sum_\alpha[\nabla^2H_\alpha+4\pi\kappa\,\mathrm{curl}\,(V_\beta\times H_\alpha)]\cdot H_\gamma r^2\sin\theta drd\theta d\phi=0\,. \qquad (2.6)$$

Executing the integrations with respect to θ and ϕ, we get

$$\int_0^a[\sum_\alpha\widehat{S_\alpha S_\gamma}+\sum_\alpha\widehat{T_\alpha S_\gamma}]r^2dr=0\,,$$

$$\int_0^a[\sum_\alpha\widehat{S_\alpha T_\gamma}+\sum_\alpha\widehat{T_\alpha T_\gamma}]r^2dr=0\,, \qquad (2.7)$$

where

$$\widehat{S_\alpha S_\gamma}=\int_0^\pi\int_0^{2\pi}[\nabla^2H_{S\alpha}+4\pi\kappa\,\mathrm{curl}\,(\sum_\beta V_\beta\times H_{S\alpha})]\cdot H_{S\gamma}\sin\theta d\theta d\phi\,,$$

$$\widehat{T_\alpha S_\gamma}=\int_0^\pi\int_0^{2\pi}[\nabla^2H_{T\alpha}+4\pi\kappa\,\mathrm{curl}\,(\sum_\beta V_\beta\times H_{T\alpha})]\cdot H_{S\gamma}\sin\theta d\theta d\phi\,, \qquad \text{etc.} \qquad (2.8)$$

We shall call $\widehat{S_\alpha S_\gamma}$, $\widehat{T_\alpha S_\gamma}$, $\widehat{S_\alpha T_\gamma}$ and $\widehat{T_\alpha T_\gamma}$ the coupling coefficients. Changing the independent and dependent variables by the following equations

$$r=a\xi, \qquad (a:\ \text{radius of the earth's core}),$$

$$\begin{pmatrix}S_n^{\ m}(r)\\ V_{S,n}^{\ m}(r)\end{pmatrix}=\frac{1}{a^{n-1}}\begin{pmatrix}S_n^{\ m}(\xi)\\ V_{S,n,m}V_{S,n}^{\ m}(\xi)\end{pmatrix}, \qquad \begin{pmatrix}T_n^{\ m}(r)\\ V_{T,n}^{\ m}(r)\end{pmatrix}=\frac{1}{a^n}\begin{pmatrix}T_n^{\ m}(\xi)\\ V_{T,n,m}V_{T,n}^{\ m}(\xi)\end{pmatrix}. \qquad (2.9)$$

we get the following expressions for the coupling coefficients.

Couplings by S-type velocity field:

$$\widehat{S_\alpha S_\gamma}=[I(\alpha,\gamma)n_\alpha(n_\alpha+1)f_S+yK(\alpha\gamma,\beta)n_\beta(n_\beta+1)g_1-yK(\gamma\beta,\alpha)n_\alpha(n_\alpha+1)g_2]n_\gamma(n_\gamma+1)S_\gamma\xi^{n_\gamma-1}$$
$$+\left[I(\alpha,\gamma)n_\alpha(n_\alpha+1)\frac{d(f_S\xi^2)}{d\xi}+yK(\alpha\gamma,\beta)n_\beta(n_\beta+1)\frac{d(g_1\xi^2)}{d\xi}-yK(\gamma\beta,\alpha)n_\alpha(n_\alpha+1)\frac{d(g_2\xi^2)}{d\xi}\right]S_\gamma\xi^{n_\gamma-2}, \qquad (2.10)$$

$$\widehat{T_\alpha S_\gamma}=yL(\gamma\alpha,\beta)n_\beta(n_\beta+1)g_3n_\gamma(n_\gamma+1)S_\gamma\xi^{n_\gamma-1}+yL(\gamma\alpha,\beta)n_\beta(n_\beta+1)\frac{d(g_3\xi^2)}{d\xi}S_\gamma\xi^{n_\gamma-2}, \qquad (2.11)$$

$$\widehat{S_\alpha T_\gamma}=\left[yL(\alpha\beta,\gamma)n_\gamma(n_\gamma+1)S_\alpha V_{S\beta}\xi^{n_\alpha+n_\beta-2}+yL(\alpha\gamma,\beta)n_\beta(n_\beta+1)\frac{d(g_1\xi^2)}{d\xi}\right.$$
$$\left.+yL(\gamma\beta,\alpha)n_\alpha(n_\alpha+1)\frac{d(g_2\xi^2)}{d\xi}\right]T_\gamma\xi^{n_\gamma-1}, \qquad (2.12)$$

$$\widehat{T_\alpha T_\gamma}=\Big[I(\alpha,\gamma)n_\alpha(n_\alpha+1)f_T+yK(\alpha\beta,\gamma)n_\gamma(n_\gamma+1)T_\alpha V_{S\beta}\xi^{n_\alpha+n_\beta-1}$$
$$+yK(\alpha\gamma,\beta)n_\beta(n_\beta+1)\frac{d(g_3\xi^2)}{d\xi}\Big]T_\gamma\xi^{n_\gamma-1}. \tag{2.13}$$

Couplings by T-type velocity field:

$$\widehat{S_\alpha S_\gamma}=[I(\alpha,\gamma)n_\alpha(n_\alpha+1)f_S+xL(\beta\gamma,\alpha)n_\alpha(n_\alpha+1)g_4]n_\gamma(n_\gamma+1)S_\gamma\xi^{n_\gamma-1}$$
$$+\Big[I(\alpha,\gamma)n_\alpha(n_\alpha+1)\frac{d(f_S\xi^2)}{d\xi}+xL(\beta\gamma,\alpha)n_\alpha(n_\alpha+1)\frac{d(g_4\xi^2)}{d\xi}\Big]\bar{S}_\gamma\xi^{n_\gamma-2}. \tag{2.14}$$

$$\widehat{T_\alpha S_\gamma}=0, \tag{2.15}$$

$$\widehat{S_\alpha T_\gamma}=-\Big[xK(\alpha\beta,\gamma)n_\gamma(n_\gamma+1)\bar{S}_\alpha T_{T\beta}\xi^{n_\alpha+n_\beta-1}+xK(\gamma\beta,\alpha)n_\alpha(n_\alpha+1)\frac{d(g_4\xi^2)}{d\xi}\Big]T_\gamma\xi^{n_\gamma-1}, \tag{2.16}$$

$$\widehat{T_\alpha T_\gamma}=[I(\alpha,\gamma)n_\alpha(n_\alpha+1)f_T+xL(\alpha\beta,\gamma)n_\gamma(n_\gamma+1)T_\alpha V_{T\beta}\xi^{n_\alpha+n_\beta}]T_\gamma\xi^{n_\gamma-1}. \tag{2.17}$$

where

$$y=4\pi\kappa a V_{2,2C}, \qquad x=4\pi\kappa a V_{1,0}, \qquad \bar{S}=\xi\frac{dS}{d\xi}+(n+1)S,$$
$$\bar{V}_S=\xi\frac{dV_S}{d\xi}+(n+1)V_S, \qquad f_{S,T}=\Big[\frac{d^2}{d\xi^2}+\frac{2(n+1)}{\xi}\frac{d}{d\xi}\Big]\Big[\begin{matrix}S\\T\end{matrix}\Big]\xi^{\binom{n-1,}{n+1,}},$$
$$g_1=\bar{S}_\alpha V_{S\beta}\xi^{n_\alpha+n_\beta-3}, \qquad g_2=S_\alpha\bar{V}_{S\beta}\xi^{n_\alpha+n_\beta-3}, \qquad g_3=T_\alpha V_{S\beta}\xi^{n_\alpha+n_\beta-2},$$
$$g_4=S_\alpha V_{T\beta}\xi^{n_\alpha+n_\beta-2}, \qquad \ldots\ldots \tag{2.18}$$

and

$$I(\alpha,\gamma)=\int_0^\pi\int_0^{2\pi} Y_\alpha Y_\gamma \sin\theta d\theta d\phi\ , \tag{2.19}$$

$$K(\alpha\beta,\gamma)=\int_0^\pi\int_0^{2\pi}\Big(\frac{\partial Y_\alpha}{\partial\theta}\frac{\partial Y_\beta}{\partial\theta}+\frac{\partial Y_\alpha}{\sin\theta\partial\phi}\frac{\partial Y_\beta}{\sin\theta\partial\phi}\Big)Y_\gamma\sin\theta d\theta d\phi\ , \tag{2.20}$$

$$L(\alpha\beta,\gamma)=\int_0^\pi\int_0^{2\pi}\Big(\frac{\partial Y_\alpha}{\partial\theta}\frac{\partial Y_\beta}{\sin\theta\partial\phi}-\frac{\partial Y_\alpha}{\sin\theta\partial\phi}\frac{\partial Y_\beta}{\partial\theta}\Big)Y_\gamma\sin\theta d\theta d\phi\ . \tag{2.21}$$

In (2.19)–(2.21), Y_α, for example, denotes $Y_{n\alpha}^{m\alpha}$.

The selection rules for the coupling coefficient integrals in (2.19)–(2.21) are as follows.

As to the integral $I(\alpha,\gamma)$, we must have

$$n_\alpha=n_\gamma, \qquad m_\alpha=m_\gamma. \tag{2.22}$$

Otherwise the integral vanishes. $K(\alpha\beta,\gamma)$ vanishes unless

$$n_\alpha+n_\beta+n_\gamma=\text{even}, \quad m_\alpha\pm m_\beta=m_\gamma. \tag{2.23}$$

$L(\alpha\beta,\gamma)$ vanishes unless

$$n_\alpha+n_\beta+n_\gamma=\text{odd}, \quad m_\alpha\pm m_\beta=m_\gamma. \tag{2.24}$$

These are the selection rules for the magneto-hydrodynamical couplings. We shall now study the magneto-hydrodynamical couplings, which are maintained by T_1^0- and S_2^{2C}-types velocities and in which S_1^0-type magnetic fields is found as an element. In Fig. 1, is shown the chain of couplings of magnetic field up to the fourth harmonics terms. It is needless to say that the chain is continued infinitely with infinite numbers of magnetic fields.

As is seen in Fig. 1, magnetic fields of S_1^0, T_2^0, T_2^{2C} and T_2^{2S} types make a closed circuit of couplings with harmonics up to the second degree. This simple chain was studied in Papers I and II. We shall call this chain the first approximation chain of the self-exciting process. Magnetic fields of S_3^0-, S_3^{2C}-

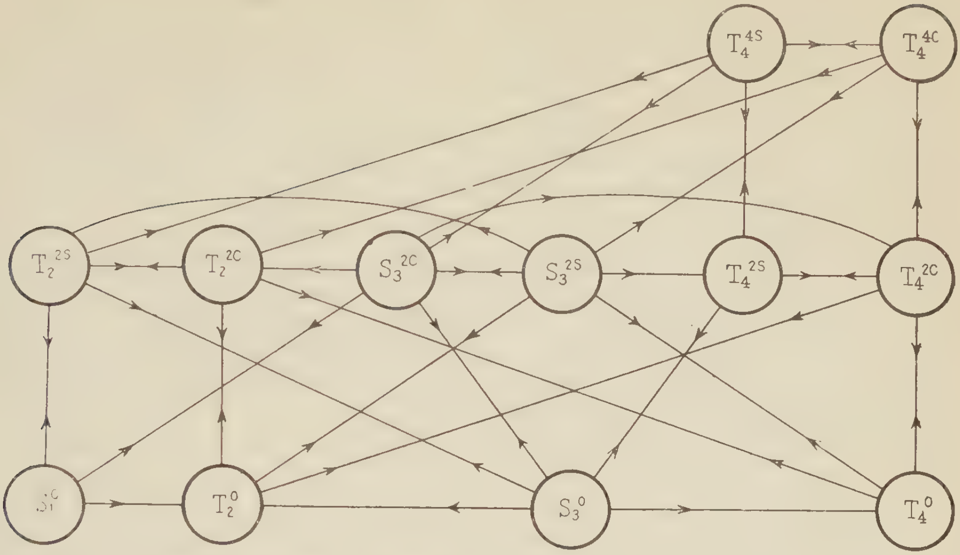

Fig. 1. Chain of induction mechanism by T_1^0– and S_2^{2C}–types fluid motions.

and S_3^{2S}–types become the elements of the coupling chain if the harmonics up to the third are taken into consideration. This step may be called the second approximation. Including harmonics up to the fourth, the chain expands and includes twelve types of magnetic fields. It will be called the third approximation chain. The numbers of elements of coupling chain increase rapidly as the higher harmonics terms are included.

§ 3. Since the coupling chain is much complicated, it is hopeless to solve the Maxwell's equation with higher harmonics terms in general. We shall consider the special case in which the T_1^0–type velocity field tends to infinity in magnitude. As we saw in Paper II, this special case is of some geophysical interests. This corresponds to the case $x\to\infty$ in Paper I, and we got the eigen-value Y for this case in Papers I and II, taking only the harmonics up to the second into consideration. We shall now try to get the eigen-value Y for this case, taking the harmonics up to the fourth into consideration. The condition $x\to\infty$ simplifies the treatment of the higher approximation considerably. This circumstance will be shown below for the first approximation already treated. From (5.2) in Paper I, we have

$$
\begin{aligned}
&\xi\frac{d^2S_1^0}{d\xi^2}+4\frac{dS_1^0}{d\xi}=\frac{9\times 24}{5}\eta\xi^3V_2^{2C}T_2^{2S},\\
&\xi\frac{d^2T_2^0}{d\xi^2}+6\frac{dT_2^0}{d\xi}=\frac{2}{3}x\frac{dV_1^0}{d\xi}S_1^0+\frac{72}{7}\frac{\eta}{\xi^2}\left[\frac{d}{d\xi}(\xi^4V_2^{2C}T_2^{2C})+\frac{d}{d\xi}(\xi^3V_2^{2C})\xi T_2^{2C}\right],\\
&\xi\frac{d^2T_2^{2C}}{d\xi^2}+6\frac{dT_2^{2C}}{d\xi}=\frac{6}{7}\frac{\eta}{\xi^2}\left[\frac{d}{d\xi}(\xi^4V_2^{2C}T_2^0)+\frac{d}{d\xi}(\xi^3V_2^{2C})\xi T_2^0\right]-2xV_1^0\xi T_2^{2S},\\
&\xi\frac{d^2T_2^{2S}}{d\xi^2}+6\frac{dT_2^{2S}}{d\xi}=2xV_1^0\xi T_2^{2C}+\frac{2}{3}\frac{\eta}{\xi^2}\left[3\xi^3V_2^{2C}\frac{d}{d\xi}\left\{\frac{dS_1^0}{d\xi}+\frac{2}{\xi}S_1^0\right\}+\left\{\frac{d}{d\xi}(\xi^3V_2^{2C})S_1^0\right\}\right].
\end{aligned}
\qquad \ldots\ldots (3.1)
$$

At first, we shall assume that S_1^0 magnetic field is of finite order. From the first equation in (3.1), we see that T_2^{2S} field is of finite order. Making $x\to\infty$ in the fourth equation, we see that T_2^{2C} field becomes zero. T_2^0 field becomes the order of x by the second and also

by the third. In short, we get $T_2^0 \sim x$ and $T_2^{2C} = 0$ when $x \to \infty$. Taking the similar way in the third approximation, we get T_2^0, $T_4^0 \sim x$ and T_2^{2C}, S_3^{2S}, T_4^{2C}, T_4^{4C} and $T_4^{4S} = 0$ as $x \to \infty$. Thus, the twelve simultaneous equations are reduced to seven in the third approximation. The seven equations will be shown in (3.3) below.

Putting

$$T_2^0 = x\bar{T}_2^0 ,\quad T_4^0 = x\bar{T}_4^0 , \tag{3.2}$$

we have $\bar{T}_2^0$ and $\bar{T}_4^0$ of the finite order. Making use of (3.2) and the results in § 2, we have

$$\frac{8}{3}\left(\frac{d^2S_1^0}{d\xi^2}+\frac{4}{\xi}\frac{dS_1^0}{d\xi}\right)-\frac{96\times 6}{5}yT_2^{2S}V_2^{2C}\xi^2$$
$$+\frac{96\times 12}{7}y\left[\left(\xi\frac{dS_3^{2C}}{d\xi}+4S_3^{2C}\right)V_2^{2C}+S_3^{2C}\left(\xi\frac{dV_2^{2C}}{d\xi}+3V_2^{2C}\right)\right]\xi^2=0 ,$$
$$-\frac{16}{5}S_1^0\frac{dV_1^0}{d\xi}\frac{1}{\xi}+\frac{24}{5}\left(\frac{d^2T_2^0}{d\xi^2}+\frac{6}{\xi}\frac{dT_2^0}{d\xi}\right)+\frac{48\times 6}{35}S_3^0\frac{dV_1^0}{d\xi}\xi=0 ,$$
$$-\frac{288\times 6}{35}y\left[\bar{T}_2^0\left(\xi\frac{dV_2^{2C}}{d\xi}+3V_2^{2C}\right)+\frac{d}{d\xi}(\bar{T}_2^0V_2^{2C}\xi^4)\frac{1}{\xi^3}\right]+\frac{96\times 6}{5}T_2^{2S}V_1^0$$
$$+\frac{96\times 12}{7}S_3^{2C}\frac{dV_1^0}{d\xi}\xi+\frac{32\times 6}{7}y\left[\bar{T}_1^0\left(\xi\frac{dV_2^{2C}}{d\xi}3V_2^{2C}\right)\xi^2+\frac{d}{d\xi}(\bar{T}_1^0V_2^{2C}\xi^6)\frac{1}{\xi^3}\right]=0 ,$$
$$\frac{288\times 6}{35}yT_2^{2S}V_2^{2C}+\frac{48}{7}\left(\frac{d^2S_3^0}{d\xi^2}+\frac{8}{\xi}\frac{dS_3^0}{d\xi}\right)$$
$$-\frac{96\times 6}{7}y\left[3\left(\xi\frac{dS_3^{2C}}{d\xi}+4S_3^{2C}\right)V_2^{2C}-2S_3^{2C}\left(\xi\frac{dV_2^{2C}}{d\xi}+3V_2^{2C}\right)\right]-\frac{480\times 6}{7}yT_1^{2S}V_2^{2C}\xi^2=0 ,$$
$$\frac{288\times 6}{7}y\bar{T}_2^0V_2^{2C}-\frac{480\times 12}{7}S_3^{2C}V_1^0-\frac{160\times 6}{7}y\bar{T}_4^0V_2^{2C}\xi^2=0 ,$$
$$-\frac{16\times 20}{21}S_3^0\frac{dV_1^0}{d\xi}\frac{1}{\xi}+\frac{80}{9}\left(\frac{d^2\bar{T}_4^0}{d\xi^2}+\frac{10}{\xi}\frac{dT_4^0}{d\xi}\right)=0 ,$$
$$-\frac{192\times 5}{7}y\left[4\bar{T}_2^0\left(\xi\frac{dV_2^{2C}}{d\xi}+3V_2^{2C}\right)-3\frac{d}{d\xi}(\bar{T}_2^0V_2^{2C}\xi^4)\frac{1}{\xi^3}\right]-\frac{480\times 20}{7}S_3^{2C}\frac{dV_1^0}{d\xi}\xi$$
$$-\frac{160\times 18}{77}y\left[10\bar{T}_4^0\left(\xi\frac{dV_2^{2C}}{d\xi}+3V_2^{2C}\right)\xi^2+17\frac{d}{d\xi}(\bar{T}_4^0V_2^{2C}\xi^6)\frac{1}{\xi^3}\right]+160\times 20T_4^{2S}V_1^0\xi^2=0 . \tag{3.3}$$

These are the simultaneous differential equations for the radial functions.

Assuming that all magnetic fields in our earth's mantle vanished at $r \to \infty$, we get the following boundary conditions

$$V_1^0(\xi)=V_2^{2C}(\xi)=\frac{dV_2^{2C}(\xi)}{d\xi}=0 ,$$
$$S_n^m(\xi)+\frac{\xi}{2n+1}\frac{dS_n^m}{d\xi}=0 ,$$
$$T_n^m(\xi)=0 ,$$

at

$$\xi=1 . \tag{3.4}$$

Thus our problem is reduced to solve (3.3) under the boundary conditions (3.4). It is, however, almost hopeless to solve this eigenvalue problem for $y=4\pi\kappa a V_{2,2C}$ by the trial and error method. We shall solve it in an approximate way, which is practically the same as that in Paper I.

At first, we shall replace the equations in (3.3) by their equivalents of the types in (2.7). As in Paper I, we shall put rather tentatively

$$V_1^0(\xi)=1-\xi ,\quad V_2^{2C}(\xi)=(1-\xi)^2 . \tag{3.5}$$

Next, taking the boundary conditions in (3.4) into consideration, we take the following trial coordinate functions.

$$S_1^0(\xi)=A_1^0\left(1-\frac{3}{4}\xi\right) ,$$

$$\begin{pmatrix} S_3^0(\xi) \\ S_3^{2C}(\xi) \end{pmatrix} = \begin{pmatrix} A_3^0 \\ A_3^{2C} \end{pmatrix} (1-\xi)^2 ,$$

$$\begin{pmatrix} T_2^0(\xi) \\ T_2^{2S}(\xi) \\ T_4^0(\xi) \\ T_4^{2S}(\xi) \end{pmatrix} = \begin{pmatrix} B_2^0 \\ B_2^{2S} \\ B_4^0 \\ B_4^{2S} \end{pmatrix} (-\xi) . \qquad \ldots\ldots (3.6)$$

where A_1^0, ... are undetermined constants. Since only one adjustable parameter A_n^m (or B_n^m) is given for each coordinate function, the present approximation using coordinate functions in (3.6) may be called the first approximation in the sense used in Paper I (see page 7 in Paper I).

The approximation using A_1^0, A_3^0, A_3^{2C}, B_2^0, B_2^{2S} is called, however, the second approximation in the sense used in § 2 of the present paper. Similarly, the approximation using A_1^0, A_3^0, A_3^{2C}, B_2^0, B_2^{2S}, B_4^0, B_4^{2S} is called the third approximation. In any case, inserting (3.6) into the equations of the types as in (2.7), we get the equations of the following types

$$-6A_1^0 - \frac{24}{35} y B_2^{2C} + \frac{96}{35\times 7} y A_3^{2C} = 0, \text{ etc.} \qquad (3.7)$$

All of these equations for the third approximation (in the sense of the present paper) is shown in Table I. This table is a generalization of Table I in Paper I. In order that these equations are compatible with one another, the determinant formed by the coefficients must be equal to zero. By putting the determinants at the first, second and the third stages (in the sense used in the present paper) equal to zero, we can determine the eigen-value

$$Y = \frac{8}{3} y , \qquad y = 4\pi\kappa a V_{2,2C} \qquad (3.8)$$

for each stage. The values of Y thus calculated are shown in Table II.

Table I. Equations for the third approximation.

A_1^0	B_2^0	B_2^{2S}	A_3^0	A_3^{2C}	B_4^0	B_4^{2S}
-6	0	$-\frac{24}{35}y$	0	$\frac{96}{35\cdot 7}y$	0	0
$\frac{1}{30}$	$-\frac{24}{35}$	0	$-\frac{12}{35\cdot 55}$	0	0	0
0	$\frac{72}{35\cdot 55}y$	$\frac{24}{35\cdot 5}$	0	$-\frac{48}{35\cdot 11}$	$-\frac{48}{35\cdot 11\cdot 13}y$	0
0	0	$\frac{24\cdot 12}{35\cdot 55}y$	$-\frac{24\cdot 8}{49}$	$-\frac{320}{77\cdot 13}y$	0	$-\frac{24\cdot 12}{49\cdot 13}y$
0	$\frac{24\cdot 12}{35\cdot 11}y$	0	0	$-\frac{24\cdot 8}{77}$	$-\frac{96}{49\cdot 13}y$	0
0	0	0	$\frac{16}{21\cdot 11\cdot 13}$	0	$-\frac{80}{99}$	0
0	$-\frac{48}{77\cdot 13}y$	0	0	$\frac{480}{77\cdot 13}$	$\frac{48\cdot 23}{77\cdot 91}y$	$\frac{800}{77\cdot 13}$

Table II. Eigen-value Y by the approximate method.

	Y
1st	68.51
2nd	77.79
3rd	80.91

The value $Y=68.51$ is nothing but the one obtained in Paper I. Other values of Y in Table II do not differ much from this. We may infer from this result that the self-exciting dynamo is driven by the fields of comparatively lower harmonics. Thus the results in Papers I and II are shown to remain

true even if we include magnetic fields of higher harmonics in our dynamo model. This result may be taken as an answer to BULLARD and GELLMAN's comment referred to at the beginning of the present paper.

References

BULLARD, E. C. & GELLMAN, H.:
1952 "On self-exciting processes in magneto-hydrodynamics". Journ. Phys. Earth, **1**, 65.

TAKEUCHI, H. & SHIMAZU, Y.
1952 "On a self-exciting process in magneto-hydrodynamics". Journ. Phys. Earth, **1**, 1.
1952 "On a self-exciting process in magneto-hydrodynamics (II)". Journ. Phys. Earth, **1**, 57.

Convective Fluid Motions in a Rotating Sphere.

By
Hitoshi TAKEUCHI and Yasuo SHIMAZU.
Geophysical Institute, Faculty of Science, Tokyo University, Tokyo.

Abstract

In connection with the self-exciting dynamo problem studies in our previous papers (referred to as Paper I, II and III), the present paper deals with the stationary convection motion of fluid within a rotating sphere. In § 3 and 4, preliminary surveys are made for plane boundary problems. In § 5, 6 and 7, the problem is reduced to solve the equations (6.16)–(6.18) under the conditions (7.15) and (7.16). This is an eigen-value problem for the Rayleigh number $\lambda=\frac{a^4\alpha\beta g}{k\nu}$ containing a parameter $\Omega=\frac{\omega a^2}{\nu}$. This eigen-value problem is solved in § 8 in an approximate way. In § 9, it is shown that the fluid motion required in Paper I–III is possible in the case when $\Omega\sim10^2$. The corresponding kinematical viscosity ν of the earth's core comes out to be about $\nu\sim10^{11}$ poise.

§ 1. In previous papers (H. TAKEUCHI and Y. SHIMAZU, 1952, 1953), which will be referred to hereafter as Paper I, II and III, the possibility of a self-exciting process was established by which the earth's main magnetic field is produced and maintained. The self-exciting process is considered to be maintained by the induction currents caused by the motions of the fluid of which the earth's core is composed. In order to make the study on the self-exciting dynamo complete, however, there remains another problem to be solved. That is the problem on the fluid motion itself. Can the required fluid motion really take place in the earth's core ? Under what condition is that fluid motion possible ? Is the admissible fluid motion appropriate to maintain the self-exciting dynamo under question ? These questions will be considered in the present paper.

§ 2. All possibilities having been considered, it is now believed that the fluid motion within the earth's core is that of convection due to the non-homogeneous heating to which it is subjected. (E. C. BULLARD, 1949 ; W. M. ELSASSER, 1950). Our previous studies in Paper I–III are made on this convection current model. The S_2^{2C}–type velocity field studied in these papers is nothing but the mathematical expression for the convection current. It is this S_2^{2C}–type velocity field that makes our self-exciting dynamo possible. In view of these circumstances, our immediate problem to solve may be stated as follows.

(1) Can the fluid motion of S_2^{2C}–type exist stationarily within the earth's core ? If it is, under what condition ?

(2) Also it must be shown that under the condition studied in (1), the S_2^{2C}–type velocity field is the easiest mode of motion to be excited. Otherwise, the S_2^{2C}–type velocity field may be overcome by fluid motions of other more powerful modes.

The stationary velocity field of S_2^{2C}–type reminds us of the well-known BENARD-cell. It may be that the fluid motion in the earth's core is essentially of the similar character as the BENARD-cell motion in a vessel which is heated from below. This will be the main point of view held in the present study. Many studies have been made about the convective motion which a viscous fluid undergoes when it is heated from below. In most of the studies, the problem is treated for plane boundaries, and the effects of earth's rotation upon the fluid motion are not taken into account. The

effects of magnetic fields are also neglected. In the next two sections, we shall take the earth's rotation and the existence of magnetic field into account, and treat the problem for plane boundaries.

§ 3. We shall consider the fluid of density ρ, viscosity μ, kinematic viscosity $\nu=\frac{\mu}{\rho}$, thermal diffusivity k and coefficient of thermal expansion α. The fluid will be considered as being contained in two parallel walls placed horizontally at a vertical distance of h. The fluid is heated from below. The temperature gradient in a state of no convection is β. Referring to the rotating rectangular coordinates as is shown in Fig. 1, we have the following equations.

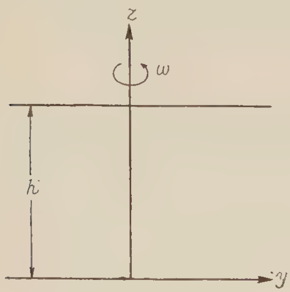

Fig. 1

$$\rho\frac{Du}{Dt}=-\frac{\partial p}{\partial x}+\mu\nabla^2 u+2\rho\omega v\,,$$
$$\rho\frac{Dv}{Dt}=-\frac{\partial p}{\partial y}+\mu\nabla^2 v-2\rho\omega u\,,$$
$$\rho\frac{Dw}{Dt}=-\frac{\partial p}{\partial z}+\mu\nabla^2 w-\rho g\,,$$
$$\frac{DT}{Dt}=k\nabla^2 T\,.$$

Customary notations are used. Attaching the suffixes $_0$ to the quantities in the states of no convection, we have

$$u_0=v_0=w_0=0,\quad p_0=p_0(z),\quad T_0=T_0(z),$$
$$\frac{dT_0}{dz}=-\beta z,\qquad \rho_0=\rho_{0,0}(1-\alpha T_0),$$
$$-\frac{dp_0}{dz}-\rho_0 g=0, \tag{3.2}$$

$\rho_{0,0}$ being a certain mean density corresponding to a certain mean temperatures (or z). We shall put

$$p=p_0+p',\quad T=T_0+T',\quad \rho=\rho_0+\rho', \tag{3.3}$$

for p, T and ρ in (3.1), and neglect the second order terms in u, v, w, p', T' and ρ'. Furthermore, we shall assume that the density variation of the fluid is caused by the thermal expansion alone and the fluid behaves otherwise as if it were an incompressible one. Thus we get

$$\rho=\rho_{0,0}(1-\alpha T),\quad \rho'=-\rho_{0,0}\alpha T', \tag{3.4}$$
$$\frac{\partial u}{\partial x}+\frac{\partial v}{\partial y}+\frac{\partial w}{\partial z}=0. \tag{3.5}$$

Inserting (3.2)–(3.4) into (3.1) and denoting p', T' and $\rho_{0,0}$ as p, T and ρ anew, we have for the state of stationary convection

$$\nu\nabla^2 u-\frac{1}{\rho}\frac{\partial p}{\partial x}+2\omega v=0\,,$$
$$\nu\nabla^2 v-\frac{1}{\rho}\frac{\partial p}{\partial y}-2\omega u=0\,,$$
$$\nu\nabla^2 w-\frac{1}{\rho}\frac{\partial p}{\partial z}+\alpha\rho g T=0\,,$$
$$k\nabla^2 T+\rho w=0\,. \tag{3.6}$$

While the above equations are derived for an incompressible fluid, H. JEFFREYS (1930) has shown that the same equations can also be applied to compressible fluid provided the density does not vary greatly within the system and provided also we interpret β as the temperature gradient in excess of the adiabatic one. Putting

$$(u,\ v,\ w,\ p,\ T)$$
$$=e^{\frac{i}{h}(mx+ny)}(u(z),\ v(z),\ w(z),\ p(z),\ T(z)), \tag{3.7}$$

we get five ordinary differential equations for five unknown functions $u(z)$, $v(z)$, ...Putting

$$m^2+n^2=(\pi b)^2,\quad z=h\zeta, \tag{3.8}$$

and eliminating $u(z)$, $v(z)$, $w(z)$ and $p(z)$ from (3.5)–(3.7), we have

$$\left[\left(\frac{d^2}{d\zeta^2}-\pi^2 b^2\right)^3+\left(\frac{2\omega h^2}{\nu}\right)^2\frac{d^2}{d\zeta^2}+\frac{\pi^2 b^2 h^4\alpha\beta g}{k\nu}\right]T$$
$$=0. \tag{3.9}$$

In order to get a quantitative result, we shall put

$$T=w=\frac{d^2 w}{d\zeta^2}=0\,, \tag{3.10}$$

at $\zeta=0$ and 1. (3.10) states that the temperature at the two free boundaries $z=0$ and h are kept constant. These boundary condi-

tions are satisfied by putting

$$T \propto \sin s\pi\zeta. \qquad (s=1,\ 2,\ \ldots\ldots) \tag{3.11}$$

Inserting (3.11) into (3.9). we get the following condition for the stationary convection

$$\lambda = \frac{\pi^4}{b^2}(b^2+s^2)^3 + \left(\frac{2\omega h^2}{\nu}\right)^2 \frac{s^2}{b^2}, \tag{3.12}$$

where

$$\lambda = \frac{h^4 \alpha\beta g}{k\nu}. \tag{3.13}$$

In the case when the value of λ in (3.13) is larger (smaller) than that given by the right-hand side of (3.12), the fluid motion is seen to be unstable (stable) and of developing (damping) character. If they are equal, that the λ is a critical value which marks the stable and unstable motions. Keeping $\left(\frac{2\omega h^2}{\nu}\right)^2$ as a parametric constant and making use of (3.12), we can determine the critical value λ as a function of wave numbers b and s. The value of the critical λ may become a minimum for certain values of b and s. As is easily understood, the mode of fluid motion corresponding to these values of b and s is nothing but the easiest one to be excited. Since λ in (3.12) monotonously increases with s, we have $s=1$ as the value of s for which λ in (3.12) becomes a minimum. Thus putting $s=1$ and $\frac{d\lambda}{db}=0$ in (3.12), we can determine the value of b for which λ becomes a minimum. The value of b thus obtained is an increasing function of $\left(\frac{2\omega h^2}{\nu}\right)^2$. In any case, inserting the value of b thus obtained into (3.12), we get the minimum critical value of λ. This minimum value is once more an increasing function of $\left(\frac{2\omega h^2}{\nu}\right)^2$. The reason for the existence of these relations is as follows. In convective fluid motions, temperature gradient is an unstabilizing factor, while viscosity and Coriolis force are stabilizing factors. The stabilizing action of Coriolis force is investigated and well recognised in dynamical meteorology. In (3.12), the second term of the right-hand side of the equation denotes this stabilizing action of Coriolis force. The first term of the right-hand side denotes also the stabilizing action due to viscosity, while the left-hand side of (3.12) does the unstabilizing action due to non-homogeneous heating. Equation (3.12) shows that the convective fluid motion can exist stationarily if these stabilizing and unstabilizing actions balance with each other. Thus we can understand the λ (minimum)$\sim\left(\frac{2\omega h^2}{\nu}\right)^2$ relation above obtained. Furthermore, as is shown in dynamical meteorology, the stabilizing action of Coriolis force is more powerful for larger scale fluid motions, while the same action due to viscosity is more powerful in smaller scale motions. These circumstances are reflected in (3.12). Thus, the first (second) term of the right-hand side of (3.12) becomes larger for larger (smaller) value of b, that is, for smaller (larger) scale motion. In short, the action of Coriolis force makes fluid motions of smaller scales easier to be excited relative to larger scale motions. This is the reason for the existence of $b\sim\left(\frac{2\omega h^2}{\nu}\right)^2$ relation above obtained. From the above physical considerations, we may safely assume that the similar λ (min.)$\sim\left(\frac{2\omega h^2}{\nu}\right)^2$ and $b\sim\left(\frac{2\omega h^2}{\nu}\right)^2$ relations as above will be obtained under other boundary conditions than assumed above. The existence of the above $b\sim\left(\frac{2\omega h^2}{\nu}\right)^2$ relation is favourable for our present study. The reason for this is as follows.

Since S_2^{2C}-type fluid motion is rather of a smaller scale, we cannot expect that the S_2^{2C} motion becomes the easiest motion to be excited (as is expected in (2) of § 2) without the above $b\sim\left(\frac{2\omega h^2}{\nu}\right)^2$ relation. In short, while the S_2^{2C} motion is not the easiest one to be excited in the case when $\omega=0$, we may expect it will become so for certain value of $\left(\frac{2\omega h^2}{\nu}\right)^2$. This is the most important result obtained in this section.

§ 4. In this section, we shall study about convective fluid motions under a uniform magnetic field. As is shown in Fig. 2, magnetic vector of the uniform field is assumed to be in the yz plane, making an angle θ with the y axis. In this case, we have

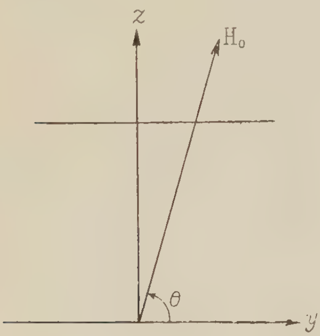

Fig. 2

$$\rho\frac{D\vec{u}}{Dt} = -\text{grad}\, p + \rho\nu\nabla^2\vec{u} - \rho\vec{g} + \mu\vec{J}\times\vec{H}\,,$$

$$\frac{DT}{Dt} = k\nabla^2 T\,. \tag{4.1}$$

$$\text{curl}\,\vec{H} = 4\pi\vec{J}, \quad \text{curl}\,\vec{E} = -\mu\frac{\partial\vec{H}}{\partial t}\,,$$

$$\text{div}\,\vec{H} = 0, \quad \vec{J} = \sigma[\vec{E} + \mu(\vec{u}\times\vec{H})]. \tag{4.2}$$

In (4.1) and (4.2), μ and σ are magnetic permeability and electric conductivity of the fluid respectively. $\vec{u}$, $\vec{H}$, $\vec{E}$ and $\vec{J}$ mean velocity, magnetic field, electric field and electric current vector respectively. From (4.2), we have

$$\frac{\partial\vec{H}}{\partial t} - \text{curl}\,(\vec{u}\times\vec{H}) = \frac{1}{4\pi\mu\sigma}\nabla^2\vec{H}\,,$$

$$\text{div}\,\vec{H} = 0\,. \tag{4.3}$$

For H, we shall assume

$$H = \begin{pmatrix} 0 \\ H_0\cos\theta \\ H_0\sin\theta \end{pmatrix} + \begin{pmatrix} h_x \\ h_y \\ h_z \end{pmatrix}, \tag{4.4}$$

in which $(h_x,\ h_y,\ h_z)$ is a deviation of H from the initial uniform field H_0 and shall be treated in the same way as $(u,\ v,\ w)$, ρ', p' and T' were in the last section. From (4.1)–(4.4), we get the following equations.

$$\frac{\partial w}{\partial t} = 0 = \frac{\mu H_0}{4\pi\rho_0}\cos\theta\left(\frac{\partial h_z}{\partial y} - \frac{\partial h_y}{\partial z}\right) + \mu\nabla^2 w - \frac{1}{\rho}\frac{\partial p}{\partial z} + \alpha g T, \quad \text{etc.}, \tag{4.5}$$

$$\frac{\partial h_x}{\partial t} = 0 = H_0\cos\theta\frac{\partial u}{\partial y} + H_0\sin\theta\frac{\partial u}{\partial z} + \frac{1}{4\pi\mu\sigma}\nabla^2 h_x\,, \quad \text{etc.}, \tag{4.6}$$

$$\frac{\partial T}{\partial t} = 0 = k\nabla^2 T + \beta w\,, \tag{4.7}$$

$$\frac{\partial u}{\partial x} + \frac{\partial v}{\partial y} + \frac{\partial w}{\partial z} = 0\,, \qquad \frac{\partial h_x}{\partial x} + \frac{\partial h_y}{\partial y} + \frac{\partial h_z}{\partial z} = 0\,. \tag{4.8}$$

Eliminating u, v, ... from (4.5)–(4.8), we get

$$\nabla^6 T = \frac{\alpha\beta g}{k\nu}\left(\frac{\partial^2}{\partial x^2} + \frac{\partial^2}{\partial y^2}\right)T + \frac{\sigma\mu^2 H_0^2}{\rho\nu}\left(\cos\theta\frac{\partial}{\partial y} + \sin\theta\frac{\partial}{\partial z}\right)^2\nabla^2 T. \tag{4.9}$$

Transforming (4.9) by the following equations

$$T = T(z)e^{\frac{i}{h}(mx+ny)}, \qquad z = h\zeta, \qquad m^2 + n^2 = (\pi b)^2, \tag{4.10}$$

we have

$$\left[\frac{d^2}{d\zeta^2} - (\pi b)^2\right]^3 T + \frac{\alpha\beta g h^4}{k\nu}(\pi b)^2 T - \frac{\sigma\mu^2 H_0^2 h^2}{\rho\nu}\left(in\cos\theta + \sin\theta\frac{d}{d\zeta}\right)^2\left(\frac{d^2}{d\zeta^2} - (\pi b)^2\right)T = 0\,. \tag{4.11}$$

Putting $\theta = \frac{\pi}{2}$ tentatively and assuming (see (3.11))

$$T \propto \sin s\pi\zeta. \qquad (s = 1,\ 2,\ 3,\ \ldots\ldots\ldots\ldots), \tag{4.12}$$

we get the following condition for the stationary convection

$$\lambda = \frac{\pi^4}{b^2}(s^2+b^2)^3 + \frac{\sigma\mu^2 H_0^2 h^2}{\rho\nu}\frac{\pi^2}{b^2}s^2(s^2+b^2)\,, \tag{4.13}$$

where

$$\lambda=\frac{\alpha g\beta h^4}{k\nu}.$$

From this equation, we see that the existence of the magnetic field stabilizes the convection current and we get $\lambda\,(\text{min.})\sim\frac{\sigma\mu^2H_0{}^2h^2}{\rho\nu}$ and $b\sim\frac{\sigma\mu^2H_0{}^2h^2}{\rho\nu}$ relations of the similar types as $\lambda\,(\text{min.})\sim\left(\frac{2\omega h^2}{\nu}\right)^2$ and $b\sim\left(\frac{2\omega h^2}{\nu}\right)^2$ relations in the last section.

§ 5. We shall now consider convective fluid motions which take place within a rotating spherical vessel of radius a. Referring to the rotating rectangular coordinates as is shown in Fig. 3, we have the following equations.

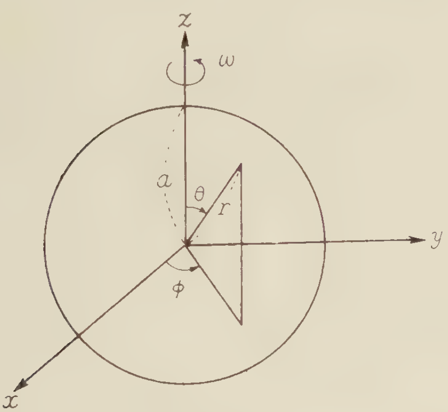

Fig. 3

$$\rho\frac{D\vec{u}}{Dt}=-\text{grad}\,p+\mu\nabla^2\vec{u}+2\rho(\vec{\omega}\times\vec{u})-\rho\vec{g},$$
$$\frac{DT}{Dt}=k\nabla^2T+\Theta, \tag{5.1}$$

where $\vec{u}$, $\vec{\omega}$ and $\vec{g}$ denote the vectors of velocity of the fluid relative to the above coordinates, of rotation of the spherical vessel and of gravity respectively. A heat generating source is supposed. The rate of heat generation is assumed such that, in the absence of conduction and convection, the temperature would rise at a uniform rate Θ. Thus in the state of no convection, we have

$$0=\frac{\partial T_0}{\partial t}=k\nabla^2T_0+\Theta. \tag{5.2}$$

In a sphere of radius a, this gives

$$T_0=\frac{\Theta}{6k}(a^2-r^2)=\frac{\beta}{2a}(a^2-r^2), \tag{5.3}$$

where

$$\beta=\frac{\Theta a}{3k}=\frac{Qa}{3\rho ck}, \tag{5.4}$$

is the temperature gradient at $r=a$. In (5.4), Q and ρck are the rate of heat generation (per unit time and volume) and the heat conductivity respectively. In the same way as in § 3, we get the following equations from (5.1)–(5.4):

$$\nu\nabla^2\vec{u}-\frac{1}{\rho}\text{grad}\,p+2(\vec{\omega}\times\vec{u})+\alpha\vec{g}T=0, \tag{5.5}$$
$$\nabla^2T=\frac{u_r}{k}\frac{dT_0}{dr}=-\frac{\beta}{ka}ru_r, \tag{5.6}$$
$$\text{div}\,\vec{u}=0. \tag{5.7}$$

In (5.6), u_r means the radial velocity in the spherical coordinates $(r,\ \theta,\ \phi)$ in Fig. 3. In these spherical coordinates, we have also

$$\vec{u}=(\vec{u}_r,\ u_\theta,\ u_\phi),\quad \vec{\omega}=(\omega\cos\theta,\ -\omega\sin\theta,\ 0),$$
$$\vec{g}=(g,\ 0,\ 0). \tag{5.8}$$

There are two types of velocity vectors $\vec{u}$ as follows which are known to satisfy (5.7). (H. Takeuchi, 1950)

Type I

$$\begin{pmatrix}u_x\\u_y\\u_z\end{pmatrix}=F_{n,m}(r)\begin{pmatrix}\frac{\partial}{\partial x}\\ \frac{\partial}{\partial y}\\ \frac{\partial}{\partial z}\end{pmatrix}W_{n,m}+G_{n,m}(r)\begin{pmatrix}x\\y\\z\end{pmatrix}W_{n,m},$$

$$ru_r=(nF_{n,m}+r^2G_{n,m})W_{n,m},$$
$$\begin{matrix}ru_\theta\\ ru_\phi\end{matrix}=F_{n,m}\begin{pmatrix}\frac{\partial}{\partial\theta}\\ \frac{1}{\sin\theta}\frac{\partial}{\partial\phi}\end{pmatrix}W_{n,m}, \tag{5.9}$$

where $W_{n,m}$ is a solid spherical harmonic of of degree n and is expressed as follows

$$W_{n,m}=r^nS_{n,m}(\theta,\ \phi)=r^nP_n{}^m(\theta)e^{im\phi}. \tag{5.10}$$

In (5.10) $S_{n,m}$ is a surface spherical harmonic, and $P_n{}^m$ is a Legendre function. For the velocity vector of type I, we have also

$$\text{div}\,\vec{u}=0$$
$$=\left[\frac{n}{r}\frac{dF_{n,m}}{dr}+r\frac{dG_{n,m}}{dr}+(n+3)G_{n,m}\right]W_{n,m}. \tag{5.11}$$

$$\begin{pmatrix} (\nabla^2\vec{u})_x \\ (\nabla^2\vec{u})_y \\ (\nabla^2\vec{u})_z \end{pmatrix} = f_{n,m}(r) \begin{pmatrix} \frac{\partial}{\partial x} \\ \frac{\partial}{\partial y} \\ \frac{\partial}{\partial z} \end{pmatrix} W_{n,m} + g_{n,m}(r) \begin{pmatrix} x \\ y \\ z \end{pmatrix} W_{n,m},$$

$$r(\nabla^2\vec{u})_r = (nf_{n,m} + r^2 g_{n,m}) W_{n,m},$$

$$\begin{pmatrix} r(\nabla^2\vec{u})_\theta \\ r(\nabla^2\vec{u})_\phi \end{pmatrix} = f_{n,m} \begin{pmatrix} \frac{\partial}{\partial\theta} \\ \frac{1}{\sin\theta}\frac{\partial}{\partial\phi} \end{pmatrix} W_{n,m}, \tag{5.12}$$

in which

$$f_{n,m} = \frac{d^2F_{n,m}}{dr^2} + \frac{2n}{r}\frac{dF_{n,m}}{dr} + 2G_{n,m},$$

$$g_{n,m} = \frac{d^2G_{n,m}}{dr^2} + \frac{2(n+2)}{r}\frac{dG_{n,m}}{dr}. \tag{5.13}$$

The other type of $\vec{u}$ satisfying (5.7) is given as follows.

Type II

$$\begin{pmatrix} u_x \\ u_y \\ u_z \end{pmatrix} = L_{n,m}(r) \begin{pmatrix} z\frac{\partial W_{n,m}}{\partial y} - y\frac{\partial W_{n,m}}{\partial z} \\ x\frac{\partial W_{n,m}}{\partial z} - z\frac{\partial W_{n,m}}{\partial x} \\ y\frac{\partial W_{n,m}}{\partial x} - x\frac{\partial W_{n,m}}{\partial y} \end{pmatrix},$$

$$u_r = 0,$$

$$u_\theta = L_{n,m}(r)\frac{1}{\sin\theta}\frac{\partial W_{n,m}}{\partial\phi},$$

$$u_\phi = -L_{n,m}(r)\frac{\partial W_{n,m}}{\partial\theta}. \tag{5.14}$$

$$\operatorname{div}\vec{u} = 0. \tag{5.15}$$

$$(\nabla^2 u)_r = 0,$$

$$(\nabla^2 u)_\theta = l_{n,m}(r)\frac{1}{\sin\theta}\frac{\partial W_{n,m}}{\partial\phi},$$

$$(\nabla^2 u)_\phi = -l_{n,m}(r)\frac{\partial W_{n,m}}{\partial\theta}, \tag{5.16}$$

where

$$l_{n,m} = \frac{d^2L_{n,m}}{dr^2} + \frac{2(n+1)}{r}\frac{dL_{n,m}}{dr}. \tag{5.17}$$

Taking (5.5) and (5.6) into consideration, we may assume

$$T = T_{n,m}(r)W_{n,m}, \quad p = \Pi_{n,m}(r)W_{n,m}, \tag{5.18}$$

for $\vec{u}$ of type I. Corresponding to $\vec{u}$ of type II, we may take

$$T = 0, \qquad p = 0. \tag{5.19}$$

The Laplacian of T in (5.18) is given as follows

$$\nabla^2 T = t_{n,m}W_{n,m},$$

$$t_{n,m} = \frac{d^2T_{n,m}}{dr^2} + \frac{2(n+1)}{r}\frac{dT_{n,m}}{dr}. \tag{5.20}$$

Accordingly equation (5.6) is satisfied by putting

$$t_{n,m} = -\frac{\beta}{ka}(nF_{n,m} + r^2G_{n,m}). \tag{5.21}$$

Furthermore, if we omit the term $2(\vec{\omega}\times\vec{u})$ in (5.5), we can make equation (5.5) to be satisfied by putting

$$\nu(nf_{n,m} + r^2g_{n,m}) - \frac{1}{\rho r^{n-1}}\frac{d(r^n\Pi_{n,m})}{dr} + \alpha grT_{n,m} = 0, \tag{5.22}$$

$$\nu f_{n,m} - \frac{1}{\rho}\Pi_{n,m} = 0, \tag{5.23}$$

$$l_{n,m} = 0. \tag{5.24}$$

The existence of the term $2(\vec{\omega}\times\vec{u})$ makes the present problem more complicated. A method of dealing with this complication will be considered in the section to follow.

§6. For the sake of convenience, we shall denote $\vec{u}$ in (5.9) and (5.14) by $\vec{u}_{n,m}(I)$ and $\vec{u}_{n,m}(II)$ respectively, and try to make (5.5) satisfied by putting

$$\vec{u} = \sum_n [\vec{u}_{n,m}(I) + \vec{u}_{n,m}(II)]. \tag{6.1}$$

The ϕ parts of all $\vec{u}_{n,m}(I)$ and $\vec{u}_{n,m}(II)$ may be taken to be $\cos m\phi (m=0, 1, 2, \ldots.)$. The reason why we may assume this form may be understood by (5.5)–(5.20) in the last section. Next, the following transformations of variables are made

$$\xi = \frac{r}{a}, \qquad F_{n,m}(\xi) = \frac{1}{a^2}F_{n,m}(r),$$

$$G_{n,m}(\xi) = G_{n,m}(r), \qquad L_{n,m}(\xi) = L_{n,m}(r),$$

$$\Pi_{n,m}(r) = \Pi_{n,m}(\xi), \qquad T_{n,m}(r) = T_{n,m}(\xi). \tag{6.2}$$

We shall denote also

$$\frac{d^2F_{n,m}(\xi)}{d\xi^2} + \frac{2n}{\xi}\frac{dF_{n,m}(\xi)}{d\xi} + 2G_{n,m}(\xi), \ \ldots.$$

by $f_{n,m}(\xi)$, ... With these notations, equations (5.21)–(5.24) are rewritten as follows.

$$t_{n,m}(\xi)=-\frac{\beta a^3}{k}[nF_{n,m}(\xi)+\xi^2G_{n,m}(\xi)] \tag{6.3}$$

$$[nf_{n,m}(\xi)+\xi^2g_{n,m}(\xi)]-\frac{1}{\rho\nu\xi^{n-1}}\frac{d(\xi^n\Pi_{n,m})}{d\xi}+\frac{\alpha g a}{\nu}\xi T_{n,m}(\xi)=0\,, \tag{6.4}$$

$$f_{n,m}(\xi)-\frac{1}{\rho\nu}\Pi_{n,m}(\xi)=0\,, \quad (6.5) \qquad l_{n,m}(\xi)=0\,. \tag{6.6}$$

Next, operating $\vec{u}_{n,m}(I)$ (which will be denoted by $\vec{u}_\beta(I)$ hereafter) to (5.5) and integrating, we get

$$\int_0^a\int_0^\pi\int_0^{2\pi}(5.5)\cdot\vec{u}_\beta(I)r^2\sin\theta drd\theta d\phi=0\,. \tag{6.7}$$

Inserting (6.1) into (5.5) in (6.7) and executing the integration with respect to θ and ϕ, we have

$$\int_0^1 C(\xi)\xi^{2n_\beta}(n_\beta F_\beta+\xi^2G_\beta)d\xi+\int_0^1 D(\xi)\xi^{2n_\beta}F_\beta d\xi=0\,, \tag{6.8}$$

where

$$C(\xi)=(6.4)_\beta+\frac{2\omega a^2}{\nu}[I_0(\beta)]^{-1}\sum_\alpha\xi^{n_\alpha-n_\beta+1}L_\alpha I_1(\beta,\alpha)\,,$$

$$D(\xi)=(6.5)_\beta+\frac{2\omega a^2}{\nu}[n_\beta(n_\beta+1)I_0(\beta)]^{-1}\sum_\alpha\xi^{n_\alpha-n_\beta+1}L_\alpha I_2(\alpha,\beta)\,. \tag{6.9}$$

In (6.9), the symbols $(6.4)_\beta$ and $(6.5)_\beta$ mean the left-hand sides of (6.4) and (6.5) with the suffix β respectively, and

$$I_0(\beta)=\int_0^\pi(P_\beta)^2\sin\theta d\theta\,, \tag{6.10}$$

$$I_1(\alpha,\beta)=\int_0^\pi P_\alpha\frac{dP_\beta}{d\theta}\sin^2\theta d\theta\,. \tag{6.11}$$

$$I_2(\alpha,\beta)=I_2(\beta,\alpha)=\int_0^\pi\left(\frac{m^2}{\sin^2\theta}P_\alpha P_\beta+\frac{dP_\alpha}{d\theta}\frac{dP_\beta}{d\theta}\right)\sin\theta\cos\theta d\theta\,, \tag{6.12}$$

$$P_\alpha=P_{n_\alpha}^{m_\alpha}(\cos\theta),\qquad F_\beta=F_{n_\beta,m_\beta},\ \cdots\cdots\,. \tag{6.13}$$

Similarly, operating $\vec{u}_\beta(II)$ to (5.5) and proceeding in the same way as above, we get

$$\int_0^1 E(\xi)\xi^{2(n_\beta+1)}L_\beta d\xi=0\,, \tag{6.14}$$

where

$$E(\xi)=(6.6)_\beta-\frac{2\omega a^2}{\nu}[n_\beta(n_\beta+1)I_0(\beta)]^{-1}\sum_\alpha\xi^{n_\alpha-n_\beta-1}[F_\alpha I_2(\alpha,\beta)+(n_\alpha F_\alpha+\xi^2G_\alpha)I_1(\alpha,\beta)]\,. \tag{6.15}$$

The symbol $(6.6)_\beta$ in (6.15) means the left-hand side of (6.6) with the suffix β, that is, l_β. From (6.8) and (6.14), we get

$$C(\xi)=D(\xi)=E(\xi)=0\,. \tag{6.16}$$

In addition to these equations, we have by (5.11), (6.2) and (6.3)

$$\frac{n_\beta}{\xi}\frac{dF_\beta}{d\xi}+\xi\frac{dG_\beta}{d\xi}+(n_\beta+3)G_\beta=0\,, \tag{6.17}$$

$$t_\beta=-\frac{\beta a^3}{k}(n_\beta F_\beta+\xi^2G_\beta)\,. \tag{6.18}$$

Equations (6.16) (6.18) should be written down for all possible β's. In writting down these equations, we should keep the values of all m_β's equal to a fixed value m (see (6.1)). By solving (6.16)–(6.18) thus obtained, we can determine F_β, G_β, L_β, Π_β and T_β. Comparing (6.16)–(6.18) to (6.3)–(6.6) and (6.17), we see that the complications brought out by Coriolis force are shown in the terms headed by $\frac{2\omega a^2}{\nu}$ in (6.9) and (6.15). In fact, if we put $\omega=0$

or all the $I_1(\alpha, \beta)$ and $I_2(\alpha, \beta)$ to be equal to 0, we have (6.3)–(6,6) and (6.17) in place of (6.16)–(6.18). In view of these circumstances, we may call $I_1(\alpha, \beta)$ and $I_2(\alpha, \beta)$ as coupling integrals. Velocity vectors $\vec{u}_\alpha$ and $\vec{u}_\beta$ with $I_1(\alpha, \beta)$, $I_2(\alpha, \beta) \neq 0$ may be considered to be coupled with the action of CORIOLIS force. Now it can easily be shown that

$$I_2(\alpha, \beta) = I_1(\alpha, \beta) + n_\beta(n_\beta+1)\int_0^\pi P_\alpha P_\beta \sin\theta \cos\theta d\theta, \tag{6.19}$$

and the coupling integrals $I_1(\alpha, \beta)$ and $I_2(\alpha, \beta)$ vanish unless $n_\alpha - n_\beta = \pm 1$. The values of $I_1(\alpha, \beta)$ and $I_2(\alpha, \beta)$ for several α and β are shown in Table I.

Table I.

$n_\alpha{}^m$	$n_\beta{}^m$	I_1	I_2
1^0	2^0	$-\frac{4}{5}$	$\frac{4}{5}$
3^0	2^0	$\frac{12}{35}$	$\frac{48}{35}$
3^0	4^0	$-\frac{40}{63}$	$\frac{40}{21}$
5^0	4^0	$\frac{40}{99}$	$\frac{80}{33}$
5^0	6^0	$-\frac{84}{11\times13}$	$\frac{15\times28}{11\times13}$
1^1	2^1	$-\frac{12}{5}$	$\frac{12}{5}$
3^1	2^1	$\frac{96}{35}$	$\frac{384}{35}$
3^1	4^1	$-\frac{200}{21}$	$\frac{200}{7}$
5^1	4^1	$\frac{320}{33}$	$\frac{640}{11}$
5^1	6^1	$-\frac{735\times4}{11\times13}$	$\frac{735\times20}{11\times13}$
2^2	3^2	$-\frac{192}{7}$	$\frac{384}{7}$
4^2	3^2	$\frac{480}{7}$	$\frac{480\times5}{7}$
4^2	5^2	$-\frac{480\times7}{11}$	$\frac{480\times28}{11}$
6^2	5^2	$\frac{2800\times24}{11\times13}$	$\frac{2800\times168}{11\times13}$
6^2	7^2	$-\frac{256\times63}{13}$	$\frac{256\times63\times6}{13}$
3^3	4^3	-800	15×160
5^3	4^3	$\frac{32\times32\times35}{11}$	$\frac{32\times32\times35\times6}{11}$
5^3	6^3	$-\frac{840\times3024}{11\times13}$	$\frac{315\times40\times1008}{11\times13}$
7^3	6^3	$\frac{120\times72\times56}{13}$	$\frac{960\times72\times56}{13}$
7^3	8^3	$-\frac{220\times126\times72}{17}$	$\frac{220\times72\times14\times63}{17}$

$n_\alpha{}^m$	$n_\beta{}^m$	I_1	I_2
2^0	1^0	$\frac{4}{15}$	$\frac{4}{5}$
2^0	3^0	$-\frac{24}{35}$	$\frac{48}{35}$
4^0	3^0	$\frac{8}{21}$	$\frac{40}{21}$
4^0	5^0	$-\frac{20}{33}$	$\frac{80}{33}$
6^0	5^0	$\frac{60}{11\times13}$	$\frac{15\times28}{11\times13}$
6^0	7^0	$-\frac{16\times7}{13\times15}$	$\frac{96\times7}{13\times15}$
2^1	1^1	$\frac{4}{5}$	$\frac{12}{5}$
2^1	3^1	$-\frac{192}{35}$	$\frac{384}{35}$
4^1	3^1	$\frac{40}{7}$	$\frac{200}{7}$
4^1	5^1	$-\frac{160}{11}$	$\frac{640}{11}$
6^1	5^1	$\frac{105\times20}{13\times11}$	$\frac{735\times20}{13\times11}$
6^1	7^1	$-\frac{16\times8\times14}{13\times5}$	$\frac{96\times8\times14}{13\times5}$
3^2	2^2	$\frac{96}{7}$	$\frac{384}{7}$
3^2	4^2	$-\frac{800}{7}$	$\frac{2400}{7}$
5^2	4^2	$\frac{32\times70}{11}$	$\frac{480\times28}{11}$
5^2	6^2	$-\frac{735\times128}{11\times13}$	$\frac{2800\times168}{11\times13}$
7^2	6^2	$\frac{192\times63}{13}$	$\frac{256\times63\times6}{13}$
7^2	8^2	$-\frac{81\times64\times7}{17}$	$\frac{567\times64\times7}{17}$

§7. As is stated in §2, we are most interested in the fluid motion of S_2^{2C}-type within the earth's core. In the way of writing down in the last section, S_2^{2C}-motion is nothing but the $\vec{u}_{2,2}(I)$ motion in (6.1). On the other hand, it is shown at the end of the last section that the $\vec{u}_{2,2}(II)$ motion cannot exist by itself under the influence of CORIOLIS force. It must be accompanied by the fluid motions of $\vec{u}_{3,2}(II)$, $\vec{u}_{4,2}(I)$, $\vec{u}_{5,2}(II)$, ...types. These fluid motions are coupled with one another as is shown in (6.16)–(6.18). The way of coupling is shown schematically as follows

$$u_{2,2}(I) \rightleftarrows u_{3,2}(II) \rightleftarrows u_{4,2}(I) \rightleftarrows u_{5,2}(II) \rightleftarrows \dots \qquad (7.1)$$

Similarly, we have groups of fluid motions as shown below

$$u_{1,0}(I) \rightleftarrows u_{2,0}(II) \rightleftarrows u_{3,0}(I) \rightleftarrows \dots \qquad (7.2)$$
$$u_{1,0}(II) \rightleftarrows u_{2,0}(I) \rightleftarrows u_{3,0}(II) \rightleftarrows \dots \qquad (7.3)$$
$$u_{1,1}(I) \rightleftarrows u_{2,1}(II) \rightleftarrows u_{3,1}(I) \rightleftarrows \dots \qquad (7.4)$$
$$u_{1,1}(II) \rightleftarrows u_{2,1}(I) \rightleftarrows u_{3,1}(II) \rightleftarrows \dots \qquad (7.5)$$
$$u_{2,2}(II) \rightleftarrows u_{3,2}(I) \rightleftarrows u_{4,2}(II) \rightleftarrows \dots \qquad (7.6)$$
$$u_{3,3}(I) \rightleftarrows u_{4,3}(II) \rightleftarrows u_{5,3}(I) \rightleftarrows \dots \qquad (7.7)$$

etc.

In general, there exist groups of fluid motions which contain $u_{n,m}(I \text{ or } II)$ with $n=m$ as their first member. As is easily understood, the case when $n=m=0$ is an exceptional one from this general rule. The problem (2) stated at the beginning in §2 is thus reduced to show that, under a certain condition, the fluid motion in (7.1) is the easiest type to be excited among (7.1)–(7.7).

Taking (6.16)–(6.18) and the results in Table I into consideration, we have the following results for the case in (7.1). In what follow, we shall omit the common suffix $m=2$, and shall write simply F_2, G_2, ... for $F_{2,2}(\xi)$, $G_{2,2}(\xi)$, ... At first, by (6.17) and (6.18), we have

$$\frac{2}{\xi}\frac{dF_2}{d\xi}+\xi\frac{dG_2}{d\xi}+5G_2=0\,, \qquad \text{(a)}$$

$$\frac{4}{\xi}\frac{dF_4}{d\xi}+\xi\frac{dG_4}{d\xi}+7G_4=0\,, \qquad \text{(b)}$$

etc. $\qquad$ .....(7.8)

$$\frac{d^2T_2}{d\xi^2}+\frac{6}{\xi}\frac{dT_2}{d\xi}=-\frac{\beta a^3}{k}(2F_2+\xi^2G_2)\,, \qquad \text{(a)}$$

$$\frac{d^2T_4}{d\xi^2}+\frac{10}{\xi}\frac{dT_4}{d\xi}=-\frac{\beta a^3}{k}(4F_4+\xi^2G_4)\,. \qquad \text{(b)}$$

etc. $\qquad$ .....(7.9)

Corresponding to $C(\xi)=0$ in (6.16), we have

$$\left[2\left(\frac{d^2F_2}{d\xi^2}+\frac{4}{\xi}\frac{dF_2}{d\xi}+2G_2\right)+\xi^2\left(\frac{d^2G_2}{d\xi^2}+\frac{8}{\xi}\frac{dG_2}{d\xi}\right)\right] -\frac{1}{\rho\nu\xi}\frac{d(\xi^2\Pi_2)}{d\xi}+\frac{\alpha g_0 a}{\nu}\xi^2T_2+\frac{5}{24}\Omega\left(-\frac{192}{7}\right)\xi^2L_3 =0\,, \qquad \text{(a)},$$

$$\left[4\left(\frac{d^2F_4}{d\xi^2}+\frac{8}{\xi}\frac{dF_4}{d\xi}+2G_4\right)+\xi^2\left(\frac{d^2G_4}{d\xi^2}+\frac{12}{\xi}\frac{dG_4}{d\xi}\right)\right] -\frac{1}{\rho\nu\xi^3}\frac{d(\xi^4\Pi_4)}{d\xi}+\frac{\alpha g_0 a}{\nu}\xi^2T_4 +\frac{1}{40}\Omega\left(\frac{480}{7}L_3-\frac{480\times 7}{11}\cdot\xi^2L_5\right)=0\,, \qquad \text{(b)},$$

etc. $\qquad$ .....(7.10)

In (7.10)

$$\Omega=\frac{\omega a^2}{\nu}\,, \qquad (7.11)$$

and g is put as

$$g=g_0\xi\,, \qquad (7.12)$$

where g_0 is the gravity at $\xi=1$, that is, at the surface of the earth's core. The gravity g in a uniform self-gravitating sphere is shown to vary as is shown in (7.12). (The gravity in the earth's core varies in a very similar way as in (7.12)). This is the reason why we have put $g=g_0\xi$. Now, corresponding to $D(\xi)=0$ in (6.16), we have

$$\frac{d^2F_2}{d\xi^2}+\frac{4}{\xi}\frac{dF_2}{d\xi}+2G_2-\frac{\Pi_2}{\rho\nu}+\frac{5}{144}\Omega\frac{384}{7}\xi^2L_3=0, \qquad \text{(a)}$$

$$\frac{d^2F_4}{d\xi^2}+\frac{8}{\xi}\frac{dF_4}{d\xi}+2G_4-\frac{\Pi_4}{\rho\nu} +\frac{1}{800}\Omega\left(\frac{480\times 5}{7}L_3+\frac{480\times 28}{11}\xi^2L_5\right)=0. \qquad \text{(b)},$$

etc. $\qquad$ .....(7.13)

Lastly, corresponding to $E(\xi)=0$ in (6.6), we have

$$\frac{d^2L_3}{d\xi^2}+\frac{8}{\xi}\frac{dL_3}{d\xi}-\frac{7}{1440}\Omega\left\{\xi^{-2}\left[-\frac{192}{7}F_2 +\frac{384}{7}(2F_2+\xi^2G_2)\right]+\left[\frac{480}{7}F_4+\frac{480\times 5}{7}(4F_4 +\xi^2G_4)\right]\right\}=0\,, \qquad \text{(a)}$$

$$\frac{d^2L_5}{d\xi^2}+\frac{12}{\xi}\frac{dL_5}{d\xi}-\frac{11}{210\times 120}\Omega\left\{\xi^{-2}\left[-\frac{480\times 7}{11}F_4+\frac{480\times 28}{11}(4F_4+\xi^2G_4)\right]+\left[\frac{2800\times 24}{11\times 13}F_6+\frac{2800\times 168}{11\times 13}(6F_6+\xi^2G_6)\right]\right\}=0\,, \qquad \text{(b)}$$

etc. .....(7.14)

If we omit $u_{n,2}$ (I or II) with $n\geq 4$ in (7.1), we get the results (a) in (7.8)–(7.14). Thereby, the F_4 and G_4 terms in (7.14) (a) must be omitted. The results thus obtained will be called the (a)–approximation. Similarly, the results obtained by taking the (a) and (b) equations in (7.8)–(7.14) and thereby omitting the F_6 and G_6 terms in (7.14) (b) will be called the (b)–approximation. In the (a)–approximation, we must solve five differential equations among five unknown functions (F_2, G_2, Π_2, T_2, L_3). In the (b)–approximation, the number of unknown functions increases to 10. In any case, proceeding in this way to (c), (d), ... –approximations, we shall obtain the required solution for the case in (7.1). Having thus established the fundamental equations, our next thing to do is to consider about the boundary conditions in this case. By the assumption of "viscous" fluid, we must have

$$\vec{u}_{n,m}(I),\quad \vec{u}_{n,m}(II)=0,\qquad \text{at}\quad \xi=1. \tag{7.15}$$

As the boundary thermal condition in this case, we shall take rather tentatively

$$T=0 \qquad \text{at}\quad \xi=1. \tag{7.16}$$

By (7.16) is meant that the temperature at $r=a$ is kept constant. This is a plausible condition to be taken for the earth's core boundary. Taking (5.9), (5.14) and (5.18) into consideration, we have

$$nF_{n,m}+\xi^2G_{n,m}=G_{n,m}=L_{n,m}=T_{n,m}=0 \qquad \text{at}\quad \xi=1. \tag{7.17}$$

$F_{n,m}$, $G_{n,m}$, ... must also be finite at $r=0$ (or $\xi=0$). Thus our problem is reduced to solve (7.8)–(7.10), (7.13) and (7.14) under the boundary conditions in (7.17). It is easily seen that our problem thus established is an eigen-value problem for $\lambda=\frac{\alpha\beta g_0a^4}{k\nu}$ containing a parameter $\Omega=\frac{\omega a^2}{\nu}$. Although the above results are obtained for the case in (7.1), similar results may be expected to be obtained for (7.2)–(7.7) equally. It is, however, almost hopeless to solve the eigen-value problem thus obtained by trial and error methods. In order to solve the problem in its simplest form, i.e., in the form of the (a)–approximation cited above, we must solve five simultaneous differential equations of second orders. A method of dealing with these difficulties will be devised in the next section.

§ 8. Taking (7.17) into consideration, we shall put

$$nF_{n,m}+\xi^2G_{n,m}=(1-\xi)^2(A_0+A_1\xi+\ldots.),$$
$$L_{n,m}=(1-\xi)(B_0+B_1\xi+\ldots.), \tag{8.1}$$

where A_0, B_0, A_1, B_1, ... are undetermined constants. In order to avoid unnecessary confusions, we shall denote $A_0(n,m)$, $B_0(n,m)$, ... for the above A_0, B_0, ... The equation (6.17) is transformed into

$$(n+1)G_{n,m}=-\frac{d(nF_{n,m}+\xi^2G_{n,m})}{\xi d\xi}. \tag{8.2}$$

The value of $G_{n,m}$ is calculated by (8.1) and (8.2). Inserting $G_{n,m}$ thus obtained into (8.1), we get $F_{n,m}$. The form of $nF_{n,m}+\xi^2G_{n,m}$ in (8.1) is so adjusted as to make $F_{n,m}$ thus obtained vanish at $\xi=1$. Next, inserting (8.1) into (6.18), we have the following differential equation for $T_{n,m}$.

$$\frac{d^2T_{n,m}}{d\xi^2}+\frac{2(n+1)}{\xi}\frac{dT_{n,m}}{d\xi}=-\frac{\beta a^3}{k}\sum_j A_j'\xi^j, \tag{8.3}$$

where A_j' is a certain constant which is a function of A_0, A_1, ... in (8.1). The equation (8.3) is solved in the form

$$T_{n,m}\left(\frac{\beta a^3}{k}\right)^{-1}=A''-\sum_j\frac{A_j'}{(j+2)(j+3+2n)}\xi^{j+2}. \tag{8.4}$$

In (8.4), A'' is a constant, which is determined so as to make $T_{n,m}$ in (8.4) satisfy the condition (7.17). The value of A'' thus adjusted is

$$A''=\sum_j\frac{A_j'}{(j+2)(j+3+2n)}. \tag{8.5}$$

Inserting (8.1) and (8.2) into $D(\xi)=0$ in (6.16), we can calculate $\Pi_{n,m}$. Thus, with $nF_{n,m}+\xi^2G_{n,m}$ and $L_{n,m}$ in (8.1), we can make

three groups of differential equations (6.17), (6.18) and $D(\xi)=0$ satisfied among the required five. There remain, still, two groups of differential equations to be solved. They are $C(\xi)=E(\xi)=0$ in (6.16). We have also two groups of undetermined constants A_0, A_1, B_0, B_1, ... We shall now try make $C(\xi)=E(\xi)=0$ satisfied approximately by choosing A_0, A_1, ...; B_0, B_1, ... adequately. Inserting (8.1)–(8.5) into (6.14) and

$$\int_0^1 C(\xi)\xi^{2n_\beta}(n_\beta F_\beta+\xi^2 G_\beta)d\xi=0\,, \tag{8.6}$$

(see (6.8) and the equation $D(\xi)=0$ above satisfied), we have equations of the following forms

$$A_0\int_0^1 C(\xi)\xi^{2n_\beta}(1-\xi)^2 d\xi=0\,,$$

$$A_1\int_0^1 C(\xi)\xi^{2n_\beta}(1-\xi)^2\xi d\xi=0\,,\ \ldots. \tag{8.7}$$

$$B_0\int_0^1 E(\xi)\xi^{2(n_\beta+1)}(1-\xi)d\xi=0\,,$$

$$B_1\int_0^1 E(\xi)\xi^{2(n_\beta+1)}(1-\xi)\xi d\xi=0,\ \ldots. \tag{8.8}$$

These equations will be used to determine the values of A_0, A_1, B_0, B_1, ... In order to show the way of determining A_0, A_1, ... by an example, we shall take up the (a)–approximation for the case in (7.1). $C(\xi)$ and $E(\xi)$ for this case are shown in the left-hand sides of (7.10) (a) and (7.14) (a). (In (7.14) (a), F_4 and G_4 have to be put equal to zero). We shall, furthermore, take only the first terms of $2F_{2,2}+\xi^2G_{2,2}$ and $L_{2,2}$ in (8.1). The results obtained in this way will be called the (a, 1)–approximation. Similarly, the results obtained by taking the first two terms of $2F_{2,2}+\xi^2G_{2,2}$ and $L_{2,2}$ will be called the (a, 2)–approximation. The (b, 1), (b, 2), (c, 1), (c, 2), ... approximations may also be defined similarly. The equations to determine A_0 and B_0 in the (a, 1)–approximation are obtained by (8.7) and (8.8) as follows.

$$\left(\frac{571}{11\cdot18\cdot30\cdot21\cdot28\cdot13}\lambda-\frac{2}{15}\right)A_0+\left(-\frac{2}{21\cdot9}\right)\Omega B_0=0,$$

$$\left(\frac{1}{6\cdot15\cdot45}\right)\Omega A_0+\left(-\frac{1}{9}\right)B_0=0. \tag{8.9}$$

In order that these equations are compatible, the determinant formed by the coefficients of A_0 and B_0 must be equal to zero. The equation for $\lambda=\dfrac{a^4\alpha\beta g}{k\nu}$ thus obtained is

$$\lambda=10602.5+1.86994\Omega^2,\quad \Omega=\frac{\omega a^2}{\nu}\,. \tag{8.10}$$

It is to be noted that this is of the same form as in (3.12). The values of λ in the (a, 1)–approximation are calculated for several Ω^2 and are shown in Table II. In Table II, are shown also the values of λ in the (a, 2)–approximation for the same Ω^2's. The values of λ in the approximation differ but little from those in the corresponding (a, 1)–approximation. The (a, 3), (a, 4), ... approximations are expected to give results practically the same as those in Table II.

Table II.

Ω^2	(a. 1)	(a. 2)
0	$1.060\cdot10^4$	$1.06\cdot10^4$
10^2	$1.079\cdot10^4$	$1.08\cdot10^4$
10^3	$1.247\cdot10^4$	$1.27\cdot10^4$
10^4	$2.930\cdot10^4$	$3.03\cdot10^4$

Thus, in order to get the value of λ in the $\lim_{j\to\infty}$ (a, j) approximation, we have only to follow the (a, 1)–approximation. Similarly, the $\lim_{j\to\infty}$ (b, j), $\lim_{j\to\infty}$ (c, j), ... approximations of λ may safely be inferred from the (b, 1), (c, 1), ... approximations. The values of λ in the (b, 1) and (c, 1)–approximations for the case in (7.1) are shown in Table III. In Table III, are shown also the values of λ in the (a, 1)–approximation for this case. The (a, 1) value is taken from Table II. The (c, 1) value of λ in Table III differs but little from the corresponding (b, 1) value. The (d, 1), (e, 1), ...approximations are expected to give results practically the same as those in Table III. Thus, we may use the (c, 1) value in Table III for the exact λ in the case (7.1). Similarly, the eigen-values for the cases (7.2)–(7.7) are calculated and are shown in Table IV. A discussion on the results in Table III and IV will be made in the next section.

Table III.

Ω^2	(a, 1)	(b, 1)	(c, 1)
0	1.060×10^4		
10^2	1.079×10^4	1.078×10^4	1.078×10^4
10^3	1.247×10^4	1.236×10^4	1.235×10^4
10^4	2.930×10^4	2.359×10^4	2.311×10^4

Table IV.

Ω^2	$u_{1,0}(I)$	$u_{1,0}(II)$	$u_{1,1}(I)$
0	0.811×10^4	1.06×10^4	0.811×10^4
10^2	0.862	1.11	0.849
10^3	1.225	1.55	1.13
10^4	2.68	3.70	2.48
	$u_{1,1}(II)$	$u_{2,2}(II)$	$u_{3,3}(I)$
0	1.06×10^4	1.53×10^4	1.53×10^4
10^2	1.10	1.55	1.54
10^3	1.48	1.79	1.64
10^4	3.47	3.52	2.44

§ 9. In this section, we shall call the motions in (7.1), (7.2), (7.3), ... as fluid motions of quasi-S_2^{2C}, quasi-S_1^0, quasi-S_2^0, ... types respectively. The reason why we call in this way is as follows. As was stated at the beginning of § 7, the $u_{2,2}(I)$ motion is nothing but the S_2^{2C} motion in the sense of Paper I, II and III. It is usually called the poloidal motion of $n=m=2$ type. Similarly, the $u_{1,0}(I)$ motion is the poloidal motion of $n=1$, $m=0$ type. It is usually denoted as S_1^0. As is seen from Table III and IV, if we put $\Omega^2=0$ in (7.1), (7.2), (7.3) ...., we have the eigen-values $\lambda=1.06\times10^4$, 0.811×10^4, 1.06×10^4 .... The eigen-functions corresponding to these eigen-values are of pure S_2^{2C}, S_1^0, S_2^0,. .... types. (H. JEFFREYS and E. M. BLAND, 1951: S. CHANDRASEKHAR, 1952). In any case, we shall now study about the problem stated in (2) in § 2. The minimum values of λ for the cases $\Omega^2=0$, 10^2, 10^3 and 10^4 are given by the fluid motions of the quasi-S_1^0, S_1^1, S_1^1, and S_2^2 types respectively. The minimum λ becomes larger for larger Ω^2. These relations correspond to the $b\sim\left(\frac{2\omega h^2}{\nu}\right)^2$ and $\lambda\,(\text{min.})\sim\left(\frac{2\omega h^2}{\nu}\right)^2$ relations in § 3. From our present point of view, it is important that we have the quasi-S_2^{2C} motion which becomes the easiest type to be excited in the case when $\Omega^2\doteqdot10^4$. Since our previous studies in Paper I, II and III were made under the assumption on the existence of S_2^{2C} motion, the result obtained above is very favourable to us. Though the existence of T_3^2, S_4^2, ... motions in the quasi S-motion may bring a little alteration to our results obtained in Paper I$\sim$III, the alteration will not be so large. We shall now estimate the value of kinematical viscosity ν corresponding to

$$\Omega^2\doteqdot10^4\,,\qquad \Omega=\frac{\omega a^2}{\nu}\doteqdot10^2\,. \tag{9.1}$$

Putting $\omega=\frac{2\pi}{86400}(\text{sec})^{-1}$ and $a=3.4\times10^8\,\text{cm}$ into (9.1), we have $\nu\doteqdot10^{11}\frac{\text{cm}^2}{\text{sec}}$. In short. if the kinematical viscosity of the fluid in the earth's core is about $10^{11}\frac{\text{cm}^2}{\text{sec}}$, so we have the fluid motion of (quasi) S_2^{2C}-type there. The viscosity ν in the earth's core was hitherto estimated to be $\nu\doteqdot10^{-2}\sim10^{-3}\frac{\text{cm}^2}{\text{sec}}$. (E. C. BULLARD, 1949) This seems contradictory with the result above obtained. It is the opinion of the present authors, however, that this contradiction is not so fatal to our studies. What our present study is concerned with is the eddy viscosity, whereas the viscosity $\nu=10^{-2}\sim10^{-3}$ above referred to is the molecular one. It is a well-known fact in dynamical meteorology and oceanography that the eddy viscosity for large-scale motions is far greater than the molecular viscosity. We shall now think over the values of λ obtained in the last section. The lowest value of $\lambda=\frac{a^4\alpha\beta g_0}{k\nu}$ in the case $\Omega^2\doteqdot10^4$ is that for the quasi-S_2^{2C} motion. In Table III, this value is shown to be

$$\lambda\doteqdot2.3\times10^4\,. \tag{9.2}$$

Inserting $g_0=10^3$, $a=3.4\times10^8$, $\alpha=10^{-5}$ and $\nu=10^{11}$ into (9.2), we have

$$\frac{\beta}{k} \doteqdot 2\times 10^{-17}. \tag{9.3}$$

For fluid motions in the earth's core, the thermal diffusivity k in (9.3) should be interpreted as the eddy diffusivity. In contrast to this, the thermal diffusivity k in (5.1)–(5.4), or in the state of no convection, should be interpreted as the molecular diffusivity. The molecular k in the earth's core is estimated to be $k=10^{-1}\frac{\text{cm}^2}{\text{sec}}$. Since the molecular k is a little greater than the molecular ν, the eddy k is considered to be a little greater than the eddy $\nu(=10^{11})$. Thus inserting $k=10^{11}\sim 10^{12}$ into (9.3), we have $\beta=10^{-5}\sim 10^{-6}$. As was stated before, β is the temperature gradient (at the surface of the earth's core) in excess of the adiabatic one. The latter is estimated to be 10^{-5}. Thus it is shown that the convection current of quasi S_2^{2C}–type can exist stationarily under the thermal gradient which is of the order of magnitude of the adiabatic one. This is the thermal state which is usually inferred to exist within the earth's core. Thus the results obtained in this section may be summed up as follows. In order that the covection current of the quasi S_2^{2C}–type exists stationarily in the earth's core, the kinematical viscosity ν there must be of the order of magnitude of 10^{11}. If ν is taken to be 10^{11}, then the thermal diffusivity k there must also be taken to be $10^{11}\sim 10^{12}$. If these values for ν and k are admitted, the thermal gradient there is shown to be of the order of magnitude of the adiabatic one. This is the thermal state which is usually supposed to exist in the earth's core.

§ 10. Since the value of ν obtained in this paper is rather too much greater than is supposed hitherto, details of the tentative convection current model in § 5 of Paper II will have to be changed a little. The magnetic field and the convection current velocity in the earth's core must be taken to be a little smaller than supposed there, but the alterations will not be so large. In the discussions in § 5–9 of the present paper, the existence of the magnetic field was not taken into account. The existence of the magnetic field within the earth's core, however, may bring no drastic changes to the results obtained in the present paper. This is seen from the equation (4.13). The result in (4.13) was obtained for plane boundaries and those for the boundary conditions other than those in § 5–9.

By the same reasoning as that at the end of § 3, we may safely conclude that the quasi S_2^{2C}–motion becomes the easiest to be excited within the earth's core in the case when the second term in the right-hand side of (4.13) becomes approximately equal to the first. In calculating the first and second terms, we may take also $s=b=1$. Thus we get the following condition for the existence of the S_2^{2C}–motion with in the earth's core

$$\frac{\sigma\mu^2 H_0^2 h^2}{\rho\nu} \sim 50 \tag{10.1}$$

Putting $\sigma=3\times 10^{-6}$, $\mu=1$, $a=3.4\times 10^8$, $\rho=10$ and $\nu=10^{11}$ in (10.1), we have $H_0\doteqdot 10$. Since the result in (4.17) is obtained by putting $\theta=\frac{\pi}{2}$ in (4.4), the value of H_0 above obtained is considered to be related to the radial component of the magnetic field within the earth's core. The value of the above H_0 interpretted in this way agrees well with that which has usually been inferred for the earth's core.

References

BULLARD, E. C.:
1949 "The magnetic field within the earth". Proc. Roy. Soc., **199**, 413.

CHANDRASEKHAR, S.:
1952 "The thermal instability of a fluid sphere heated within". Phil. Mag., Ser. 7, **43**, 1317.

ELSASSER, W. M.:
1950 "Causes of motions in the earth's core". Trans. Amer. Geophys. Union, **31**, 454.

JEFFREYS, H.:
1930 "The instability of a compressible fluid heated below". Proc. Camb. Phil. Trans., **26**, 170.

JEFFREYS, H. & BLAND, M. E. M.:
1951 "The instability of a fluid sphere heated

within". M.N.R.A.S. Geophys. Suppl., **6**, 148.

TAKEUCHI, H.:

1950 "On the earth tide of the compressible earth of variable density and elasticity". Trans. Amer. Geophys. Union, **31**, 651.

TAKEUCHI, H. & SHIMAZU, Y.:

1952 "On a self-exciting process in magneto-hydrodynamics". Jour. Phys. Earth. **1**, 1.

1952 "On a self-exciting process in magneto-hydrodynamics (II)", Jour. Phys. Earth, **1**, 57.

1953 "On a self-exciting process in magneto-hydrodynamics (III)", Jour. Phys. Earth, **2**, 5.

Propagation of Tremors over the Surface of an Elastic Solid.

By
Hitoshi Takeuchi
Geophysical Institute, Faculty of Science, Tokyo University, Tokyo.
and
Naota Kobayashi.
Department of Precision Mechanics, Faculty of Technology, Chūō University, Tokyo.

Abstract

Wave phenomena which are seen along the surface of a semi-infinite elastic solid when subjected to an impulsive line force in the direction normal to its surface have been studied. The results obtained are as follows.

(1) Immediately after the impulsive force is removed, the vertical displacement is downward in the neighbourhood of the origin, and it is upward outside that downward domain. (§ 3)

(2) In the downward (upward) domain, the horizontal displacement is toward (away from) the origin. (§ 4)

(3) The surface deformations thus produced are propagated with the velocity of Rayleigh wave without conspicuous changes in form. (§ 3 and § 4)

(4) The wave length of the Rayleigh wave is proportional to the time of duration of the impulse, and is of the same order of extent as that of the downward domain at the moment when the force is removed. (§ 3)

§ 1. Wave phenomena which are seen along the surface of a semi-infinite elastic solid when subjected to an external impulsive force were studied by H. Lamb (1904). His results are chiefly concerned with the phenomena which are to be observed at the places far distant from the wave origin. The deformation of the elastic solid in the neighbourhood of the origin was not studied in his paper. On the other hand, an experimental approach to this problem has recently been made by K. Kasahara (1952, 1953). In his experiments, an apparently curious phenomenon has been found in the neighbourhood of the origin. He has stated: "When an impulsive vertical force acts downwards on the surface of an elastic medium, a part of the surface within a certain region begins in upward motion. The disturbance which occurs in such a way is propagated as time passes on. Such a phenomenon seems rather curious from the stand point of the theory of the statical deformation of elastic bodies. Because, as Boussinesq has studied, every part of the surface of a semi-infinite elastic body subjected to an external vertical force acting downwards at a point, is displaced downwards and no part showing upward displacements can exist on the surface. In fact, a statical experiment carried out on the same medium produces such results". Kasahara has shown theoretically the possibility of swelling up of the surface of an elastic solid when subjected to an impulsive downward force, but has failed to bring a unified view in connecting this upward motion with the phenomena observed at the places far distant from the origin (1953). It is the purpose of the present paper to show a simple way of calculating the surface displacement of the elastic solid at any time and at any point and to fill up the gap between the knowledges concerning two extremes above cited.

§ 2. It was shown by Lamb (1904, his equation (93)) that the vertically downward displacement v_0 at $(x, y=0, t)$ due to the

vertically downward force $Q(t)$ at the origin ($x=0$, $y=0$) is given as follows.

$$v_0 = -\frac{1}{\pi\mu}\int_a^b \frac{b^2(2\theta^2-b^2)^2\sqrt{\theta^2-a^2}}{(2\theta^2-b^2)^4+16\theta^4(\theta^2-a^2)(b^2-\theta^2)}Q(t-\theta x)d\theta$$
$$-\frac{1}{\pi\mu}\,p\int_b^\infty \frac{b^2\sqrt{\theta^2-a^2}}{(2\theta^2-b^2)^2-4\theta^2\sqrt{\theta^2-a^2}\sqrt{\theta^2-b^2}}Q(t-\theta x)d\theta\,. \tag{2.1}$$

In (2.1), x is the distance of the point from the origin and t is the time, a and b in (2.1) are

$$a=\frac{1}{V_P}=\sqrt{\frac{\rho}{\lambda+2\mu}}\,,\qquad b=\frac{1}{V_S}=\sqrt{\frac{\rho}{\mu}} \tag{2.2}$$

respectively and the symbol p denotes the principal part of the integral which follows it. It is to be noted that the equation (2.1) is valid for any x and t. Equation (2.1) can be rewritten as follows.

$$v_0\frac{V_P}{V_S}\pi\mu = p\int_{-\infty}^{+\infty} V\left(\frac{t-t_0}{ax}\right)Q(t_0)\,d\left(\frac{t-t_0}{ax}\right)$$
$$= p\int_{-\infty}^{\infty} V\left(\frac{V_P(t-t_0)}{x}\right)Q(t_0)\,d\left(\frac{V_P(t-t_0)}{x}\right), \tag{2.3}$$

in which $V(\theta')=V(\theta/a)$ is

$$V(\theta')=-\frac{m^3(2\theta'^2-m^2)\sqrt{\theta'^2-1}}{(2\theta'^2-m^2)^4+16\theta'^4(\theta'^2-1)(m^2-\theta'^2)}$$
$$\text{for}\qquad 1\le\theta'\le m$$
$$V(\theta')=-\frac{m^3\sqrt{\theta'^2-1}}{(2\theta'^2-m^2)^2-4\theta'^2\sqrt{\theta'^2-1}\sqrt{\theta'^2-m^2}}$$
$$\text{for}\qquad m\le\theta'$$
$$m=\frac{b}{a}=\frac{V_P}{V_S}\,. \tag{2.4}$$

The value of $V(\theta')$ for the case $\lambda=\mu$ is given in the LAMB's paper. We reproduce it in Fig. 1.

We shall now calculate the value of v_0 in the case when

$$Q(t_0)=\text{const}\,Q,\quad \text{for}\quad -\tau\le t_0\le\tau$$
$$\text{and}\qquad Q(t_0)=0,\quad \text{otherwise.} \tag{2.5}$$

Putting $\quad t=\tau t' \qquad t_0=\tau t_0'$ (2.6)

in (2.4), we have

$$-\frac{m\pi\mu}{Q}v_0 = p\int_{\frac{V_P\tau}{x}(t'-1)}^{\frac{V_P\tau}{x}(t'+1)} (-V(\theta'))d\theta'. \tag{2.7}$$

This is the formula by which the value of v_0 at any x and t can be calculated. The hatched area which is shown in Fig. 1 represents the integral on the right hand side of (2.7) corresponding to a certain t'. In executing this integration for various values of t', we come across a difficulty when the domain of the integral $\int(-V(\theta'))d\theta'$ includes $\theta'=1.88\ldots$. At $\theta'=1.88\ldots$ the integrand $-V(\theta')$ in (2.7) becomes infinite of the order of $(\theta'-1.88\ldots)^{-1}$. This difficulty is similar to that encounterd in executing the integral $\int_{-1}^{+1}\frac{dx}{x}$, for instance. The limiting process by the aid of the principal value expressed the symbol p in (2.7) removes the difficulty stated above. Thus making use of (2.7), we can calculate the value of $-v_0$ (upward displacement) for any x and t. The results of calculation for the case when $\lambda=\mu$ are shown in Fig. 2.

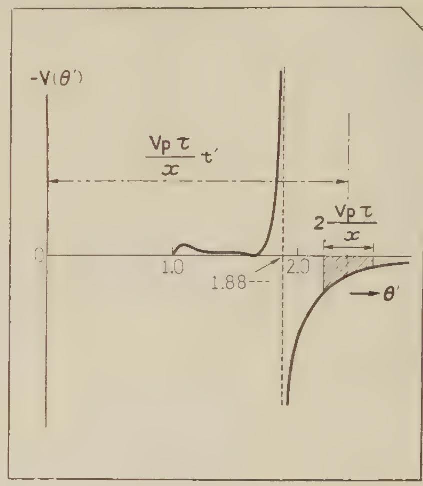

Fig. 1. The function $V(\theta')$

§3. As is seen in Fig. 2, the vertical displacement at $t=0$ or $t=\tau$ is downward for $\frac{x}{\tau V_P}\le 0.49$ or $\frac{x}{\tau V_P}\le 0.98$ respectively. It is of

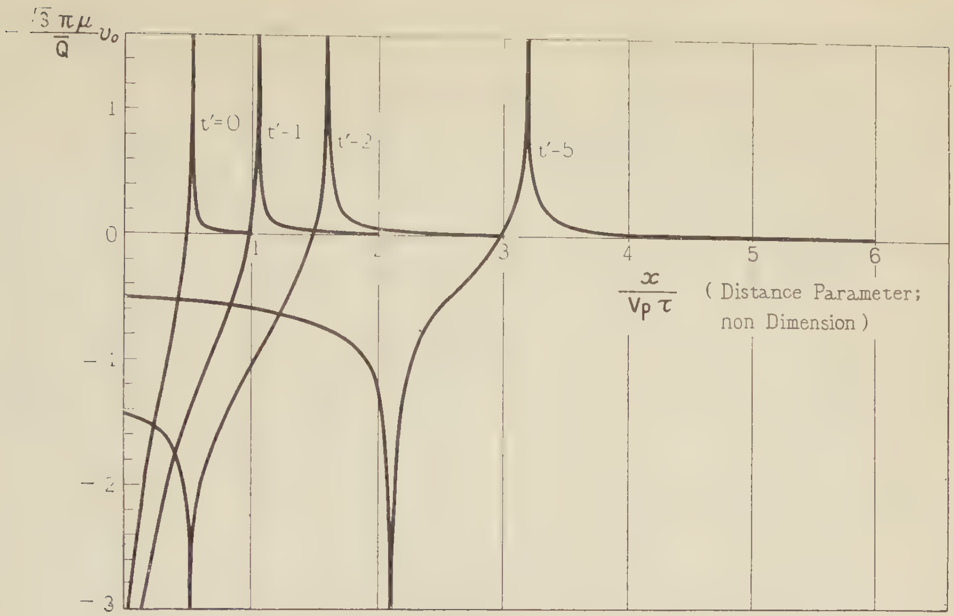

Fig. 2. Upward deformation $-v_0$

interest to note that the linear extension of the downward domain is proportional to τ (half the time of duration of the downward force). Thus if we make $\tau\to\infty$, we have the downward displacement everywhere on the surface of the elastic solid. This is nothing but the result obtained by BOUSSINESQ in the case of a statical downward force. There is a domain of the upward displacement outside the downward domain above stated. In the two dimensional problem as ours, the points of zero displacements lie on a straight line x=const. at a fixed time. As time passes on, this line of zero displacement, i.e., the boundary line between the upward and the downward domains is propagated from the origin with the velocity of RAYLEIGH wave. On the other hand, the front of the upward displacement is propagated from the origin with the velocity of P wave (compressional wave). The origin times of these two "waves" are both $t=-\tau$. Thus the upward (and also of the downward) domain increases in its extent according to time. The peak of the upward displacement is propagated from the origin with the velocity of RAYLEIGH wave. The origin time of this upward peak is also $t=-\tau$, i.e., at the time when the vertical force begins to act. The trough of the downward displacement is propagated from the origin also with the velocity of RAYLEIGH wave. The origin time of this trough is $t=+\tau$, i.e., at the time when the vertical force is removed. The time interval at any point between the arrival times of the upward peak and the downward trough is 2τ. The corresponding "wave length" L of the RAYLEIGH wave is $V_R\cdot 4\tau$, that is, the RAYLEIGH wave velocity times twice the time of duration of the downward force. As was stated at the beginning of the present section, the domain of the downward displacement at $t=\tau$ is characterised by the relation $|x|\leq 0.98\tau V_P$. and the width D of the domain of the downward displacement is $2\times 0.98\tau V_P$. Making use of the relation $V_R=0.53V_P$ for the case when $\lambda=\mu$, we have $D=3.7\tau V_R$. This is approximately equal to the wave length $L=4\tau V_R$ of the generated RAYLEIGH wave.

In Fig. 2 are shown only the displacements up to the time $t=5\tau$. The approximate pattern of the displacement for $t'>5$, however, can be obtained as follows. The front of the upward displacement is at $x=V_P(t+\tau)$. The

peak of the upward displacement and the trough of the downward displacement are at $x=V_R(t+\tau)$ and $V_R(t-\tau)$ respectively. The displacement in the neighbourhood of the origin decreases gradually as time goes on. In other respect, the pattern of the displacement is similar to that at $t\geqq 5\tau$.

The curve of displacement at $x=0$ is shown in Fig. 3.

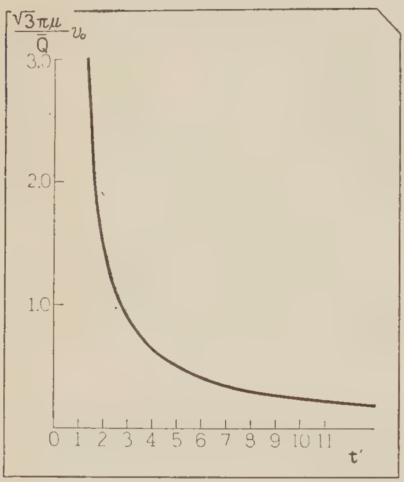

Fig. 3. Displacement at the origin

For the large values of $t=\tau t'$, the curve is expressed approximately by the equation

$$-\frac{\sqrt{3}\,\pi\mu}{Q}v_0=\frac{3\sqrt{3}}{4}\log_e\left(1+\frac{2}{t'}\right). \qquad (3.1)$$

The equation (3.1) is obtained as follows. From (2.4), we have

$$-V(\theta')=\frac{3\sqrt{3}}{4}\theta'^{-1} \qquad (3.2)$$

for the large θ'. Inserting (3.2) into (2.7), we get the equation (3.1). It can readily be seen that all of the numerical results above obtained are closely connected to the infinity point at $\theta'=1.88\ldots$ of the function $-V(\theta')$ in Fig. 1. This infinity point at $\theta'=1.88\ldots$ is, in turn, closely connected to the RAYLEIGH wave velocity for the case when $\lambda=\mu$. In fact, the numerical factor 0.53 in the relation $V_R=0.53V_P$ is nothing but the reciprocal of this $1.88\ldots$. It is therefore expected that the similar results as those obtained above will be obtained for the elastic solid for which $\lambda\fallingdotseq\mu$. KASAHARA's experiment referred to at the beginning of the present paper is made with an elastic solid (agar-agar) for which $\lambda=4\sim5\mu$. Adopting this value of λ/μ, his experimental results agree quite well with the above theoretical results. According to KASAHARA, for example, the peak of the upward deformation in his experiment is propagated with the velocity of about 1 cm/5m sec $=200$ cm/sec. (see Fig. 4 in his paper II) and this is seen from Table II in the same paper of his to be about the velocity of the RAYLEIGH wave in his experiment, just as is expected from our calculations.

§ 4. By the similar methods as adopted in the preceding sections, we can calculate the horizontal displacement $u_0(x, y=0, t)$. The equation by which the value of u_0 is to be calculated is as follows

$$\frac{m\pi\mu}{Q}u_0=-m\pi H\delta\left(t'-t_0-\frac{x}{V_P\tau}\right)$$

$$+2\int_{\frac{V_P\tau}{x}(t'-1)}^{\frac{V_P\tau}{x}(t'+1)}U(\theta')d\theta', \qquad (4.1)$$

in which δ is the DIRAC's function, and

$$U(\theta')=-\frac{m^3\theta'(2\theta'^2-m^2)\sqrt{\theta'^2-1}\sqrt{m^2-\theta'^2}}{(2\theta'^2-m^2)^4+16\theta'^4(\theta'^2-1)(m^2-\theta'^2)},$$

$$1\leqq\theta'\leqq m$$

$$U(\theta')=0, \qquad \theta'\leqq 1, \quad \theta'>m$$

$$H=0.12500 \quad (\lambda=\mu). \qquad (4.2)$$

The equation (4.1) and (4.2) are derived from the equation (92) in the LAMB's paper, and the value of $U(\theta')$ for the case when $\lambda=\mu$ was calculated also in the LAMB's paper. Thus making use of (4.1), we can calculate the value of u_0 for any x and t. The results of calculation for the case when $\lambda=\mu$ are shown in Fig. 4.

As is seen from Fig. 4, the horizontal displacement at $t=0$ or $t=\tau$ is towards the origin for x less than about $0.57\tau V_P$ or $1.15\tau V_P$ respectively. This domain of inward displacement roughly corresponds to the downward domain referred to at the beginning of the last section. Outside this domain, there is also a

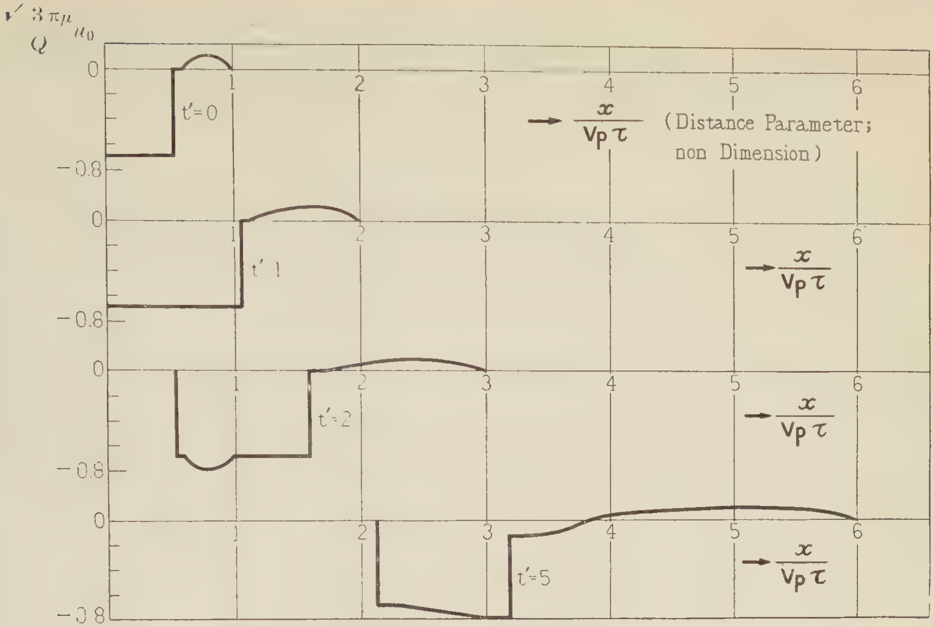

Fig. 4. Horizontal Displacement u_0

domain in which the horizontal displacement is outward from the origin. In the "outward domain", the vertical deformation is upward. The front of this horizontal displacement is propagated with the velocity of P wave. The origin time of this wave is $t=-\tau$. The principal part of the horizontal displacement at t is limited in the interval

$$V_R(t-\tau) \leq x \leq V_R(t+\tau) .$$

The value of u_0 in this part is about $-0.7\frac{Q}{\sqrt{3\pi\mu}}$. The front and rear of the principal part are propagated from the origin with the velocity of RAYLEIGH wave. The origin time of these front and rear waves are $t=-\tau$ and $t=\tau$ respectively.

§5. Throughout the present study, a line source of wave has been assumed, and the problem has been treated as a two-dimensional one. In the two-dimensional problem as ours, it is to be noted that the waves are propagated without conspicuous changes in form. In a three-dimensional problem with a point source of force, this is not the case. This latter problem will be studied in another paper.

References

KASAHARA, K.:

1952 "Experimental studies on the mechanism of generation of elastic waves 1". Bull. Earthq. Res. Inst., **30**, 259.

1953 "Experimental studies on the mechanism of generation of elastic waves 2". Bull. Earthq. Res. Inst., **31**, 71.

LAMB, H.:

1904 "On the propagation of tremors over the surface of an elastic solid" Phil. Trans., A **203**, 1.

Determination of Elastic Wave Velocities in Rocks by Means of Ultrasonic Impulse Transmission.

By

Akira KUBOTERA.

Geophysical Institute, Faculty of Science, Kyoto University, Kyoto.

Abstract

Velocities of longitudinal and transversal elastic waves in rock specimens have been determined from the transmission times of ultrasonic impulse (50 KC—300 KC) through them at ordinary temperatures and pressures. POISSON's ratios have also been calculated from the velocities of the two kinds of elastic waves.

18 specimens of granite and 34 of marble, all collected from various localities of Japan, were examined. In addition, 12 apecimens of marble from Italy and various other kinds of rock, such as andesite, sandstone, tuff, etc. were also examined. The experimental results are summarised as follows:

	longitudinal wave (km/sec.)	transversal wave (km/sec.)	POISSON's ratio
Granite	4.09–5.89	2.51–3.55	0.19–0.28
Marble	3.75–6.94	2.02–3.86	0.18–0.35

Within the frequency range of our experiments, dispersion phenomena have been found in none of the rock specimens examined.

§ 1. Introduction

The elastic constants of rocks for low and audio-frequencies have been measured by a number of workers. In experimental loboratories, the constants can be determined from the resonance frequency of a rod of rock specimen which is subjected to standing elastic vibrations (K. IIDA: 1939). In fields, on the other hand, the constants can most directly be determined from the time of transmission of artificial or natural seismic waves. If one wishes to use this direct method in laboratories, an inconveniently long specimen of rock will be needed, because the specimen must be at least several times as long as the wave-length of the elastic wave used. This difficulty will disappear if ultrasonic frequency is used instead of audio-frequency. In the present paper, the writer is going to describe the results of his loboratory determinations of elastic constants of rocks from the time of transmission of ultrasonic waves (50 KC–300 KC) in rock specimens. The dimensions of the specimens are 20 cm × 17 cm × 6 cm in case of granite and 12 cm × 9 cm × (2∼1) cm in case of marble.

§ 2. Apparatus and Experimental Method

Fig. 1 shows the general view of the apparatus used and Fig. 2 is its schematic diagram. The apparatus consists of a pulse generator, pulse amplifier, sweep circuit, time mark circuit and cathod-ray oscillograph.

$BaTiO_3$ crystals were used to generate and receive ultrasonic waves of 50 KC, while quartz crystals were used for 150 KC and 300 KC. For the latter case, X-cut crystals were used for longitudinal waves, while Y-cut crystals were used for transversal waves. D. S. HUGHES and J. H. CROSS (1951) used X-cut crystals for both kinds of waves, but according to the writer's experiences, Y-cut crystals are more adapted for transversal waves.

The pulse generator (including power am-

plifier) which excites the crystals has been so designed that the pulse is sent into the specimen a short time after the sweep circuit bigins to operate. Sweep signals are fed to the horizontal plate circuit of the cathod-ray oscillograph while the imput impulse to the rock specimen and the output impulse from it are both fed to the vertical plate circuit of

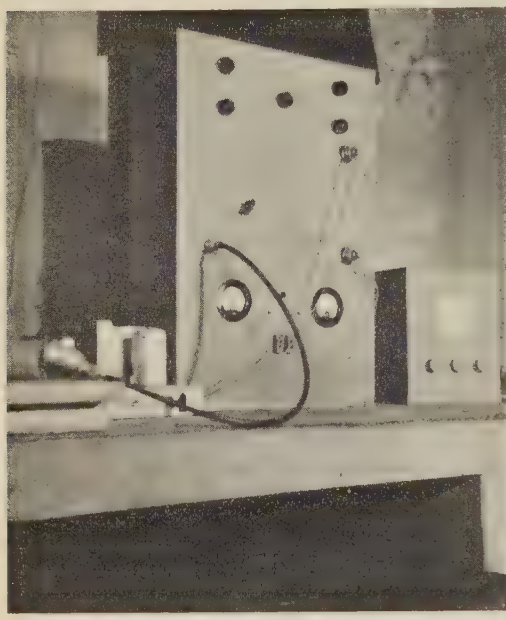

Fig. 1. General view of the experimental apparatus.

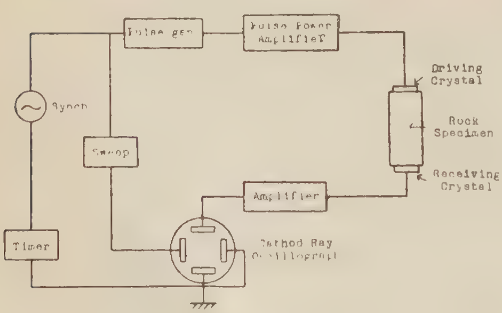

Fig. 2. Schematic diagram of the experimental apparatus.

the oscillograph together with time marks. The time marks are given at every 3±0.06 microseconds. The apparatus was designed by Assistant Professor F. KONDO of the Department of Electrical Engineering, Kyoto University, and was constructed by his assistant, Mr. T. YAMADA.

§ 3. Rock Specimens

The rock specimens examined are as follows:

Granite	18	Japan
Marble	33	Japan
Marble	12	Italy
Marble	1	Korea,

all collected by Mr. S. NAGAOKA. These were placed at the writer's disposal by the kindness of Professor S. MATSUSHITA. The localities from which they were collected are listed in Tables I and II. Each of the rock specimens has its own characteristic appearance and has the proper name according to its place of occurrence as also listed in the tables. The properties of these specimens of granite and marble are believed to be such that they well represent those of the corresponding rocks which occur in their respective places. Unfortunately, however, chemical and mineralogical compositions of the specimens have not yet been determined.

§ 4. Results

The cathod-ray oscillograms due to longitudinal and transversal waves in rock specimens were taken photographically. Fig. 3 is one of the records obtained for a granite specimen. On the first record are shown the incident and received wave pulses due to the X-cut quartz crystal oscillations, while the third those due to the Y-cut crystal oscillations. The second and fourth records are time marks corresponding to the records above them. As is clear from the records, when the X-cut crystal is used, only one phase can be seen in the wave trains received. This phase corresponds to the longitudinal wave. In contrast to this, when the Y-cut crystal is used, the wave trains received show two sharply distinguishable phases, the first smaller one corresponding to the longitudinal wave and the latter larger one to the transversal wave. It is likely that in case of the Y-cut, while the main oscillations of the

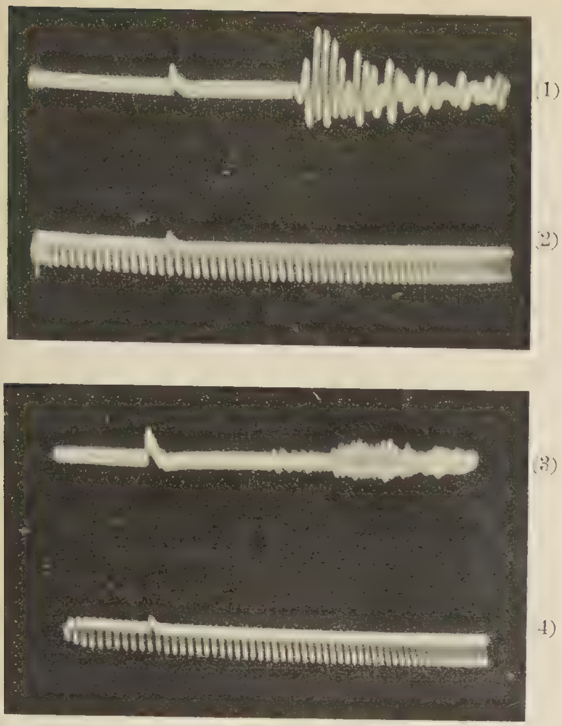

(1) Longitudinal wave of X-cut crystal.
(2) Time Mark.
(3) Longitudinal and transversal waves of Y-cut crystal.
(4) Time Mark.

Fig. 3. An example of records obtained for a granite specimen.

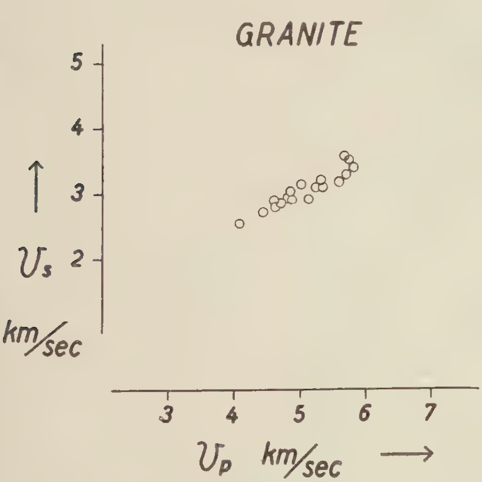

Fig. 4. Longitudinal and transversal wave velocities in granite specimens.

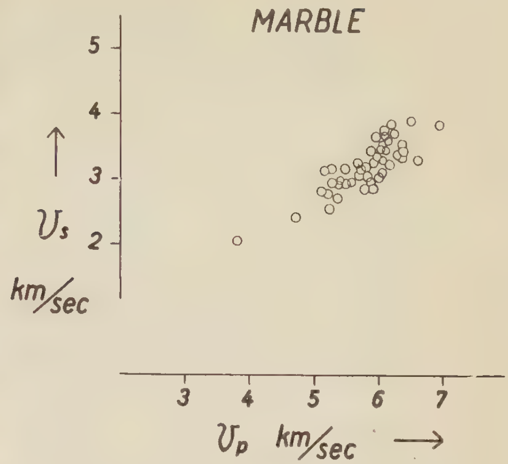

Fig. 5. Longitudinal and transversal wave velocities in marble specimens.

crystal are in X-direction and produce the transversal wave, those in Y-direction due to the thickness oscillation produce the longitudinal wave.

The velocities of longitudinal and transversal waves obtained for various specimens are listed in Tables I and II for granite and marble specimens respectively. Figs. 4 and 5 have been obtained by taking the transversal wave velocity v_s in ordinate and the longitudinal wave velocity v_p in abscissa. The points in these figures are seen to lie approximately on a straight line within a certain range of velocity values. The velocities of elastic waves in granite and marble range as follows:

	v_p (km/sec.)	v_s (km/sec.)
Granite	4.09–5.89	2.51–3.55
Marble	3.75–6.94	2.02–3.86

Poisson's ratios as well as densities of the rock specimens are also given in Tables I and II. The range and the average values of Poisson's ratio are as follows:

	range	average
Granite	0.19–0.28	0.23
Marble	0.18–0.35	0.27

Table I. Locality, Proper Name, Longitudinal and Transversal Wave Velocities, POISSON's Ratio and Density of Granite.

No.	Locality	Proper Name (Japanese)	V_p km/sec.	V_s km/sec.	POISSON's ratio	Density gr/cm³
1	Hyogo-Pref.	Akao-ishi	5.75	3.27	.26	2.86
2	〃	Hon-mikage (I)	5.77	3.50	.21	2.77
3	〃	〃 (II)	5.38	3.16	.28	2.79
4	Ôsaka-Pref.	Kitazima-ishi	5.89	3.37	.26	2.76
5	〃	〃	5.63	3.16	.27	2.77
6	Aichi-Pref.	Kuro-sansyu-mikage	4.91	2.89	.24	2.65
7	Ehime-Pref.	Oshima-ishi	4.45	2.70	.21	2.78
8	Kagawa-Pref.	Yoshima-ishi	4.86	3.00	.19	2.77
9	〃	Agi-ishi	4.56	2.78	.21	2.71
10	〃	Shokai	5.40	3.05	.27	2.70
11	Okayama-Pref.	Kitaki	4.83	2.96	.20	2.68
12	〃	Sabi-ishi	5.02	3.10	.19	2.62
13	〃	〃	5.30	3.03	.26	2.94
14	〃	Inushima-ishi	5.18	2.88	.28	2.87
15	〃	Aoki-ishi	4.09	2.51	.20	2.77
16	〃	Kitaki-ishi	5.71	3.55	.19	2.70
17	〃	Mansei-ishi	4.77	2.81	.24	2.70
18	〃	Muneage-ishi	4.62	2.85	.19	2.77

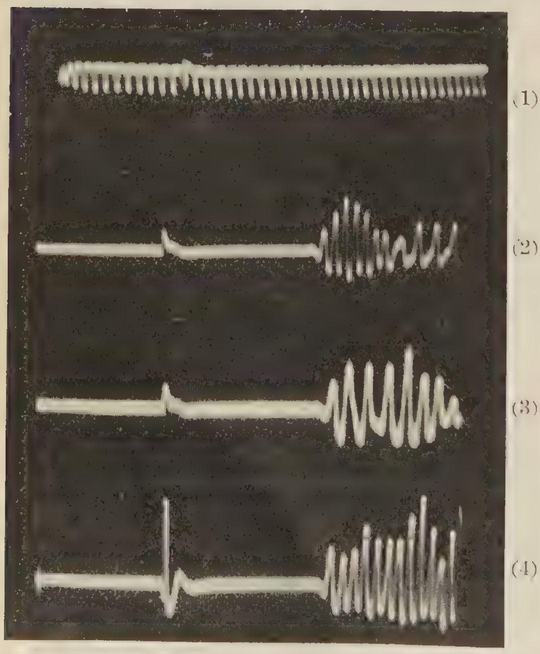

Fig. 6. Longitudinal waves in a sandstone specimen excited by different frequencies.

(1) Time mark. (3 microseconds.)
(2) 300 kc/sec. X-cut crystal.
(3) 150 kc/sec. X-cut crystal.
(4) 50 kc/sec. $BaTiO_3$.

The average values of POISSON's ratio as determined by our experiments agree with BIRCH's value (1938). The averages of the ratios of the longitudinal and transversal wave velocities are as follows:

	ratio
Granite	1.69
Marble	1.78

Finally, no tendency has been found that the velocity of elastic waves depends on the ultrasonic frequency within our frequency range (50 KC–300 KC) and also within the accuracy of our experiments. One of the experimental results which indicates this conclusion is shown in Fig. 6. This record was taken with a sandstone specimen. Although

Table II. Locality, Proper Name, Longitudinal and Transversal Wave Velocities, Poisson's Ratio and Density of Marble.

No.	Locality		Proper Name (Japanese)	V_p km/sec.	V_s km/sec.	Poisson's ratio	Density gr/cm³
1	Yamaguchi-Pref.	Akiyoshi	Shiro	5.62	3.26	.25	2.66
2	〃	〃	Hakuchuzitu	5.97	3.32	.28	2.73
3	〃	〃	Midoriiriishi	5.34	2.96	.28	2.80
4	〃	〃	Shirakumo	6.08	3.73	.20	2.93
5	〃	〃	Usugumo	5.48	2.92	.30	2.76
6	〃	〃	Hakuyo	6.14	3.22	.31	2.76
7	〃	〃	〃	5.09	2.80	.28	2.73
8	〃	〃	Oka sarasa	5.89	2.96	.33	2.73
9	〃	〃	Kinmon	5.85	3.46	.23	2.79
10	〃	〃	Kinteki	5.89	2.83	.35	2.74
11	〃	〃	〃	6.02	3.54	.24	2.72
12	〃	〃	Oka	3.75	2.02	.29	2.68
13	〃	〃	〃	5.11	3.12	.21	2.66
14	〃	Omine	Hakuyo	5.25	3.13	.24	2.83
15	〃	〃	Shisuiseki	6.15	3.84	.18	2.66
16	〃	〃	Uzura	6.05	3.48	.26	2.72
17	〃	Ota	Sarasa	6.37	3.31	.31	2.70
18	〃	〃	Okibuse	5.92	3.64	.19	2.80
19	Tokushima-Pref.	Tokushima	Kamo	6.48	3.92	.21	2.76
20	〃	〃	Kinkamo	6.34	3.43	.29	2.76
21	〃	〃	Aka-kamo	5.98	3.04	.33	2.76
22	〃	Akaishi	Sato-shima	5.80	3.07	.31	2.72
23	〃	〃	Kinkaseki	6.10	3.70	.27	2.79
24	Kochi-Pref.	Kochi	Ao-keiryu	5.41	3.15	.24	2.72
25	〃	〃	Keiryu	5.67	3.10	.29	2.82
26	Gifu-Pref.	Akasaka	Ki-sarasa	6.94	3.86	.28	2.74
27	〃	〃	Aka-sarasa	6.16	3.76	.21	2.70
28	〃	〃	〃	6.10	3.70	.21	2.69
29	〃	〃	Kuro-sarasa	6.01	3.50	.24	2.62
30	〃	〃	Kuro	6.19	3.75	.21	2.70
31	Ibaragi-Pref.	Mayumiyama	Shimanezumi	6.23	3.38	.29	2.72
32	Okayama-Pref.	Naruha	Aiko	5.72	3.18	.28	2.72
33	Wakayama-Pref.	Yuasa	Kamo	6.02	3.10	.32	2.73
34	Yamanashi-Pref.		Shihanseki	5.14	2.72	.30	2.80
35	Ryukyu Islands		〃	5.38	3.00	.28	2.39
36	Korea, Heizyo		Akagasumi	6.00	3.30	.28	2.70
37	Italy			6.33	3.51	.26	2.66
38	〃			5.90	3.28	.28	2.58
39	〃			5.70	3.20	.27	2.75
40	〃			5.53	2.99	.29	2.59
41	〃			5.25	2.92	.28	2.62
42	〃			4.68	2.43	.28	2.88
43	〃			5.31	2.75	.32	2.82
44	〃			6.62	3.31	.33	2.64
45	〃			5.20	2.53	.35	2.75
46	〃			5.74	2.84	.34	2.72

three different frequencies were used as indicated in the figure, no difference is seen in the time between the imput and arrival of waves.

So far, the results for granite and marble have been described. We have made similar experiments for about 150 specimens of other kinds of rock. The results of these experiments will be reported in the near future.

Acknowledgements

The writer wishes to express his gratitudes to Professor K. SASSA, Professor E. NISHIMURA, both of the Geophysical Institute of Kyoto University, and Professor S. MATSUSHITA of the Geological Institute, and Assistant Professor F. KONDO of the Department of Electrical Engineering of the same university, for their many valuable discussions. Many thankes are also due to Mr. K. NAKAZAWA, Mr. T. YAMADA and Mr. T. SHINOHARA for their assistance in the experiments. The present study has been supported by the Grant in Aid for the Miscellaneous Scientific Researches of the Department of Education.

References

BIRCH, F., and BANCROFT, D.:
1936 "The Effect of Pressure on the Rigidity of Rocks." Journ. Geol.. **46**, 59–141.

HUGHES, D.S., and CROSS, J.H.:
1951 "Elastic Wave Velocities at High Pressures and Temperatures." Geophysics, **16**, 577–593.

IIDA, K.:
1938 "Determining YOUNG's Modulus and the Solid Viscosity Coefficients of Rocks by the Vibration Method." Bull. Earthq. Res. Inst., **17**, 79–92.

Fluid Motions near the Core Boundary and the Irregular Variations in the Earth's Rotation.

By

Hitoshi TAKEUCHI

Geophysical Institute, Faculty of Science, Tokyo University, Tokyo.

and

W. M. ELSASSER

Department of Physics, University of Utah, Salt Lake City, Utah, U.S.A.

Abstract

The transmission of mechanical forces of the magnetic field through the top layers of the core into mantle is studied. It is shown that moderate fluctuations of the toroidal field near the boundary of the core are large enough to produce the observed variations in the rate of rotation of the mantle. A simple theoretical analysis of the motions near the boundary of the core shows that the equations of the geostrophic wind in meteorology can be applied to the layer.

§1. It has been suspected for some time that the observed irregular fluctuations in the earth's rate of rotation (D. BROUWER, 1952) can be explained by an exchange of angular momentum between the earth's mantle and core. W. MUNK and R. REVELL (1952, see also E. H. VESTINE 1953) have studied all the available geophysical evidences and found that this explanation is by far the most plausible one. E. C. BULLARD and collaborators (1950) have shown that the observed westerly drift of the geomagnetic secular variation requires the existence of an electromagnetic couple between the core and mantle. In Bullard's model the earth is represented by three concentric solid spheres in mutual electrical contact and rotating relative to each other. In this paper, we go a step further by using the actual hydrodynamic equations for the region of the core near its boundary, and thereby investigate the transmission of electromagnetic torques from the core to the mantle. Simple numerical estimates show that the mechanical forces exerted by the magnetic field in the neighbourhood of the core boundary are at least as large as any other force acting in the fluid. Hence this problem involves hydromagnetic theory and is closely related to the dynamo models which have been developed to account for the earth's magnetic field (W.M. ELSASSER, 1950; H. TAKEUCHI and Y. SHIMAZU, 1952, 53 and 54; E. C. BULLARD, 1949 and 1954).

As the following treatment shows, the motion near the boundary will break up into large-scale eddies, similar to the major perturbations of the atmosphere. This is due, mainly, to the deflecting action of the Coriolis force, which leads to instabilities and eddy formation. In a previous paper (W. M. ELSASSER and H. TAKEUCHI, 1955), we have approached this problem by using averages over circles of latitude and lumping the effects of the eddies together in a mechanical and a magnetic eddy viscosity, which both are very large. It seems desirable to show how far we can go in a quantitative analysis without making this radical assumption. In the present paper, the frictional terms are considered to correspond to molecular viscosities and are small compared with other terms, especially the Coriolis and pressure terms in the equations of motion. This does not lead to a specification of the mean flow in the boundary layer, as in the preceding paper; nevertheless it is possible to show that electro-magnetic torques transmitted from the core to the mantle are of the right order

of magnitude to account for the observed variations in the earth's rate of rotation.

§ 2. Let us take a local Cartesian coordinate system in Fig. 1, which has its origin at a point on the surface of the earth's core. The equations to be solved are

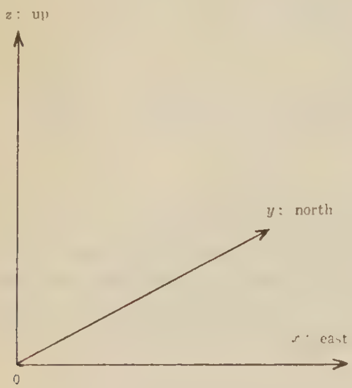

Fig. 1

$$\frac{\partial H}{\partial t}=\frac{1}{4\pi\mu\sigma}\nabla^2 H+\text{ curl }(V\times H) \tag{2.1}$$

$$\text{div } H=0 \tag{2.2}$$

$$\text{div } V=0 \tag{2.3}$$

$$\frac{\partial V}{\partial t}=-\text{grad}\left(\frac{p}{\rho}+gz\right)-2(\omega\times V)+\frac{\mu}{4\pi\rho}(\text{curl } H\times H)+\nu\nabla^2 V, \tag{2.4}$$

where H is the magnetic field, μ the permeability, σ the electrical conductivity, all in electro-magnetic units. V is the velocity field, ω the rotation vector, p the pressure, ρ the density. Expecting that the boundary layer, where the westward drift of the earth's magnetic field is taking place, is thin compared with the lateral dimensions concerned, we shall assume

$$\frac{\partial}{\partial x},\ \frac{\partial}{\partial y}\ll\frac{\partial}{\partial z}. \tag{2.5}$$

This will essentially be the only assumption required in this paper. Using this assumption in (2.2) and (2.3), we find that H_z and V_z are independent of z:

$$\frac{\partial H_z}{\partial z}=\frac{\partial V_z}{\partial z}=0 \tag{2.6}$$

Since the velocity V_z is relative to the earth's mantle, which is in the region $z>0$ in Fig. 1, and since $V_z=0$ at $z=0$, we may take

$$V_z=\text{constant}=0 \tag{2.7}$$

in the boundary layer. Inserting (2.5)−(2.7) into (2.1), we get

$$\frac{\partial H_x}{\partial t}=\frac{1}{4\pi\mu\sigma}\frac{\partial^2 H_x}{\partial z^2}+H_z\frac{\partial V_x}{\partial z} \tag{2.8}$$

$$\frac{\partial H_y}{\partial t}=\frac{1}{4\pi\mu\sigma}\frac{\partial^2 H_y}{\partial z^2}+H_z\frac{\partial V_y}{\partial z} \tag{2.9}$$

$$\frac{\partial H_z}{\partial t}=0 \tag{2.10}$$

By (2.6) and (2.10) is meant that H_z is a constant, independent of both (x, y, z) and t. Using the preceding relations, we find from (2.4)

$$\frac{\partial V_x}{\partial t}=-\frac{\partial p'}{\partial x}+2\omega_z V_y+\frac{\mu H_z}{4\pi\rho}\frac{\partial H_x}{\partial z}+\nu\nabla^2 V_x, \tag{2.11}$$

$$\frac{\partial V_y}{\partial t}=-\frac{\partial p'}{\partial y}-2\omega_z V_x+\frac{\mu H_z}{4\pi\rho}\frac{\partial H_y}{\partial z}+\nu\nabla^2 V_y, \tag{2.12}$$

$$0=-\frac{\partial p'}{\partial z}+2\omega_y V_x-\frac{\mu}{8\pi\rho}\frac{\partial}{\partial z}(H_x^2+H_y^2) \tag{2.13}$$

where $\rho p'=p+\rho gz$ is the pressure deviation from the corresponding hydrostatic pressure. The reason why we retain the terms $-\frac{\partial p'}{\partial x}$ and $-\frac{\partial p'}{\partial y}$ in the above equations is that although $\frac{\partial}{\partial x}$ and $\frac{\partial}{\partial y}$ are assumed to be small, p' might be large and might keep $-\frac{\partial p'}{\partial x}$ and $-\frac{\partial p'}{\partial y}$ finite.

§ 3. In the stationary state, we get from (2.8) and (2.9)

$$\frac{\partial V_x}{\partial z}=-\frac{1}{4\pi\mu\sigma H_z}\frac{\partial^2 H_x}{\partial z^2},$$

$$\frac{\partial V_y}{\partial z}=-\frac{1}{4\pi\mu\sigma H_z}\frac{\partial^2 H_y}{\partial z^2} \tag{3.1}$$

Integrating (3.1) with respect to z, and putting $(V_x)_{z=0}=(V_y)_{z=0}=0$, we find

$$V_x = -\frac{1}{4\pi\mu\sigma H_z}\left[\frac{\partial H_x}{\partial z} - \left(\frac{\partial H_x}{\partial z}\right)_{z=0}\right]$$
$$V_y = -\frac{1}{4\pi\mu\sigma H_z}\left[\frac{\partial H_y}{\partial z} - \left(\frac{\partial H_y}{\partial z}\right)_{z=0}\right] \qquad (3.2)$$

In our present problem, H_z may be considered the z component of the dipole field in the boundary layer. Since $H_z<0$ (or >0) in the northern (or southern) hemisphere, the first equation in (3.2) will give the following condition for the stationary westward drift $V_x<0$:

$$\frac{\partial H_x}{\partial z} - \left(\frac{\partial H_x}{\partial z}\right)_{z=0} \begin{cases} < 0 : \text{northern hemisphere} \\ > 0 : \text{southern hemisphere} \end{cases} \qquad (3.3)$$

The distribution of H_x as shown in Fig. 2 will satisfy the above condition. Thus we have the distributions of the fields shown schematically in Fig. 3. These are nothing

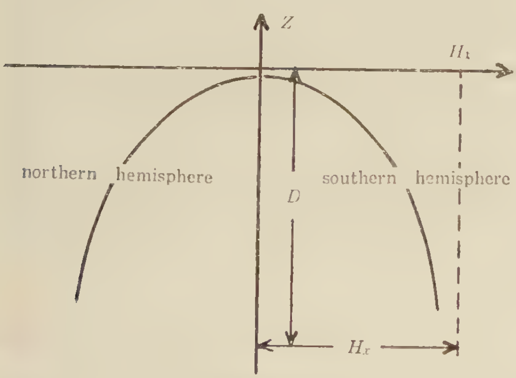

Fig. 2.

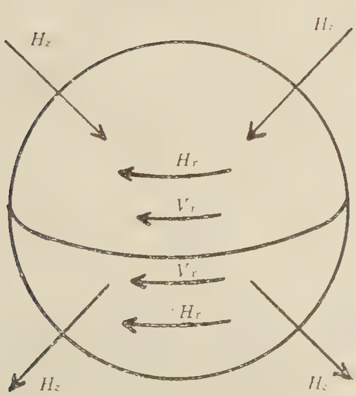

Fig. 3.

but the distributions which have been supposed hitherto to exist in the boundary layer of the earth's core. The first equation in (3.2) will also give a quantitative result of the following type

$$H_x \sim 4\pi\mu\sigma\, V_x\, D H_z, \qquad (3.4)$$

where D is the thickness of the boundary layer and H_x is the toroidal magnetic field at the bottom of the boundary layer (see Fig. 2). (3.4) is of the same type as obtained by BULLARD (E. C. BULLARD, 1949, especially his equations (1) and (2)). In BULLARD's paper, H_x and H_z are written as H_ϕ and H_0, respectively. Putting $\mu=1$, $\sigma=3\times10^{-6}$, $V_x=0.03$ and $H_z=4$ (all in c. g. s. e. m. u) in (3.4), we find

$$H_x \simeq 0.5\, D\,, \qquad (3.5)$$

where D is meassured in Km. (3.5) will give $H_x=5$, 25 and 50 gauss for $D=10$, 50 and 100 Km., respectively. These are plausible values for the boundary layer. Inserting the above results into (2.12), we see that the second term on the right-hand side $2\omega_z V_x \sim 10^{-4}\times3\times10^{-2}=3\times10^{-6}$ is about 10 times the third term $\sim\frac{H_zH_y}{10^2 D}\sim\frac{1}{6D}$ (H_y was taken to be 4 gauss). Although we have no experimental evidence on the magnitude of V_y, we may assume that it is of the same order of magnitude as V_x. Thus, in order that the fourth term $\frac{\nu V_y}{D^2}$ on the right-hand side of (2.12) is of the same order of magnitude as the third term, we must have

$$V \sim 10^{-2}\frac{H_zH_yD}{V_y} \qquad (3.6)$$

With $D=10$ Km., $V_y=0.03$ cm/sec and $H_z=H_y=4$ gauss, (3.6) will give $\nu\sim5\times10^6$, which is much larger than hitherto supposed. For smaller values of ν, the fourth term will become very small compared even with the third term. Thus, in the stationary state, it is very likely that the second term balances the first term and we have

$$-\frac{1}{\rho}\frac{\partial p}{\partial y} - 2\omega_z V_x = 0 \qquad (3.7)$$

Similary, we get from (2.11) and (2.13)

$$-\frac{1}{\rho}\frac{\partial p}{\partial x}+2\omega_z V_y=0\,,$$

$$-\frac{\partial p'}{\partial z}+2\omega_y V_x-\frac{\mu}{8\pi\rho}\frac{\partial}{\partial z}(H_x^2+H_y^2)\doteqdot$$

$$-\frac{1}{\rho}\frac{\partial p}{\partial z}-g=0 \qquad (3.7)$$

(3.7) is nothing but the equation for the geostrophic wind in meteorology, and (3.7) and (3.2) are the fundamental equations in the stationary state.

§ 4. On eliminating H_y, V_x and V_y from (2.8), (2.9), (2.11) and (2.12), we find

$$\frac{\partial}{\partial z}L\,H_x=(p') \qquad (4.1)$$

where (p') is a functiou of p' and

$$L=\left[\left(\frac{\partial}{\partial t}-\nu\frac{\partial^2}{\partial z^2}\right)\left(\frac{\partial}{\partial t}-\nu_m\frac{\partial^2}{\partial z^2}\right)-c^2\frac{\partial^2}{\partial z^2}\right]^2$$
$$+4\omega_z^2\left(\frac{\partial}{\partial t}-\nu_m\frac{\partial^2}{\partial z^2}\right)^2 \qquad (4.2)$$

$$\nu_m=\frac{1}{4\pi\mu\sigma},\qquad c^2=\frac{\mu H_z^2}{4\pi\rho} \qquad (4.3)$$

If we put $\omega_z=0$ and $\nu=\nu_m=0$ in (4.1) and (4.2), we have the following homogeneous equation for H_x

$$\left(\frac{\partial^2}{\partial t^2}-c^2\frac{\partial^2}{\partial z^2}\right)H_x=0\,, \qquad (4.4)$$

which will give

$$H_x\propto e^{in(z-ct)} \qquad (4.5)$$

This is nothing but the equation for a magnetohydrodynamical wave first obtained by H. ALFVEN (1950). When ω_z, ν, $\nu_m\neq 0$, the homogeneous equation of H_x in (4.1) will give

$$H_x\propto e^{-qt+inz} \qquad (4.6)$$

$$[(-q+\nu n^2)(-q+\nu_m n^2)+c^2n^2]^2$$
$$+4\omega_z^2(-q+\nu_m n^2)^2=0 \qquad (4.7)$$

This is the expression for the characteristic time $\tau=$(real part of q) in which the stationary state will be reestablished after having been disturbed by a disturbance of wave length $\lambda=\frac{2\pi}{n}$. Putting the values in the neighbourhood of (3.5), $\rho=10$ and $\lambda=4D$ (rather tentatively) into (4.7), we find the values of the longest characteristic times τ in Table 1.

D : Km	H_x : gauss	τ : year
10	5	0.5
50	25	12
100	50	50

Table 1.

§ 5. In this section, using the results obtained above, we shall study the problem on the irregularities in the rotation of the earth, which has recently been discussed in connection with the westward drift of the earth's magnetic field (W. MUNK and R. REVELLE, 1952 and E. H. VESTINE, 1953). Since the boundary layer is very thin, we have effectively two layers, the mantle and the core. Thus denoting the moments of inertia and angular velocities of the mantle and the core by I_m, I_c; ω_m and ω_c, respectively, we have

$$I_m\Delta\omega_m+I_c\Delta\omega_c=0\,, \qquad (5.1)$$

where $\Delta\omega_m$ and $\Delta\omega_c$ are the deviations of the angular velocities from their stationary values. Since $I_m\,(\doteqdot 7.2\times10^{44})\gg I_c\,(\doteqdot 8.6\times10^{43})$, (5.1) will give $|\Delta\omega_c|\gg|\Delta\omega_m|$. Thus, we may write

$$\Delta\omega_m=-\frac{I_c}{I_m}\Delta\omega_c\doteqdot-\frac{I_c}{I_m}\Delta(\omega_c-\omega_m)\,, \qquad (5.2)$$

where $\Delta(\omega_c-\omega_m)$ is the variation of angular velocity of the core relative to the mantle, which may be observed as the variation of the westward drift of the earth's magnetic field. On the other hand, from the relation $\omega_m T=2\pi$, where $T=86400$ is the length of a day in sec., we find

$$\Delta T=-\frac{T^2}{2\pi}\Delta\omega_m\doteqdot\frac{T^2}{2\pi}\frac{I_c}{I_m}\Delta(\omega_c-\omega_m)$$

or

$$\frac{\Delta T}{\Delta(\omega_c-\omega_m)}\doteqdot\frac{T^2}{2\pi}\frac{I_c}{I_m}=1.4\times10^8\,\frac{\text{sec}^2}{\text{radian}}$$
$$=7.9\,\frac{\text{millisec.}}{\text{degree}/\text{decade}}\,, \qquad (5.3)$$

which agree quite well with the formula obtained by MUNK and REVELLE using a little different model than ours. In their formula, $8.2 \frac{\text{msec.}}{\frac{\text{deg}}{\text{decade}}}$ stands for our 7.9 in the above formula, the difference of which is only trivial. The stationary value of $\omega_c - \omega_m$ is $-0.18°$/year (E.C. BULLARD, 1950). Putting $\Delta(\omega_c - \omega_m)$ in (5.3) equal to 0.18°/decade, that is, one tenth of the stationary value, we have $\Delta T = 1.4$ msec. This means that when the westward drift of the earth's magnetic field is changed by one tenth of its stationary value, the length of a day will be changed by 1.4 millisecond. According to D. BROUWER (1950) (see E. H. VESTINE, 1953, Fig. 5), the length of a day (a year) was increased linearly by 3.8 msec. (1.0 sec) from 1890 to 1915 and decreased by almost the same amount from 1910 to 1930. These changes correspond to those in the westward drift of the magnetic field by 0.3 to 0.4 of its stationary value. These are plausible variations to occurr during the above periods. With the symbol in (5.3) the above results may be written as

$$\Delta T = at, \text{ where } a = \pm \frac{3.8 \text{ msec.}}{20 \text{ year}} \tag{5.4}$$

or

$$\frac{d\Delta\omega_m}{dt} = -\frac{2\pi}{T^2} a = \mp 5.0 \times 10^{-21} \tag{5.5}$$

Multiplying with the moment of inertia $I_m = 7.2 \times 10^{44}$, we get the torque acting on the mantle

$$I_m \frac{d\Delta\omega_m}{dt} = \mp 3.6 \times 10^{24} \text{ c.g.s.} \tag{5.6}$$

We shall now show that moderate fluctuations of the toroidal field near the boundary of the core are adequate to produce the electro-magnetic couple of the above order of magnitude. If the earth's mantle were an insulator, the toroidal field there would vanish and there would be no electromagnetic couple acting on the mantle. It is, however, a kind of mathematical idealization to assume that the mantle is an insulator. For the conducting mantle, the electrical conductivity of which may be much smaller than that of the core, a fraction of the toroidal field in the core will penetrate into the mantle in the way schematically shown in Fig. 4. In spherical coordinates (r, θ, ϕ), the polar axis of which coincides with the rotation axis of the earth, the ϕ component of the electro-magnetic force F_ϕ and the electro-magnetic couple Γ acting on the mantle are given by

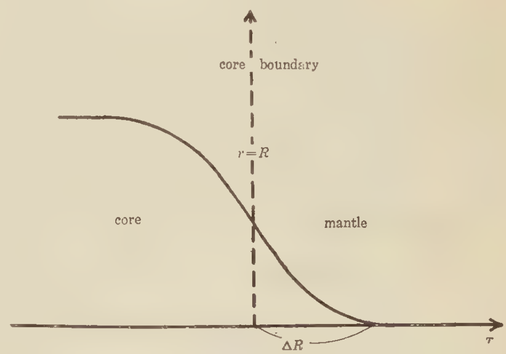

Fig. 4.

$$4\pi F_\phi = \frac{H_\theta}{r\sin\theta}\left[\frac{\partial}{\partial\theta}(H_\phi \sin\theta) - \frac{\partial H_\theta}{\theta\phi}\right] - \frac{H_r}{r\sin\theta}\left[\frac{\partial H_r}{\partial\phi} - \frac{\partial}{\partial r}(rH_\phi \sin\theta)\right], \tag{5.7}$$

$$\Gamma = \int_R^{R+\Delta R}\int_0^\pi\int_0^{2\pi} F_\phi \cdot r^3 \sin^2\theta \, dr\, d\theta\, d\phi\,, \tag{5.8}$$

respectively. In (5.8), the integration is carried out in the region between $r=R$ (the core boundary) and $r=R+\Delta R$, where the toroidal field H_ϕ is appreciable. In the above region, we have

$$\frac{\partial}{\partial r} \gg \frac{1}{r}, \quad \frac{1}{r\sin\theta}, \quad \frac{1}{r\sin\theta\,\partial\phi} \sim \frac{1}{R}$$

$$4\pi F_\phi \sim H_r \frac{\partial H_\phi}{\partial r} \tag{5.9}$$

$$4\pi\Gamma \sim -R^3\int_0^\pi\int_0^{2\pi}(H_r H_\phi)_{r=R} \sin^2\theta\, d\theta\, d\phi \tag{5.10}$$

In order to get a concrete result on the net torque on the mantle, we speciallize the poloidal and toroidal field to be a pure dipole and a pure quadrupole, respectively (W. M. ELSASSER, 1946 and 47), say

$$H_r = b_r P_1(\cos\theta), \quad H_\phi = b_\phi \frac{\partial P_2(\cos\theta)}{\partial\theta} \tag{5.11}$$

where P_1 and P_2 are Legendre functions. Inserting (5.11) into (5.10), we find.

$$\Gamma = \frac{2}{5} R^3 b_r b_\varphi \tag{5.12}$$

Equating (5.12) to (5.6) and putting $R=3.5 \times 10^8$cm, and $b_r=4$ gauss, we have

$$b_\phi = 0.05 \text{ gauss}, \tag{5.13}$$

which is small enough to be a fraction of the toroidal field in the earth's core.

Acknowledgement: The authors should like to express their thanks to Dr. S. K. RUNCORN of Cambridge University for his helpful discussions during his stay in the Department of physics, University of Utah.

References

ALFVEN, H. (1950): Cosmical electrodynamics, Oxford, Clarendon Press.

BROUWER, D. (1952): A new discussion of the changes in the earth's rate of rotatlon, Proc. Nat. Acad. Sci., 38, 1.

BULLARD, E. C. (1949): The magnetic field within the eartn, Proc. R. Soc,, 197, 433.

——— (1954): In press in Phil. Trans.

BULLARD, E. C., FREEDMAN, C., GELLMAN, H. and NIXON, J. (1950): The westward drift of the earth's magnetic field, Phil. Trans. 243, 67.

ELSASSER, W. M. (1946): Induction effects in terrestrial magnetism (Part 1), Phys. Rev., 69, 106. (Part 2), Phys. Rev., 70, 202.

——— (1947): (Part 3), Phys. Rev., 72, 821.

——— (1950): The earth's interior and geomagnetism, Rev. Mod. Phys. 22, 1.

——— and TAKEUCHI, H (1955): In press in Trans. Amer. Geophy. Union.

MUNK, W and REVELLE, R. (1952): On the geophysical interpretation of irregularities in the rotation of the earth, M.N.R.A.S., Geophy. Suppl. 6, 331.

TAKEUCHI, H and SHIMAZU, Y. (1952): On a self-exciting process in magneto-hydrodynamics (Part 1), J. Phys. Earth. 1,1. (Part 2), J. Phys. Earth., 1, 56.

——— (1953): On a self-exciting process in magnetohydrodynamics, J. Geophy. Res., 58, 497.

——— (1954): (Part 3), J. Phys. Earth., 2, 5.

VESTINE, E. H. (1953): On variations of the geomagnetic field, fluid motions, and the rate of the earth's rotation, J. Geophys. Res., 58, 127.

A Simple Method for Calculating the Deflection of the Vertical From Gravity Anomalies, with its Applications to 16 Selected Stations in U. S. A.

By

Chuji TSUBOI* and Akio HAYATU

Department of Geophysics Faculty of Science, Tokyo University Tokyo, Japan

§ **1.** To calculate the ξ- and η-components of the deflection of the vertical at a point situated on the earth's surface from gravity anomalies which are known on the same surface is one of the classical problems in physical geodesy since the day of C.G. STOKES. The well-known formula which was derived by STOKES for this purpose is theoretically beautiful but unfortunately it cannot be used in its original form at present because of our rather poor knowledge concerning the gravity anomaly distribution all over the world, which is essential for the application of that method. Among the many efforts which have since been made to make this method of STOKES competent for practical applications, the derivation of a useful formula by Vening MEINESZ (1928) is to be particularly mentioned. In this formula, the effect of the gravity anomaly in an elementary compartment of the earth's surface upon the deflection of the vertical at a certain point on the same surface is given in terms of the angular distance ψ of the compartment from the point and of its azimuth θ as seen from the same point. The total deflection is obtained if such an elementary effect is integrated over the entire surface of the earth, that is, from 0 to π with respect to ψ and from 0 to 2π with respect to θ.

SOLLIN's table (1947) which was published later is an important contribution to this field of study. In this table are given numerical values of the quantities needed if one wishes to apply MEINESZ's formula to actual problems.

Making use of this table, Donald A. RICE of U. S. Coast and Geodetic Survey (1952) calculated the ξ- and η-components of the deflections of the vertical at 16 stations selected in U. S. A. using free-air anomalies known around them. RICE gave curves showing how the calculated ξ and η tend to their respective definite values according as the limit of integration with respect to ψ is successively increased. Looking at these interesting curves of RICE, it was noticed that the greatest distance taken by RICE in the direction of ψ was a little over 600 km at most, which is only a small fraction of the earth's radius. So far as RICE's calculations are concerned, therefore, no appreciable part seems to have been played by the assumption of the sphericity of the earth which underlies MEINESZ's formula. It naturally occurred to the present writers that it will be interesting to see what will happen if the sphericity of the earth is ignored altogether in this problem. There can be two ways of approach to investigate this, say (A) and (B): the one (A) to solve the plane problem from the outset, while the other (B) to find the approximate expression of MEINESZ's formula in case when ψ is made small. It might well be expected that the two will turn to the same formula after all and that this formula when applied to the actual problems in U. S. A. will give results that differ little from those obtained by RICE with much higher approximations.

§ **2.** First, we shall follow the way (A). Taking the cylindrical co-ordinate system with its origin at the point at which the

---

* The preliminary report was published in Proc. Japan Acad., **30** (1954), 461.

deflection is to be calculated, the gravity potential U (anomalous part only) can be expressed by a FOURIER-BESSEL series such as

$$U=\sum_n\int_0^\infty \frac{B^c_{nk}}{k} J_n(kr)\exp(-kz)dk\cdot\cos n\theta$$
$$+\sum_n\int_0^\infty \frac{B^s_{nk}}{k} J_n(kr)\exp(-kz)dk\cdot\sin n\theta \quad \ldots(1)$$

using customary notations. From (1), the gravity anomaly Δg at any r, θ, and z is given by

$$\Delta g=-\frac{\partial U}{\partial z}=\sum_n\int_0^\infty B^c_{nk}J_n(kr)\exp(-kz)dk\cdot\cos n\theta$$
$$+\sum_n\int_0^\infty B^s_{nk}J_n(kr)\exp(-kz)dk\cdot\sin n\theta\,. \quad \ldots(2)$$

Since $z=0$ at the earth's surface, (2) reduces into

$$\Delta g=\sum_n\int_0^\infty B^c_{nk}J_n(kr)dk\cdot\cos n\theta$$
$$+\sum_n\int_0^\infty B^s_{nk}J_n(kr)dk\cdot\sin n\theta$$
$$=\int_0^\infty B^c_{0k}J_0(kr)dk$$
$$+\int_0^\infty B^c_{1k}J_1(kr)dk\cdot\cos\theta$$
$$+\int_0^\infty B^c_{2k}J_2(kr)dk\cdot\cos 2\theta+\cdots\cdot$$
$$+\int_0^\infty B^s_{1k}J_1(kr)dk\cdot\sin\theta$$
$$+\int_0^\infty B^s_{2k}J_2(kr)dk\cdot\sin 2\theta+\cdots\cdot$$
$$\equiv C_0(r)+C_1(r)\cos\theta+C_2(r)\cos 2\theta+\cdots\cdot$$
$$+S_1(r)\sin\theta+S_2(r)\sin 2\theta+\cdots\cdot \quad \ldots(3)$$

where $C_0(r)\equiv\int_0^\infty B^s_{0k}J_0(kr)dk$,

$$C_1(r)\equiv\int_0^\infty B^c_{1k}J_1(kr)dk\,,$$
$$S_1(r)\equiv\int_1^\infty B^s_{1k}J_1(kr)dk\,,$$
$$\cdots\cdot$$

On the other hand, the ξ- and η-components of the deflection of the vertical at the origin are given if r in the following expressions, (4) and (5), is made to tend to 0.

$$\xi=\frac{1}{g}\left(\frac{\partial U}{\partial r}\right)_{\substack{\theta=0\\z=0}}$$
$$=\frac{1}{g}\left\{\int_0^\infty B^c_{0k}J_0'(kr)\,dk+\int_0^\infty B^c_{1k}J_1'(kr)dk+\cdots\cdot\right\},\quad \ldots(4)$$

$$\eta=\frac{1}{g}\left(\frac{\partial V}{\partial r}\right)_{\substack{\theta=\pi/2\\z=0}}$$
$$=\frac{1}{g}\left\{\int_0^\infty B^s_{1k}J_1'(kr)dk+\cdots\cdot\right\}. \quad \ldots(5)$$

If, in doing this, the following mathematical relations concerning BESSEL functions are noticed,

$$J_1'(0)=\frac{1}{2}\,,\quad J_1'(0)=J_2'(0)=\cdots\cdot=0\,,\quad \ldots(6)$$

the following expressions are obtained,

$$\xi=\frac{1}{2g}\int_0^\infty B^c_{1k}\,dk\,,\quad \ldots(7)$$
$$\eta=\frac{1}{2g}\int_0^\infty B^s_{1k}\,dk\,,\quad \ldots(8)$$

B^c_{1k} and B^s_{1k} being the constants which already appeared in the expression (3). The next task then is to evaluate the integrals in (7) and (8). If the following mathematical relation again concerning a BESSEL function is noticed,

$$\int_0^\infty \frac{J_1(kr)}{r}\,dr=1\,,\quad \ldots(9)$$

the integration with respect to k can be replaced by that with respect to r, thus

$$\int_0^\infty B^c_{1k}dk=\int_0^\infty\int_0^\infty B^c_{1k}\frac{J_1(kr)}{r}\,dk\,dr$$
$$=\int_0^\infty \frac{C_1(r)}{r}\,dr\,,\quad \ldots(10)$$

and similarly

$$\int_0^\infty B^s_{1k}dk=\int_0^\infty \frac{S_1(r)}{r}\,dr\,.\quad \ldots(11)$$

The final expressions for ξ and η are therefore simply

$$\xi=\frac{1}{2g}\int_0^\infty \frac{C_1(r)}{r}\,dr\,,\quad \ldots(12)$$
$$\eta=\frac{1}{2g}\int_0^\infty \frac{S_1(r)}{r}\,dr\,.\quad \ldots(13)$$

These expressions state that what are needed for our purpose are only $C_1(r)$ and $S_1(r)$ which are the first order coefficients when the

gravity anomalies along a circle $r=r$ drawn around the origin are expressed by the FOURIER series of azimuth. So our method for calculating ξ and η practically consists in :

1) drawing a series of concentric circles around the point for which ξ and η are to be calculated,

2) reading the values of Δg along each of the circles at a reasonably many number of points,

3) calculating the first order coefficients $C_1(r)$ and $S_1(r)$ for expressing Δg along each of the circles by the FOURIER series of azimuth,

4) dividing $C_1(r)$ and $S_1(r)$ by corresponding r,

5) integrating $C_1(r)/r$ and $S_1(r)/r$ with respect to r from 0 to ∞ and lastly,

6) dividing the integrals by $2g$.

The integrals $\int_0^\infty \frac{C_1(r)}{r}dr$ and $\int_0^\infty \frac{S_1(r)}{r}dr$ may first appear to diverge at $r=0$, since r is contained in the denominators of the integrands. But this is not actually the case, because $C_1(r)$ and $S_1(r)$ themselves tend to 0 also as the first power of r if r tends to 0. If r is small, $C_1(r)$ is a linear function of r and may be written as

$$C_1(r)=\alpha r\,, \qquad 0\leqq r\leqq R\,, \qquad \ldots.(14)$$

where R is the limit up to which $C_1(r)$ may be regarded to change linearly as αr. The integral from 0 to ∞ may be split into two parts : the one from 0 to R and the other from R to ∞, and may be written as

$$\begin{aligned}\xi&=\frac{1}{2g}\int_0^\infty \frac{C_1(r)}{r}dr\\ &=\frac{1}{2g}\left\{\int_0^R \frac{C_1(r)}{r}dr+\int_R^\infty \frac{C_1(r)}{r}dr\right\}\\ &=\frac{1}{2g}\left\{\alpha R+\int_R^\infty \frac{C_1(r)}{r}dr\right\}\\ &=\frac{1}{2g}\left\{C_1(R)+\int_R^\infty \frac{C_1(r)}{r}dr\right\}. \qquad \ldots.(15)\end{aligned}$$

The value of ξ as given by (15) is evidently finite. The splitting of the integrals into the two parts, however, need not be necessarily exactly at the very limit up to which $C_1(r)$ changes linearly with r. If, by any method, $\xi(R')$ is known to be the total contribution of Δg within $r=R'$, ξ may be written as

$$\xi=\xi(R')+\frac{1}{2g}\int_{R'}^\infty \frac{C_1(r)}{r}dr\,, \qquad \ldots.(16)$$

where R' may take any value. Also

$$\eta=\eta(R')+\frac{1}{2g}\int_{R'}^\infty \frac{S_1(r)}{r}dr\,. \qquad \ldots.(17)$$

§ 3. Now in order to investigate its feasibility, our new method will be applied to calculate the values of ξ and η at the same 16 points in U. S. A. for which RICE's values have been known. The comparison of the values by RICE and by the present writers will make it clear how far the new method can safely be used.

On the map of Δg_0 published by RICE, concentric circles were drawn at every 20km distance interval around the point at which ξ and η are to be calculated. $C_1(r)$ and $S_1(r)$ were calculated from 24 equidistant readings of Δg_0 along each of the circles around the origin by the ordinary harmonic analysis method. As to the values of $\xi(20)$ and $\eta(20)$, however, no accurate estimations have been possible for us for the map published by RICE was unfortunately of too large a scale to admit them. What could be done was only to calculate $\frac{1}{2g}\int_{20}^\infty \frac{C_1(r)}{r}dr$ and $\frac{1}{2g}\int_{20}^\infty \frac{S_1(r)}{r}dr$, according to (16) and (17), and to the calculated values to add the values of ξ (20.09) and η (20.09) obtained by RICE. At the writers' request, the values of ξ (20.09) and η (20.09) were kindly supplied by RICE. He sent also the values for larger distances for reference.

In order to demonstrate the procedures followed in our calculations, the results for Meades Ranch, one of the 16 stations, are given in Table I as an example.

Since the integrands in (16) and (17) contain r in the demominators and $C_1(r)$ and $S_1(r)$ do not increase systematically at large r, the integrals decrease with r. Owing to this reason, the values of $\int_{20}^r \frac{C_1(r)}{r}dr$ and $\int_{20}^r \frac{S_1(r)}{r}dr$ do not change much at larger r, so that the

integrals from 0 to ∞ can be approximated by those from 0 to a reasonably large r. If $\xi(r)$ and $\eta(r)$ have the following meaning:

$$\xi(r)=\xi(20)+\frac{1}{2g}\int_{20}^{r}\frac{C_1(r)}{r}\,dr\,, \qquad \ldots(18)$$

$$\eta(r)=\eta(20)+\frac{1}{2g}\int_{20}^{r}\frac{S_1(r)}{r}\,dr\,, \qquad \ldots(19)$$

Table II will show the values of $\xi(r)$ and $\eta(r)$ found by our calculations for all the 16 points. The values by RICE are also entered in the table for the sake of comparison and are printed in gothic type.

TABLE I

Meades Ranch

ξ-Component

r(km)	$C_1(r)$ (magl)	$C_1(r)/r$ 10^{-9}	$\int_{20}^{r}\frac{C_1(r)}{r}dr$ 10^{-3}	ξ (second)	ξ (second)
0					″
20	0.33	0.17	—	—	−0.28*
40	6.42	1.61	1.77	0.19	−0.09
60	6.40	1.07	4.44	0.47	0.19
80	2.26	0.28	5.79	0.61	0.33
100	3.81	0.38	6.46	0.68	0.40
120	1.12	0.09	6.93	0.73	0.45
140	−2.86	−0.20	6.82	0.72	0.44
160	−2.76	−0.17	6.44	0.68	0.40
180	−4.08	−0.23	6.05	0.64	0.36
200	−7.34	−0.37	5.45	0.57	0.29
220	−10.78	−0.49	4.60	0.48	0.20

* RICE's value

η-Component

r	$S_1(r)$	$S_1(r)/r$	$\int_{20}^{r}\frac{S_1(r)}{r}dr$	η	η
0					″
20	−5.48	−2.74	—	—	−0.96*
40	−3.66	−0.92	−3.65	−0.38	−1.34
60	0.11	0.02	−4.55	−0.48	−1.44
80	4.29	0.54	−4.00	−0.42	−1.38
100	7.49	0.75	−2.71	−0.28	−1.24
120	0.50	0.04	−1.92	−0.20	−1.16
140	−6.16	−0.44	−2.32	−0.24	−1.20
160	−4.11	−0.26	−3.02	−0.32	−1.28
180	−4.34	−0.24	−3.51	−0.37	−1.33
200	−4.39	−0.22	−3.97	−0.42	−1.38
220	−1.37	−0.06	−4.26	−0.45	−1.41

* RICE's value

The values of $\xi(r)$ and $\eta(r)$ are plotted in Fig. 1 against r up to which integrations were extended. It is clearly seen that the values of RICE and ours agree satisfactorily well. At a few points, Little Rock Longitude for instance, however, there is some systematic difference between the two which amounts to 0.3″. The origin of such a difference is not yet clear.

§4. Now the second way of approach (B) will be taken to see what will happen if ϕ is made small in MEINESZ's formula. The formulas as given by MEINESZ are as follows:

$$\xi=-\frac{1}{2\pi g}\int_0^{2\pi}\int_0^{\pi}\Delta g(\phi\theta)\,\frac{df(\phi)}{d\phi}\sin\phi\cos\theta\,d\phi\,d\theta\,, \qquad \ldots(20)$$

$$\eta=-\frac{1}{2\pi g}\int_0^{2\pi}\int_0^{\pi}\Delta g(\phi\theta)\,\frac{df(\phi)}{d\phi}\sin\phi\sin\theta\,d\phi\,d\theta\,, \qquad \ldots(21)$$

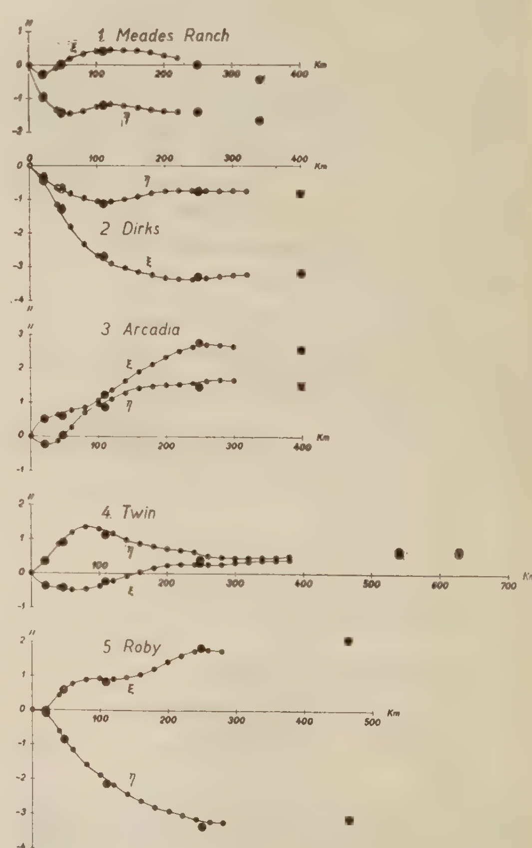

Fig. 1

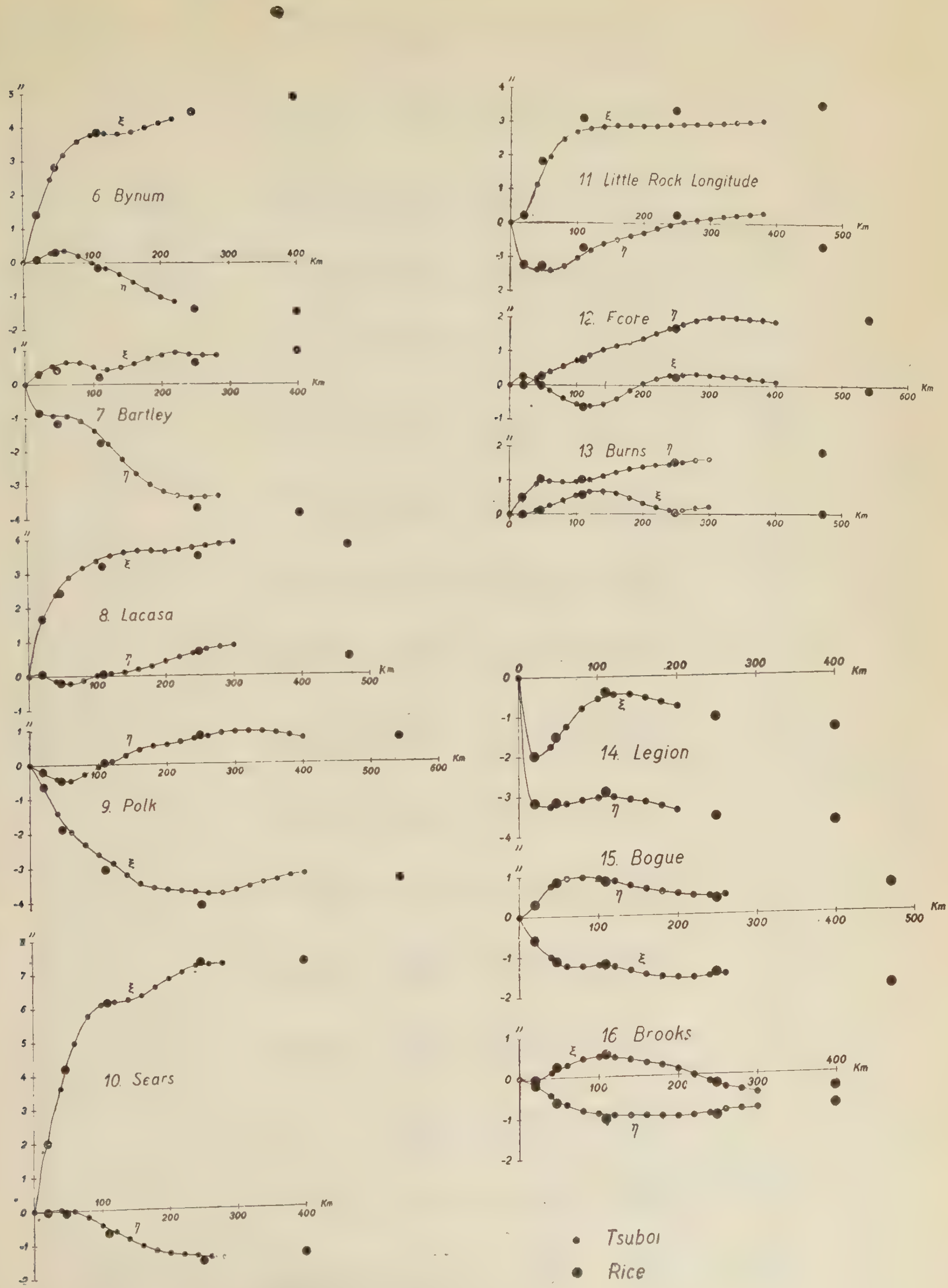
6 Bynum
7 Bartley
8 Lacasa
9 Polk
10 Sears
11 Little Rock Longitude
12 Fcore
13 Burns
14 Legion
15 Bogue
16 Brooks
Km
Tsuboi
Rice

Fig. 1.

TABLE II. Deflections of the Vertical at 16 Stations in U. S. A.

Comparison with RICE's Values (Gothic Type)

r km	1 Meadels Ranch		2 Dirks		3 Arcadia		4 Twin		Roby		6 Bynum		7 Bartley		8 Lacasa	
	ξ	η	ξ	η	ξ	η	ξ	η	ξ	η	ξ	η	ξ	η	ξ	η
20	-0.28	-0.96	-0.44	-0.38	-0.23	0.52	-0.36	0.34	-0.02	-0.10	1.43	0.10	0.31	-0.86	1.68	0.08
40	-0.09	-1.34	-1.16	-0.64	-0.12	0.63	-0.42	0.84	0.44	-0.62	2.48	0.30	0.54	-0.94	2.40	-0.14
47.0	**0.00**	**-1.24**	**-1.30**	**-0.70**	**0.03**	**0.60**	**-0.41**	**0.90**	**0.60**	**0.86**	**2.83**	**0.31**	**0.43**	**-1.16**	**2.45**	**-0.20**
60	0.19	-1.44	-1.82	-0.83	0.26	0.76	-0.48	1.20	0.78	-1.16	3.19	0.35	0.63	-0.95	2.91	-0.19
80	0.33	-1.38	-2.33	-0.96	0.69	0.85	-0.46	1.36	0.90	-1.57	**3.60**	0.19	0.63	-1.09	3.20	-0.10
100	0.40	-1.24	-2.69	-1.06	1.07	0.95	-0.36	1.30	0.93	-1.89	3.79	-0.01	0.51	-1.39	3.38	0.02
109.0	**0.40**	**-1.19**	**-2.71**	**-1.13**	**1.23**	**0.87**	**-0.23**	**1.13**	**0.82**	**-2.13**	**3.85**	**-0.15**	**0.22**	**-1.74**	**3.21**	**0.07**
120	0.45	-1.16	-2.92	-1.08	1.37	1.11	-0.21	1.15	0.92	-2.18	3.84	-0.17	0.43	-1.78	3.54	0.09
140	0.44	-1.20	-3.05	-1.01	1.64	1.29	-0.08	0.99	0.97	-2.42	3.83	-0.36	0.48	-2.23	3.64	0.13
160	0.40	-1.28	-3.17	-0.92	1.90	1.42	0.04	0.87	1.05	-2.64	3.90	-0.57	0.60	-2.65	3.69	0.19
180	0.36	-1.33	-3.25	-0.83	2.14	1.48	0.15	0.78	1.20	-2.81	4.02	-0.80	0.74	-2.98	3.68	0.29
200	0.29	-1.38	-3.33	-0.77	2.34	1.51	0.23	0.72	1.42	-2.93	4.16	-1.02	0.85	-3.19	3.68	0.43
220	0 20	-1.41	-3.38	-0.76	2.52	1.54	0.26	0.68	1.60	-3.03	4.28	-1.15	0.90	-3.31	3.72	0.56
240			-3.38	-0.75	2.65	1.58	0.26	0.62	1.73	-3.14			0.88	-3.37	3.78	0.66
248.0	**0.04**	**-1.41**	**-3.30**	**-0.79**	**2.77**	**1.47**	**0.40**	**0.32**	**1.83**	**-3.36**	**4.49**	**-1.38**	**0.64**	**-3.68**	**3.52**	**0.72**
260			-3.34	-0.75	2.71	1.63	0.26	0.52	1.77	-3.22			0.85	-3.36	3.83	0.75
280			-3.29	-0.76	2.71	1.67	0.28	0.46	1.74	-3.25			0.84	-3.32	3.87	0.84
300			-3.25	-0.77	2.66	1.66	0.32	0.46							3.93	0.88
320			-3.23	-0.78			0.35	0.46								
340							0.38	0.47								
341.2	**-0.42**	**-1.64**														
360							0.40	0.48								
380							0.40	0.50								
399.0			**-3.18**	**-0.82**	**2.56**	**1.51**					**4.93**	**-1.46**	**0.98**	**3.84**		
400																
465.5									**2.06**	**-3.11**					**3.83**	**0.54**
541.5							**0.67**	**0.61**								
628.1							**0.66**	**0.63**								

TABLE II. Continued.

r	9		10		11		12		13		14		15		16	
	Polk		Sears		Little Rock Longitude		Ecore		Burns		Legion		Bogue		Brooks	
km	ξ	η	ξ	η	ξ	η	ξ	η	ξ	η	ξ	η	ξ	η	ξ	η
20	-0.64	-0.19	2.00	-0.01	0.21	-1.24	0.24	0.00	0.00	0.50	-1.97	-3.18	-0.58	0.32	-0.05	-0.17
40	-1.41	-0.41	3.63	0.04	1.12	-1.38	0.09	0.21	0.11	0.89	-1.74	-3.26	-1.01	0.75	0.13	-0.43
47.0	**-1.88**	**-0.45**	**4.21**	**-0.06**	**1.83**	**-1.27**	**-0.01**	**0.26**	**0.12**	**1.02**	**-1.51**	**-3.16**	**-1.11**	**0.87**	**0.26**	**-0.62**
60	-1.97	-0.47	4.96	0.00	1.96	-1.40	-0.15	0.40	0.25	0.98	-1.24	-3.17	-1.24	0.95	0.30	-0.68
80	-2.35	-0.27	5.77	-0.18	2.47	-1.29	-0.38	0.56	0.41	0.96	-0.80	-3.09	-1.23	0.98	0.43	-0.82
100	-2.64	-0.07	6.09	-0.43	2.71	-1.04	-0.55	0.72	0.56	0.96	-0.56	-3.02	-1.22	0.94	0.49	-0.89
109.0	**-3.08**	**0.05**	**6.16**	**-0.68**	**3.14**	**-0.73**	**-0.64**	**0.75**	**0.59**	**1.02**	**-0.38**	**-2.90**	**-1.20**	**0.86**	**0.55**	**-1.03**
120	-2.93	0.09	6.19	-0.65	2.81	-0.80	-0.62	0.89	0.66	1.02	-0.46	-3.02	-1.29	0.86	0.48	-0.95
140	-3.27	0.26	6.24	-0.86	2.86	-0.62	-0.57	1.03	0.67	1.12	-0.47	-3.08	-1.39	0.76	0.42	-0.96
160	-3.53	0.42	6.36	-1.07	2.89	-0.50	-0.40	1.16	0.60	1.23	-0.54	-3.16	-1.47	0.68	0.34	-0.97
180	-3.65	0.52	6.59	-1.22	2.90	-0.40	-0.17	1.27	0.46	1.33	-0.64	-3.25	-1.53	0.60	0.26	-1.00
200	-3.70	0.57	6.83	-1.31	2.89	-0.29	0.04	1.38	0.31	1.39	-0.77	-3.36	-1.57	0.52	0.15	-1.02
220	-3.75	0.65	7.04	-1.36	2.91	-0.16	0.19	1.52	0.18	1.43			-1.57	0.48	0.01	-1.00
240	-3.80	0.74	7.19	-1.41	2.93	-0.05	0.28	1.68	0.10	1.47			-1.54	0.46	-0.16	-0.96
248.0	**-4.15**	**0.82**	**7.31**	**-1.56**	**3.35**	**0.24**	**0.23**	**1.69**	**0.02**	**1.51**	**-1.03**	**-3.53**	-1.45	**0.40**	**-0.22**	**-1.01**
260	-3.84	0.81	7.26	-1.45	2.95	0.04	0.31	1.81	0.10	1.53			-1.51	0.46	-0.31	-0.91
280	-3.83	0.88	7.26	-1.49	2.95	0.10	0.32	1.92	0.15	1.58					-0.41	-0.88
300	-3.77	0.93			2.97	0.15	0.30	1.99	0.20	1.62					-0.47	-0.85
320	-3.67	0.94			2.99	0.19	0.28	2.02								
340	-3.56	0.93			3.02	0.24	5.25	2.01								
341.2																
360	-3.46	0.88			3.04	0.27	0.20	1.98								
380	-3.37	0.81			3.06	0.30	0.15	1.94								
399.0			**7.30**	**-1.37**							**-1.34**	**-3.70**			**-0.33**	**-0.78**
400	-3.30	0.73					0.11	1.89								
465.5					**3.55**	**0.67**			**0.00**	**1.82**			**-1.82**	**0.69**		
541.5	**-3.44**	**0.72**					**-0.14**	**2.00**								
628.1																

$$\frac{df}{d\psi}=\frac{1}{2}\Big[-\frac{\cos\psi/2}{2\sin 2\psi/2}-3\cos\frac{2}{\psi}+5\sin\psi$$
$$+3\sin\psi\log\left(\sin\frac{\psi}{2}+\sin^2\frac{\psi}{2}\right)$$
$$-\frac{3}{2}\,\frac{1+2\sin\psi/2}{1+\sin\psi}\cot\frac{\psi}{2}\,\cos\psi\Big] \quad \ldots(22)$$

in which ψ is the angular distance between a compartment on the earth's sruface where Δg is known and the point at which the deflection of the vertical is to be calculated. θ is the azimuth of the direction that connect the two.

As already stated by SOLLINS (1947), if ψ is small, (22) can be written approximately as

$$\frac{df}{d\psi}=-\frac{1}{\psi^2}-\frac{3}{2\psi}. \quad \ldots(23)$$

Therefore

$$\xi=\frac{1}{2\pi g}\int_0^{2\pi}\int_0^{\pi}\Delta g(\psi\theta)\frac{1}{\psi}\cos\theta\, d\psi\, d\theta, \quad \ldots(24)$$

and

$$\eta=\frac{1}{2\pi g}\int_0^{2\pi}\int_0^{\pi}\Delta g(\psi\theta)\frac{1}{\psi}\sin\theta\, d\psi d\theta. \quad \ldots(25)$$

But since

$$\frac{1}{\pi}\int_0^{2\pi}\Delta g(\psi\theta)\cos\theta\, d\theta=C_1(\psi), \quad \ldots(26)$$

and

$$\frac{1}{\pi}\int_0^{2\pi}\Delta g(\psi\theta)\sin\theta\, d\theta=S_1(\psi), \quad \ldots(27)$$

ξ and η are given by

$$\xi=\frac{1}{2g}\int_0^{\pi}\frac{C_1(\psi)}{\psi}d\psi, \quad \ldots(28)$$

and

$$\eta=\frac{1}{2g}\int_0^{\pi}\frac{S_1(\psi)}{\psi}d\psi, \quad \ldots(29)$$

If, by the reason already stated, the integration with respect to ψ is extended up to ψ instead of up to π, (28) and (29) reduce to

$$\xi=\frac{1}{2g}\int_0^{\psi}\frac{C_1(\psi)}{\psi}d\psi, \quad \ldots(30)$$
$$\eta=\frac{1}{2g}\int_0^{\psi}\frac{S_1(\psi)}{\psi}d\psi. \quad \ldots(31)$$

On the other hand, if the earth's radius is a, $a\psi$ is our r. Thus (30) and (31) may be written as

$$\xi=\frac{1}{2g}\int_0^{r}\frac{C_1(r)}{r}dr, \quad \ldots(32)$$
$$\eta=\frac{1}{2g}\int_0^{r}\frac{S_1(r)}{r}dr, \quad \ldots(33)$$

which are nothing but the expressions already obtained in (12) and (13).

Proceeding to the second approximation, if the term $\frac{3}{2\psi}$ in the expression (23) is retained, ξ and η are given

$$\xi=\frac{1}{2g}\int_0^{\psi}C_1(\psi)\left(\frac{1}{\psi}+\frac{3}{2}\right)d\psi$$
$$=\frac{1}{2g}\int_0^{r}C_1(r)\left(\frac{1}{r}+\frac{3}{2a}\right)dr, \quad \ldots(34)$$
$$\eta=\frac{1}{2g}\int_0^{\psi}S_1(\psi)\left(\frac{1}{\psi}+\frac{3}{2}\right)d\psi$$
$$=\frac{1}{2g}\int_0^{r}S_1(r)\left(\frac{1}{r}+\frac{3}{2a}\right)dr. \quad \ldots(35)$$

The following is the summary of what have been sta'ed,

a) in the first approximation,

$$\xi=\frac{1}{2g}\int_0^{\infty}\frac{C_1(r)}{r}dr,$$
$$\eta=\frac{1}{2g}\int_0^{\infty}\frac{S_1(r)}{r}dr, \quad \ldots(36)$$

b) in the second approximation,

$$\xi=\frac{1}{2g}\int_0^{\infty}C_1(r)\left(\frac{1}{r}+\frac{3}{2a}\right)dr,$$
$$\eta=\frac{1}{2g}\int_0^{\infty}S_1(r)\left(\frac{1}{r}+\frac{3}{2a}\right)dr, \quad \ldots(37)$$

c) in the third approximation.

$$\xi=-\frac{1}{2g}\int_0^{\pi}C_1(\psi)\frac{df(\psi)}{d\psi}\sin\psi\, d\psi,$$
$$\eta=-\frac{1}{2g}\int_0^{\pi}S_1(\psi)\frac{df(\psi)}{d\psi}\sin\psi\, d\psi \quad \ldots(38)$$

The three curves in Fig. 2 show the values of

a) $\frac{1}{2\pi}\int_{0.1}^{\psi}\frac{1}{\psi}d\psi,$

b) $\frac{1}{2g}\int_{0.1}^{\psi}\left(\frac{1}{\psi}+\frac{3}{2}\right)d\psi,$

c) $-\frac{1}{2g}\int_{0.1}^{\psi}\frac{df}{d\psi}\sin\psi\, d\psi,$

as plotted against ψ or r. These are ξ's

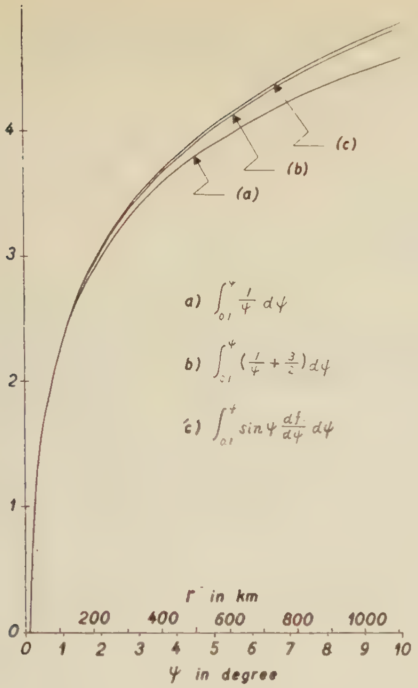

Fig. 2.

when C_1 or S_1 are dropped out in (36), (37) and (38). The three curves are very much similar with each other and it will be understood that even when $C_1(r)$ and $S_1(r)$ do not depend on r, the error in the values of ξ and η introduced by our first approximation is very small and may safely be ignored.

Thus the conclusion is that the formulas (12) and (13) proposed by the present writers are very satisfactory ones and are widely recommended owing to simplicity of use and reasonable accuracy which can be attained by them. But if one wishes to get more accurate results, the formulas (34) and (35) are to be recommended. These formulas give almost the same values as the exact ones do, provided, of course, $C_1(r)$ and $S_1(r)$ do not increase much as r increases.

In conclusion, the present writers wish to thank Dr. Donald A. Rice of U S. Coast and Geodetic Survey for kindly placing his unpublished values of ξ and η at the 16 American stations at the writers' disposal.

Reference

Meinesz: F. A. Vening.:
1928 A formula expressing the deflection of the plumb-line in the gravity anomalies and some formula for the gravity-field and gravity-potential outside the geoid. Kon. Akad. van Wet. Amesterdam, **31**. 315.

Rice: Donald A.:
1952 Deflections of the vertical from gravity anomalies. Bull. géod.. No. 25, 285.

Sollins, A. D.:
1947 Table for the computatien of deflections of the vertical from gravity anomalies. Bull. géod., No. 6, 279.

Equation of State for the Earth's Mantle Based Upon a Theory of Pressure- and Temperature-Dependences of Elasticity of Solid

By

Yasuo SHIMAZU

Institute of Earth's Science, Nagoya University, Nagoya.

The pressure at the center of the earth is generally accepted to be of the order of three millon atmospheres. The temperature there is believed to be several thousand degrees. In order to understand the physical state of materials at such a high pressure and temperature, experimental studies in high pressure and temperature physics are highly useful. But the highest pressure that could be produced so far in the laboratory is about 1.5×10^5 atmospheres, which corresponds to the pressure at 300 km depth of the earth, only 5 per cent of its radius. The highest temperature that could be produced experimentally under high pressures is only a thousand degrees. It must be admitted therefore that these man-made pressure and temperature conditions are as yet rather far from those prevailing in the central parts of the earth. Thus theoretical considerations are naturally needed particulary concerning with the equation of state of materials of which the earth is composed.

The materials of which the earth is composed are in a state of finite initial deformations caused by the high pressure to which they are subjected. From the propagation of seismic waves within the earth and the periodic deformation of the earth by tidal forces, we know that the mantle of the earth is an elastic solid. Seismic waves are propagated through this elastic solid which is under finite initial deformations. Since the velocities of seismic waves are known at any depth of the earth from observations, we can estimate from them the order of initial deformations, if the behavior of elastic waves propagated through the finitely deformed solid be known.

Let us first try to extend the theory of finite elastic strains due to F. D. MURNAGHAN, L. BRILLOUIN, R. KAPPUS, R. FÜRTH, etc. to obtain exact stress-strain relations *(1, II). In our theory, the strain under considerations must be perfectly reversible. We shall study the effect of initial dilatation and shear upon the elastic constants of both isotropic solid (1, III) and cubic crystal (1, V). The case when hydrostatic compression is working is also included in our calculations. Elastic constants are expressed in terms of the initial elastic constants and of the applied initial strains or stresses. For example, the bulk modulus K and rigidity G have the forms as follows:

Isotropic solid

$$K=K_0+\frac{P}{3K_0}\left(12\lambda+8\mu-18l-6m-\frac{2}{3}n\right)+\ldots,$$

$$G=G_0+\frac{P}{3K_0}(3\lambda+9\mu+1.5m+0.5n)+\ldots, \qquad \ldots(1)$$

Cubic crystal

$$K=K_0+\frac{P}{3K_0}\left(4C_{11}+8C_{12}-2D_{111}-4D_{112}-\frac{2}{3}D_{123}\right)+\ldots,$$

$$G=G_0+\frac{P}{3K_0}\left(C_{11}+2C_{12}+7C_{44}-\frac{D_{144}}{2}-D_{166}\right)+\ldots, \qquad \ldots(2)$$

where K_0, G_0 are their respective initial values and P is the applied hydrostatic pressure. (l, m, n) and $(D_{111}, \ldots)$ are the elastic constants of the second order.

* (1, II) denotes Chapter II of Paper 1. The present paper is the summary of that paper.

Now We shall discuss the propagation of elastic waves through an isotropic solid under initial strains (1, IV). Since anisotropy is introduced when initial strains are applied, velocities of the waves become dependent upon the direction of propagation. Isotropy is kept only for hydrostatic strain. The initial (unstrained) coordinates will be denoted by (a, b, c) and the final (strained) coordinates (of the same particle) by (x, y, z). When uni-axial tension is applied along a-axis, the displacement is expressed by $(x-a=\alpha a,\ y-b=-\beta b,\ z-c=-\beta c)$. In this case, the velocities of elastic waves along several special directions of propagation are as follows:

TABLE I

direction cos. of the wave propagation	displacement of a particle corresponding to the wave	Velocity	Remarks
$q_1=0$	$l_1=1$	$W_D=V_s\left\{1+\varepsilon\left(\frac{-\lambda-3\mu-0.5m}{2\mu}\right)+\varepsilon'\left(\frac{-2\lambda-3\mu-m-0.5n}{2\mu}\right)\right\}$	purely transversal wave
	$l_1=0,\ \frac{l_2}{l_3}=\frac{q_2}{q_3}$	$W_{B'}=V_p\left\{1+\varepsilon\left(\frac{-3\lambda-6l+2m}{2(\lambda+2\mu)}\right)+\varepsilon'\left(\frac{-10\lambda-14\mu+12l+2m}{2(\lambda+2\mu)}\right)\right\}$	quasi-longitudinal wave
	$l_1=0,\ \frac{l_2}{l_3}=-\frac{q_3}{q_2}$	$W_E=V_s\left\{1+\varepsilon\left(\frac{-\lambda-0.5m-0.5n}{2\mu}\right)+\varepsilon'\left(\frac{-2\lambda-6\mu-m}{2\mu}\right)\right\}$	quasi-transversal wave
$q_2=0$	$l_2=1$	$\bar{W}_E=W_E+V_s\left\{\varepsilon\left(\frac{-3\mu+0.5n}{2\mu}\right)+\varepsilon'\left(\frac{3\mu-0.5n}{2\mu}\right)\right\}q_1^2$	polarized wave
	$l_2=0$	$\bar{W}_{B'}=W_{B'}+V_p\left\{\varepsilon\left(\frac{-4\lambda-14\mu-2m}{2(\lambda+2\mu)}\right)+\varepsilon'\left(\frac{4\lambda+14\mu+2m}{2\lambda+2\mu}\right)\right\}q_1^2$	polarized wave
		$\bar{W}_D=W_D$	
$q_3=0$	Similar to the case $q_2=0$ by putting q_2 for q_3.		

In Table I, $V_p=\sqrt{\frac{\lambda+2\mu}{\rho_0}}$ and $V_s=\sqrt{\frac{\mu}{\rho_0}}$ are the initial values of velocities. ε and ε' are defined by $(1+\alpha)^2=(1-2\varepsilon)^{-1}$, $(1-\beta)^2=(1-2\varepsilon')^{-1}$. Only the first order terms of ε and ε' are shown in Table I, whereas our calculation includes the second orders. Putting $\varepsilon=\varepsilon'=-f$, the results obtained above become in the case of hydrostatic compression:

$$\rho W_p^2=\lambda+2\mu+f\,(16\lambda+20\mu-18l-4m)+f^2(62.5\lambda+65\mu-207l-55m-3n),$$

$$\rho W_s^2=\mu+f\,(3\lambda+9\mu+1.5m+0.5n)+f^2(15\lambda+27.5\mu-27l+1.5m+2.5n),$$

$$\rho=\rho_0(1+2f)^{3/2} \quad \ldots\ldots(3)$$

For the finite plane shear which can be denoted by $(x-a=\tau b,\ y-b=\tau' a,\ z-c=0)$, the results similar to those in Table I are obtained as follows :

TABLE II

direction cos. of the wave propagation	displacement of a particle corresponding to the wave	Velocity
$q_1=1$	$l_3=0$, l_1, l_2 : complicated	$W_{\mathrm{I}}=V_p$; $W_{\mathrm{II}}=V_s$
	$l_3=1$, $l_1=l_2=0$	$W_{\mathrm{III}}=V_s$
$q_2=1$	similar to the case $q_1=1$ by putting τ for τ'	
$q_3=1$	$l_3=1$	$W_1=V_p$
	$l_3=0$, $\dfrac{l_1}{l_2}=+1$	$\dfrac{W_{\mathrm{II}}}{W_{\mathrm{III}}}=V_s\left[1\pm\left(\dfrac{-3\mu+0.5n}{\mu}\right)(\tau+\tau')\right]$
$q_3=0$	$l_3=0$, l_1, l_2 : complicated	$W_{\mathrm{I}}=V_p\left[1+\left(\dfrac{-2\lambda-7\mu-m}{\lambda+2\mu}\right)(\tau+\tau')q_1q_2\right]$; $W_{\mathrm{II}}=V_s$
	$l_3=1$	$W_{\mathrm{III}}=V_s\left[1+\dfrac{1}{2}\left(\dfrac{-3\mu+0.5m}{\mu}\right)(\tau+\tau')q_1q_2\right]$

It can be seen that the effects of initial strains upon velocities of waves are small. Variation in velocities will be 1 per cent at most when a linear extension of 0.5 per cent or a shear of 40′ is applied. The range of perfect elasticity of materials of which the upper part of the earth is composed is much less than 0.5 per cent for extension. If any variation in velocities be detected before or after great earthquakes as some-one insist the cause for it is not likely due to the change in working pressure, and therefore it is beyond of the present study.

As we see in (1), (2), or Tables I, II, second order elastic constants appear in our calculations. All high pressure experiments to date to determine the orders of magnitude of these constants have not been sufficiently accurate except for bulk modulus. The only way left to predict the order of magnitude of second order constants is to develop a theory of finite strain for crystats (1, V). For crystals with a given lattice structure and with a given force law between constituent atoms, the potential energy is a known function of deformation (=strain invariants) and the elastic constants of any order can be expressed as the coefficients of each term in this function. The potential energy between two particles of the lattice will be assumed to be of the form

$$\varphi(r)=u\frac{nm}{n-m}\left[-\frac{1}{m}\left(\frac{r_0}{r}\right)^m+\frac{1}{n}\left(\frac{r_0}{r}\right)^n\right], \quad \ldots\ldots(4)$$

$$(n>m)$$

By thermodynamical considerations, we get

$$\left(\frac{\partial K}{\partial P}\right)_{P=0}=\frac{m+n+6}{3} \quad \ldots\ldots(5)$$

$\left(\frac{\partial K}{\partial P}\right)_{P=0}$ can also be obtained from the theory of finite strains as

$$\left(\frac{\partial K}{\partial P}\right)_{P=0}=4-\frac{2}{3}\frac{3D_{111}+D_{123}+6D_{112}}{C_{11}+2C_{12}}. \quad \ldots(6)$$

It is confirmed by BRIDGMAN's experiments that $\left(\frac{\partial K}{\partial P}\right)_{P=0}$ for both single and polycrystals is about 4 for 24 elements and 4-5 for 40 compounds. These results lead us to the conclusion

$$6<m+n<9 \quad \ldots(7)$$

from (5). Then we get

$$\frac{2D_{111}+4D_{112}+\frac{2}{3}D_{123}}{4C_{11}+8C_{12}}\sim 0 \quad \ldots(8)$$

in (1). From the above considerations, we see that the second order term in bulk modulus is nearly equal to zero. Unlike for the bulk modulus, the second order term for rigidity cannot be obtained by such thermodynamical considerations. Calculating the lattice sums for face-centered cubic crystals, we get the second order term for rigidity as

$$0.40>\frac{-\frac{D_{144}}{2}-D_{166}}{C_{11}+2C_{12}+7C_{44}}>0.13, \quad \ldots(9)$$

corresponding to $6<m+n<9$. Of course, $\frac{\partial K}{\partial P}$ can also be obtained by calculating the lattice sums, and this gives the same result as (5). Simple and body-centered cubic crystals are found to be mechanically unstable for such comparatively small values of m and n. We see that the contribution of the second order term to rigidity is much larger than that to bulk modulus. Although experimental values for $\left(\frac{\partial G}{\partial P}\right)_{P=0}$ are scattered, we may say $4<m+n<12$. Then we obtain

$$0<\frac{-18l-6m-\frac{2}{3}n}{12\lambda+8\mu}<0.25,$$

$$0.40>\frac{1.5m+0.5n}{3\lambda+9\mu}>0.13 \quad \ldots(10)$$

for isotropic solid by comparing (1) and (2).

Since we get the equation of state of solid as

$$P=\frac{1}{2}\left[\left(\frac{V_0}{V}\right)^{7/3}-\left(\frac{V_0}{V}\right)^{5/3}\right]\left[C_{11}+2C_{12}\right.$$
$$\left.+\frac{1}{2}(3D_{111}+D_{123}+6D_{112})\left\{1-\left(\frac{V_0}{V}\right)^{2/3}\right\}+\ldots\right] \quad \ldots(11)$$

from the theory of finite strains, we may say that

$$P\sim\left[\left(\frac{V_0}{V}\right)^{7/3}-\left(\frac{V_0}{V}\right)^{5/3}\right], \quad \ldots(12)$$

and $m=2$, $n=4$, when $\frac{3D_{111}+D_{123}+6D_{112}}{2(C_{11}+2C_{12})}\sim 0$ from (8).

Equation of state for a simplified model of the earth's mantle in accordance with the theory of finite strains will be discussed as follows (1, VI). If the hydrostatic equilibrium is satisfied within the earth, density-pressure ($\rho-P$) relation is found from

$$\frac{\partial P}{\partial \rho}=W_P^2-\frac{4}{3}W_S^2=\phi=\frac{K_S}{\rho}, \quad \ldots(13)$$

where K_s denotes the adiabatic bulk modulus. The relation between the adiabatic modulus and the isothermal modulus in (1) can be obtained by thermodynamical considerations. (13) is the fundamental equation in BULLEN's density distribution and we adopt it here too. In this model, chemical homogeneity is also assumed. The physical state of a material can be described by four variables: pressure P, density ρ, temperature T, and chemical concentration n (SHIMAZU, Y: 1952). The equation of state is usually expressed by $\rho=\rho(P,T,n)$. Although there are many studies on the constitution of the earth based upon the density distribution, we must note that observable quantities within the earth are W_P and W_S, but not ρ. We shall discuss directly the earth's model based upon W_P and W_S. From (13) we get

$$\frac{\partial K_S}{\partial P}=1-\frac{1}{g}\frac{d\phi}{dr}. \quad \ldots(14)$$

Using seismic data, we see that $\frac{\partial K}{\partial P}$ is nearly

constant (=3.7) for the layer between 1,000—2,900 km depths. The layer shallower than 1,000 km depth is not in this consideration on account of an apparent scattering in the distribution of $\frac{\partial K_S}{\partial P}$. Then we get $m+n\sim 5$ for the deeper layer of the mantle. Considering the effect of temperature gradient, $m+n$ may become slightly larger, say, $m+n\sim 6$. Thus the effect of second order elastic constants of the constituent material may be sufficiently small in virtue of (8), and the equation of state can be expressed by (12). Assumption of chemical homogeneity is also valid for this layer.

Even if the second order terms in ϕ are nearly epual to zero, those in W_P and W_S may be large (1, VI). Calculating initial strain (f)-depth relation and using observed W_P, W_S distribution, we can derive W_P, W_S $-f$ relation. We see that W_P and W_S are linear functions of f. Comparing these results with (3), we get

$$\lambda=1.01\,\mu,$$
$$18l+4m=9.46\,\mu$$
$$1.5m+0.5n=-4.76\,\mu. \quad \ldots(15)$$

We see that the effect of second order term upon the shear wave is greater than upon the longitudinal wave.

In the preceding discussion, we see that the pressure is the predominant variable in the deeper layer of the mantle. It has been proved that the shear wave cannot be propagated through the core of the earth. This may lead to the fact that fusion takes place within the core. Melting of materials there is related to the temperature. We shall study, for the next step, the effect of temperature upon the elastic constants of solid. Our main object is to calculate the temperature dependence of rigidity of a solid.

Now we shall study the behavior of an isotropic solid using Debye's approximation (1, IX). We may safely say that the mantle of the earth is in a high temperature region, that is, the temperature there is far above the Debye's characteristic temperature $\Theta_D\left(=\frac{h\nu_0}{k}\right)$ of its constituent materials. ν_0 in the above expression is the Debye's characteristic frequency. Then the free energy density (=the elastic potential energy density) is given by

$$\phi=\phi_0+\frac{3RT}{V}\log\frac{\Theta_D}{T}, \quad \ldots(16)$$

where ϕ_0 and Θ_D are expanded by $e(=-f$ in(3)) using (3). Grüneissen's parameter γ_G is given by $\gamma_G=-\frac{d\log\nu_0}{d\log V}$. We get $e=\frac{\gamma_G RT}{KV_0}$ because $\frac{\partial\phi}{\partial e}$ must vanish because of the assumption that solid is in the state of zero stress at any temperature under no external force. The mean value of the coefficient of thermal expansion is then found as $\alpha=\frac{3e}{T}=\frac{3R\gamma_G}{KV_0}$ which gives the Grüneissen's equation of state. $\left(\frac{\partial K}{\partial T}\right)_P$ is obtained from

$$\left(\frac{\partial K}{\partial T}\right)_P=\left(\frac{\partial K}{\partial T}\right)_e+\left(\frac{\partial K}{\partial e}\right)_T\left(\frac{\partial e}{\partial T}\right)_P.$$

Finally we get

$$\gamma_G=1.833, \quad \left(\frac{\partial K}{\partial T}\right)_P=-19.69\frac{R}{V_0} \quad \ldots(17)$$

for $\lambda=\mu$ at $T=0$. We notice that γ_G is a function of volume while it is independent of temperature. Bulk modulus decreases linearly under rising temperature at high temperature region.

Suppose an isotropic solid is placed in a rigid tube. Raising the temperature, the solid will be expanded in one direction. Therefore, thermal strain is of the unilateral dilatation type. Calculations of velocities of elastic waves propagated through the solid with finite unilateral dilatation are given in Table I. Using these result, we obtain the temperature dependence of $\lambda+2\mu$. As it is very tedious to calculate the temperature dependence of rigidity using the finite strain theory for shear, we obtain $\left(\frac{\partial G}{\partial T}\right)_P$ by combining the results for $\lambda+2\mu$ and $K=\lambda+\frac{2}{3}\mu$.

The result of the calculation is (1, IX)

$$\left(\frac{\partial \lambda}{\partial T}\right)_P = -4.18\,\frac{R}{V_0},\quad \left(\frac{\partial \mu}{\partial T}\right)_P = -23.27\frac{R}{V_0} \qquad \ldots.(18)$$

for $\lambda=\mu$ at $T=0$, and finally

$$\left(\frac{\partial K}{\partial T}\right)_P = -19.69\,\frac{R}{V_0},\quad \left(\frac{\partial K_S}{\partial T}\right)_P = -9.61\,\frac{R}{V_0},$$
$$\left(\frac{\partial G}{\partial T}\right)_P = -23.27\,\frac{R}{V_0}. \qquad \ldots.(19)$$

Our result shows that the rigidity decreases linearly and reduces to about one-half at the so-called melting point. There are many experimental works on the temperature dependence of elasttc constants. Attention has specially been given to the decrease in rigidity under rising temperature in relation to the study of the fusion mechanism. It has been shown that rigidity reduces to about one-half at several degrees below the melting point beyond which it decreases rapidly to nearly zero. That rapid decrease near the melting point and its relation to the mechanism of fusion are beyond the scope of our study.

From the equation

$$\frac{d}{dr}\left(\frac{K}{G}\right) = -\rho g\left[\frac{\partial}{\partial P}\left(\frac{K}{G}\right)\right]_T + \left[\frac{\partial}{\partial T}\left(\frac{K}{G}\right)\right]_P \frac{dT}{dr}, \qquad \ldots.(20)$$

we find (1, X) that the effect of temperature upon K or G, for 1,000—2,900 km depths, is only 5 per cent or 13 per cent respectively of the effect of pressure. In that calculation $\frac{dT}{dr}$ is assumed to be adiabatic. Adiabatic temperature gradient is obtained as shown later. If the melting point gradient obtained by R. J. UFFEN, which gives thc maximum temperature gradient, is inserted into $\frac{dT}{dr}$, the effect for K and G is nearly 16 per cent and 40 per cent respectively. However, when we examine the thermal state of the earth's interior, it is likely that the thermal convection exists within the mantle, and that the actual temperature gradient would be nearly equal to adiabatic. Thus we see that our model for 1,000—2,900 km depths is valid. It is not confirmed, however, that our model is valid for shallower mantle. Finally we find that the temperature at which the rigi. dity of a rock reduces to one-half is 6,000 °K at the pressure of the core boundary, whereas it is 1,790°K at the surface. At the core boundary, the adiabatic gradient gives the temperature of 1,600—3,200°K corresponding to the assumed temperature of 1,000—2,000°K near the surface.

If the mean atomic weight of the constituent material is assumed, DEBYE's characteristic frequency ν_0 and GRÜNEISEN's parameter γ_G at any depth can be estimated from seismic data. We take $A=20$ from the mean value of rocks. Further, the distributions of the coefficient of thermal expansion α and the adiabatic temperature gradient $\left(\text{from } \frac{d \log T}{dr} = -\frac{\alpha}{C_p}g\right)$ can also be estimated. There is a comparatively rapid decrease of α with depth. Using the distribution of ν_0, we can estimate the dlstributions of some other physical quantities. There may be an increase in electrical conductivity $\left(\propto \exp\left(-\frac{W}{RT}\right),\ W=W(\nu_0)\right)$ and a decrease in viscosity $\left(\propto \exp\left(\frac{W'}{RT}\right)\right)$ with the depth. Thermal conductivity $(\propto \rho^{1/3}\nu_0)$ may increase moderately to reach 2.3 times the surface value at the bottom of the mantle.

Is it likely that the thermal convection exists within the mantle? To find one answer, we study energy transfer within the mantle (1, X). According to a theory of the origin of the geomagnetic field, (TAKEUCHI, H. and SHIMAZU, Y: 1952–54), the heat flow from the core to the mantle is of the order of 2×10^{-6} cal/cm² sec at the bottom of the mantle. The heat which is transported through the mantle by thermal conduction may be, at most, of the order of 10^{-6} cal/cm² sec. Once the convection takes place, the amount of heat transfer may reach 3×10^{-6} cal/cm² sec. This result suggests that

the convection is sufficient but the conduction is insufficient to transfer the heat energy generated in the core to the surface of the earth. Worthly to be noted is that the mean heat flow through the surface of the earth outward is of the order of 1×10^{-6} cal/cm^2 sec.

References

(1) Yasuo SHIMAZU:
"Equation of state of materials composing the earth's interior", Jour. Earth Sci., Nagoya Univ., Vol. 2, (1954), 15-93; 95-172.

(1, I) Chapter 1. General introdnction.

(1, II) Chapter 2. Theory of finite elastic strains.

(1, III) Chapter 3. Effects of initial strains upon the elastic parameters of isotropic solids.

(1, IV) Chapter 4. Propagation of elastic waves in a medium under finite initial strains.—An application to the problem of seismology.

(4, V) Chapter 5. Theory of finite elastic strains of cubic crystals and third order elastic constants.

(1, VI) Chapter 6. Equation of state for a simplified model of the earth's mantle in accordance with the theory of finite strains.

(1, VII) Chapter 7. Equation of state of solid at high temperature derived from statistical machanics.

(1, VIII) Chapter 8. Thermal dependence of elastic constants of a cubic crystal.

(1, IX) Chapter 9. Thermal dependence of elastic constants of an isotropic solid.

(1, X) Chapter 10. Grüneisen's parameter and the temperature distribution within the earth.

(2) Yasuo SHIMAZU:
"Density distribution and concentration of heavy materials in the mantle of the earth", Jour. Phys. Earth, Vol. 1, (1952), 11-17.

(3) Hitoshi TAKEUCHI & Yasuo SHIMAZU:
"On a self-exciting process in magneto-hydrodynamics", (I), Jour. Phys. Earth, Vol. 1, (1952), 1-9; (II), ibid., Vol. 1, (1952), 57-64; (III), ibid., Vol. 2, (1954), 5-12.

Hitoshi TAKEUCHI & Yasuo SHIMAZU:
"On a self-exciting process in magneto-hydrodynamics", Jour. Geophys. Res., Vol. 58, (1953), 497-518.

Hitoshi TAKEUCHI & Yasuo SHIMAZU:
"Convective fluid motions in a rotating sphere", Jour. Phys. Earth, Vol. 2, (1954), 13-26.

Quantitative Prediction of Earthquake Occurrence as Stochastic Phemomena

By

Keiiti AKI

Geophysical Institute, Faculty of Science, Tokyo University, Tokyo, Japan.

Abstract

In this paper, the occurrence of earthquakes is regarded as a stochastic process and to it the theory of stochastic process is applied with an intention to investigate the possibility of the earthquake predictions by this procedure. At first the theory of prediction is roughly sketched. Discussions follow as to what quantity in the phenomena should be taken as the stochastic variable. As the result $[n(t)-E(n(t))]$ is found to be the most appropriate quantity, where $n(t)$ is the number of earthquakes belonging to specified range of magnitude which occurred in a specified area from $t=0$ to $t=t$ and $E(n(t))$ is the average of $n(t)$ at $t=t$. The theory is applied to conspicuous earthquakes occurred near Shiriyasaki between 1900 and 1945, and the occurrence is predicted or extrapolated up to 1947 and compared with the actual.

Introduction—One of the essential problems in Seismology is to establish the law of occurrence of earthquakes which, with the knowledge based on the present and past natural conditions concerned, can give us an information about their future occurrences. This law, different from the deterministic ones in various other sciences, must have a statistical character for the present, because of our present ignorance about the conditions by which the occurrence of earthquakes is influenced and the deterministic laws by which it is governed under such conditions. It is hoped that the statistical method used in the present paper will give us a certain macroscopic information about the phenomena which can not otherwise be obtained for the present.

Many statistical studies have been made about the occurrence of earthquakes since the beginning of this century. The outline of these studies can be seen in the text-book by MATUZAWA,(1) for instance. In these studies, two sorts of method are important; the one is to regard the occurrence of earthquakes as a MARKOV process as is done in the papers by WATANABE,(2) KITAGAWA(3) and others. The other is to establish the periodicity in the sequence of occurrence of earthquake as is done by MATUZAWA(4).

The method used in the present paper is somewhat different from the above two and is applicable to a stationary stochastic process. Therefore the occurrence of earthquakes to be studied by this method must be the one which can be regarded as stationary. But this is not always possible. For example, a series of after-shocks occurring exactly according to the OMORI's law can ot be regarded as stationary. Another example is the so called trend, although this can be a part of a phenomenon which, if observed long enough, may well be a stationary one. In the former case, however, we can regard the total series as an element of a stationary process if the time interval is taken long enough and if we give up to get any information about the process occurring within that time interval. In the latter case, we can pick up the stationary process only, by eliminating the trend from the total process.

The material on which the studies will be made in the present paper is the series of 210 conspicuous earthquakes which occurred

in the area of about $3\times10^4\mathrm{km}^2$ near Shiriya-saki between 1900 and 1945. The data were supplied by the Central Meteorogical Obsesvatory, Tokyo[5].

Theory of prediction—Regarding a stationary stochastic process we have the following theorems[6].

Theorem (1) A stationary stochastic process $X(t)$, of which the mean value is zero, can be seperated into two parts as

$$X(t)=U(t)+V(t), \tag{1}$$

wherc $U(t)$ has a continuous spectrum only and can be expressed as

$$U(t)=\sum_{k=0}^{\infty} b_k Y(t-k). \tag{2}$$

Here $Y(t)$ is a stochastic process of which the mean value is zero and its every autocorrelation coefficient is zero.

$V(t)$ is a singular process which has a discontinuous spectrum only.

Theorem (2) When there is no singular process in $X(t)$, we have

$$X(t)=\sum_{k=0}^{\infty} b_k Y(t-k) \tag{3}$$

$$Y(t)=\sum_{k=0}^{\infty} a_k X(t-k) \tag{4}$$

where

$$\sum_{i=0}^{\infty} a_i b_{k-i}=0 \quad (k=1, 2, 3, \ldots.), \tag{5}$$

$$a_0=b_0=1 \text{ and } a_k=b_k=0 \ (k<0).$$

The derivation of these theorems is in the papers about time series, e. g., OGAWARA's[6]. Hereafter we shall consider the case when there is no singular process in $X(t)$, for the correlogram of our time series which will be given later has no definite singularity.

It is important that the value of $X(t)$ for the time t can be expressed as a weighted sum of a series of $Y(t)$ for the time previous to t, where the mean values of $X(t)$ and $Y(t)$ are both zero and every autocorrelation coefficient of $Y(t)$ is zero, that is,

$$\frac{E(Y(t)Y(t-k))}{D^2(Y)}=0 \quad (k=1, 2, 3, \ldots.). \tag{6}$$

Here $D^2(Y)$ is the variance of $Y(t)$ and $E(\ )$ is the operation to average the term in the bracket.

Inserting (4) into (6), we have

$$E(Y(t)X(t-k))=D(Y)D(X)\sum_{i=0}^{\infty} a_i \rho_{k-i} = 0 \quad (k=1, 2, 3, \ldots.), \tag{7}$$

where $\rho_k=\dfrac{E(X(t)X(t-k))}{D^2(X)}$. This is the autocorrelation coefficient of $X(t)$, and can be expressed by the relation (3) as follows,

$$\rho_k=\frac{\sum_{i=0}^{\infty} b_i b_{i+k}}{\sum_{i=0}^{\infty} b_i^2} \tag{8}$$

The relations (7) and (8) are important for obtaining the prediction operators a_k and b_k from the known quantity ρ_k.

The predicted or expected value for the time $t+k$ $(k=1, 2, 3, \ldots.)$ is the conditional mean value of

$$X(t+k)$$

under the conditions

$$X(t-i)=x_{t-i} \qquad (i=0, 1, 2, 3, \ldots.),$$

where x_{t-i} is the actual or sample value of the process for the time $t-i$.

If x_{t-i} is known, y_{t-i} can be obtained by the formula (4) as follows,

$$y_{t-i}=\sum_{k=0}^{\infty} a_k x_{t-i-k} \tag{9}$$

Then the conditional average of $X(t+k)$ is given by the following formula,

$$\begin{aligned} E_c(X(t+k)) &= E\left(\sum_{i=0}^{k-1} b_i Y(t+k-i)+\sum_{i=0}^{\infty} b_{k+i}\, y_{t-i}\right) \\ &= \sum_{i=0}^{\infty} b_{k+i}\, y_{t-i} \end{aligned} \tag{10}$$

Otherwise, from the formula (4), we have

$$E_c(X(t+k)) = -\sum_{i=0}^{k-1} a_i E_c(X(t+k-i))-\sum_{i=0}^{\infty} a_{k+i}\, x_{t-i} \tag{11}$$

In this case the expectation is carried out step by step. (10) and (11) were called the extrapolation formulas of the first and second kinds in the work by OGAWARA[6].

The accuracy of prediction is measured by its variance

$$(12)\qquad E[(X_e(t+k)-E_e\{X(t+k)\})^2] = \sum_{i=0}^{k-1} b_i^2 D^2(Y) = \sum_{i=0}^{k-1} b_i^2 \kappa^2 D^2(X)$$

where

$$\kappa^2=\frac{D^2(Y)}{D^2(X)}=\sum_{i=0}^{\infty} a_i \rho_i$$

In the practical application of the above theory, we obtain a_k and b_k not from the formulus (8) and (9) but by regarding the process of autoregressive scheme as follows. A stochastic process $X(t)$ of autoregressive scheme is one which satishes the following relation

$$(13)\qquad \sum_{i=0}^{h} a_i X(t-i)=Y(t),$$

where h is finite, and $Y(t)$ is as before the process of which every autocorrelation coefficient is zero. Then we have

$$(14)\qquad \sum_{i=0}^{h} a_i \rho_{k-i}=0 \qquad (k=1, 2, 3, \ldots)$$

Thus, when we have the correlogram of the time series, we choose a proper value h such that the assumed correlation function of this scheme of rank h chosen may interpret the whole correlogram, and solve the system of initial h equations in (14) and obtain a_k. And then b_k is calculated from (5).

Refering to the above theory, WOOD[7] dealed with the time series in a similar way as above, and also WIENER[8] referred to the discrete time series in his book "Cybernetics".

Application.—Before the application of the above theory to our problem, it must be considered what quantities in the phenomena should be taken as the stochastic variable. The idea of taking the energy of earthquakes as the variable seems reasonable because it has an obvious physical meaning. But the energies of large and small earthquakes differ considerably and the largest earthquakes play a predominant role. It is therefore difficult to regard the series of energy as stationary during our period of observation. For the present, therefore, more preferable one is the number of earthquakes occurring in a specified area in a specified range of magnitude. In the present paper, the following three expressions based on this number are discussed and the above theory is applied to the best of them:

(a) series of time interval between successive earthquakes.

(b) series of number of earthquakes per unit time e.g. per month.

(c) $n(t)-E(n(t))$
where $n(t)$ is the number of earthquakes between $t=0$ and $t=t$ and $E(n(t))$ is the average of $n(t)$ at $t=t$. If α is the average number of earthquakes per unit time, $E(n(t))$ is equal to αt.

In the followings, these three time series will be constructed from the data referred to before and their statistical property and the applicability of the theory of prediction will be examined.

(a) Series of time interval between successive earthquakes.

The principal probability density of this time series is shown in Fig. 1. It seems to be in a good accordance with the exponential density curve also shown in the figure. But, for the effective use of our method, it is required that the distribution function should be normal i. e. Gaussian. Therefore our series must be transformed into a new one of which the distribution function is normal, and the correlogram of this new series must be formed. The result is given in Fig. 2. The figure shows that in the correlogram for the first period (1900–1910), the hypothesis that all the autocorrelation coefficients are zero cannot be rejected on the 10% level of significance except one which may be assumed as positive. This is the same in the

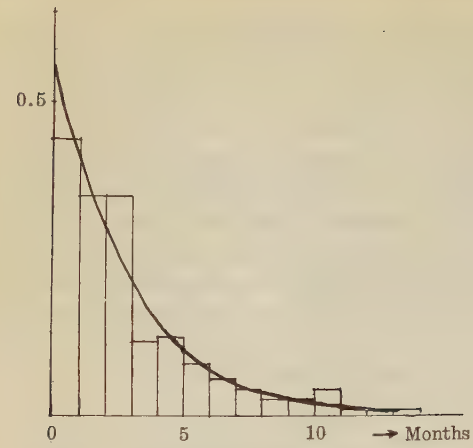

Fig. 1. Principal probability density of the series of time interval

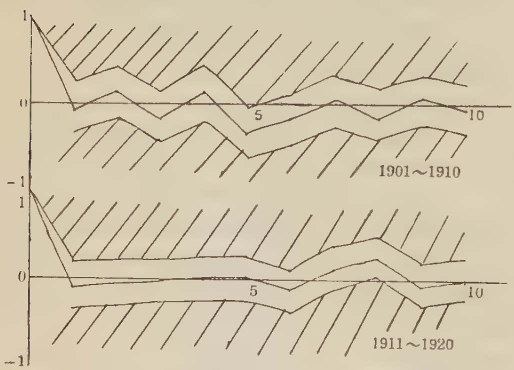

Fig. 2. Correlograms of the series of time interval

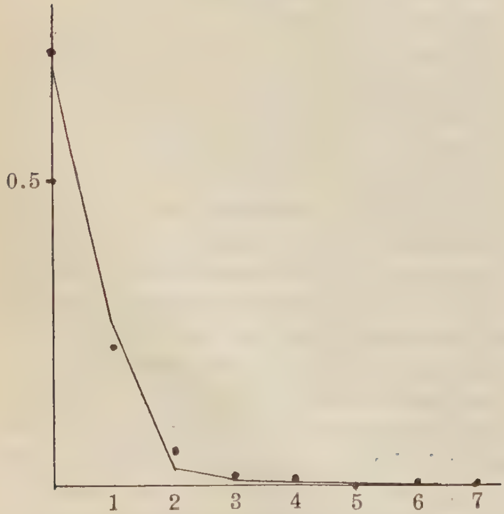

Fig. 3. Principal distribution of the series of number of earthquakes per month

second period (1910–1920), but in this case one significant autocorrelation coefficient is negative. It is almost hopeless that we can, from such a sample correlogram, get any theoretical model of autocorrelation function for a non purely random process to which we shall apply the theory. So this expression of occurrence of earthquakes should be abandoned.

(b) Series of number of earthquakes per month. The principal distribution of this series is shown by dots in Fig. 3, in which the curve shows the Poisson's distribution of mean value 0.4. In this c se the correlogram is formed without the normalization of distribution. Since the number of earthquakes per month is almost always one or zero, the correlation coefficient of those numbers which are mutually t months apart has an almost linear relation to the probability that an earthquake occurs t months after the time when an earthquake took place, i. e. the simplest transition probability, and we can test the uniformity of the probability about months by the method of χ square test and at the same time the significance of the correlation coefficient. The result is that the correlation coefficients are more significant than in the focmer case. But as shown in Fig. 4, if we

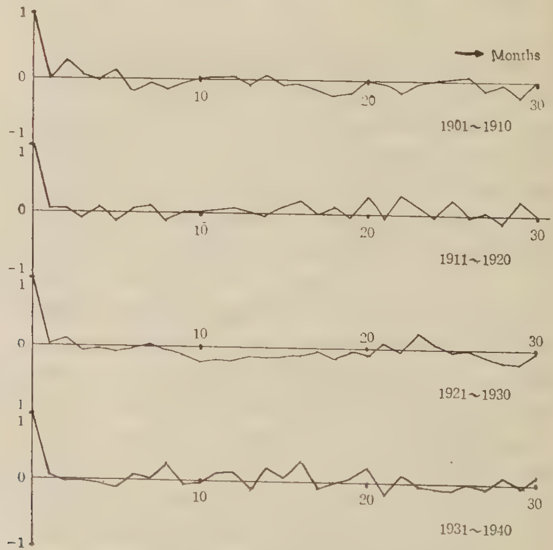

Fig. 4. Correlograms of the series of number of earthquakes per month.

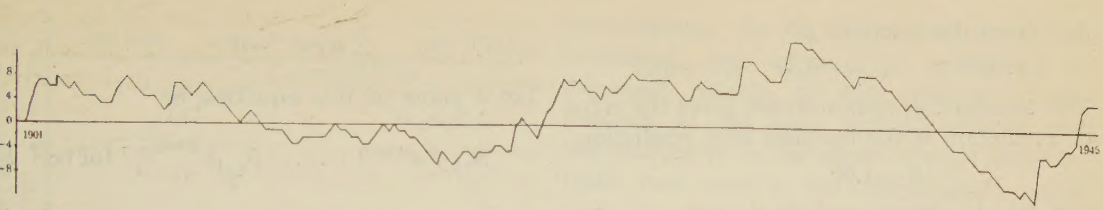

Fig. 5. $n(t)-E(n(t))$ obtained from the data which contains 210 major earthquakes occurred near Shiriya-saki from 1901 to 1945.

fit continuous autocorrelation functions to those sample correlograms, the sample points must vary largely about the function. And other more suitable expressions are required.

(c) $n(t)-E(n(t))$. The meaning of this quantity was given before. The actual variation of this function for our sample is shown in Fig. 5. For the convenience of analysis this is seperated into two parts ; one is a long period variation and the other is a short period variation. Smoothing the original variation by the method of moving average, the former is obtained and subtracting this from the original the latter is given. These two variations can be regarded to have a negligible correlation, and the seperation is justified.

(1) Short period variation. The principal probability density of this variation is given in Fig. 6 and seems in a good accordance with the normal probability density of mean value 0 and standard deviation 1.4. The correlogram can be immediately formed in

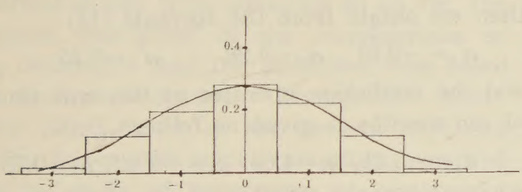

Fig. 6. Principal probability density of the short period variation

this case and is show in Fig. 7. In this case the correlograms are sufficiently smooth that we can reduce significant and continuous autocorrelation functions from them and regard them as the samples of these functions. But, as shown in the figure, these four correlograms are considerably different from each other and it is not preferable to regard

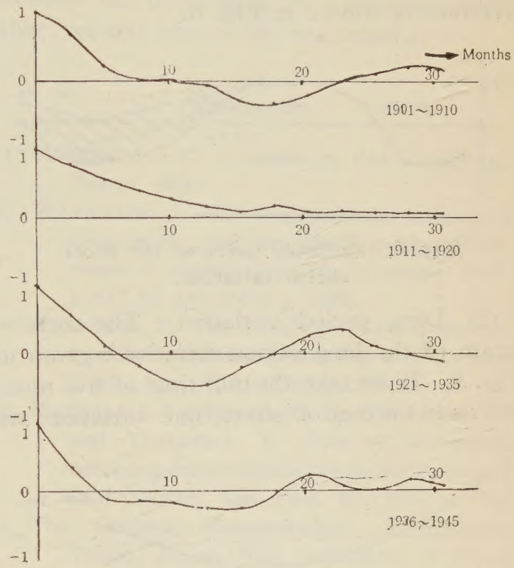

Fig. 7. Correlograms of the short period variation.

them as samples of a single autocorrelation function. The correlogram for 1910–1920 has no negative values and diminishes almost exponentially, and others are like a damped oscillation. From a very simple idea that the correlogram for 1921–1936 and that for 1936–1945 are comparatively similar and that the correlogram after 1945 will be the similar one, the prediction operators are obtained from the correlogram for 1921–1936.

Assuming that the correlogram is one of the autoregressive scheme of $h=3$, and taking unit time of five months, we get from the correlogram

$$\rho_1=0.1 \qquad \rho_2=-0.4 \qquad \rho_3=-0.2$$

then we obtain from the formula (14)

$$a_1=-0.18 \quad a_2=0.42 \qquad a_3=0.12$$

and from the formura (5)

$$b_1=0.18 \qquad b_2=-0.39 \qquad b_3=-0.27$$

The standard deviation which gives the error of prediction is for the first step prediction

$$E_1=1.07$$

and for the second and third steps

$$E_2=1.10 \qquad E_3=1.21.$$

The result of prediction for the short period ariation is shown in Fig. 8.

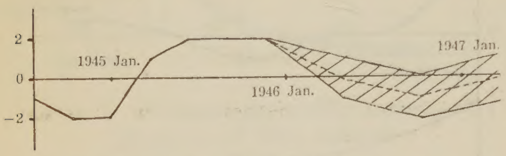

Fig. 8. Precicted curve of the short period variation.

(2) Long period variation. The correlogram of the long period variation is given in Fig. 9. If we take the unit time of five months as in the case of short time variation, we

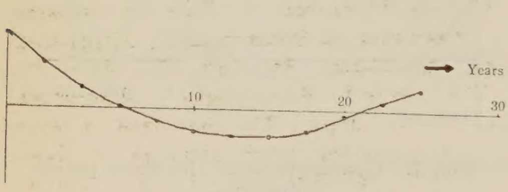

Fig. 9. Correlogram of the long period variation.

can hardly get an autocorrelation function of autoregressive scheme of relatively small h which should interprete the whole correlogram. In order to avoid this difficulty a method developed by OGAWARA is used. At first letting the unit time be a necessary length τ, we solve the next equations and obtain a'_k,

$$(15) \qquad \sum_{i=0}^{h} a'_i \rho'_{k-i}=0 \quad (k=1,2,3,\dots,h)$$

from the definition of the autoregressive scheme. The next equations hold for $k>h+1$

$$(16) \qquad \sum_{i=0}^{h} a'_i \rho'_{k-i}=0\,.$$

The characteristic equation corresponding to this difference equation is

$$(17) \qquad \sum_{i=0}^{h} a'_i z^{h-i}=0$$

Let h roots of this equation be

$$\beta_0,\ \beta_1 e^{\pm 2\pi i f_1},\ \dots,\ \beta_{\frac{h-1}{2}} e^{\pm 2\pi i f_{\frac{h-1}{2}}} \text{ for odd } h$$

$$\beta_1 e^{\pm 2\pi i f_1},\ \beta_2 e^{\pm 2\pi i f_2},\ \dots,\ \beta_{\frac{h}{2}} e^{\pm 2\pi i f_{\frac{h}{2}}}$$

for even h,

where f_i is the component frequency and β_i is the component damping ratio contained in the correlogram. Then we set up a h-th order algebraic equation of which h roots are, e. g. for odd h, $\frac{\beta_0}{n},\ \frac{\beta_1}{n}e^{\pm 2\pi i \frac{f_1}{n}},\ \dots,$ $\frac{\beta_{\frac{h-1}{2}}}{n} e^{\pm 2\pi i f_{\frac{h-1}{2}}}$,

$$(18) \qquad \left(z-\frac{\beta_0}{n}\right)\left(z-\frac{\beta_1}{n}e^{2\pi i\frac{f_1}{n}}\right)\left(z-\frac{\beta_1}{n}e^{-2\pi i\frac{f_1}{n}}\right)$$

$$\cdots\left(z-\frac{\beta_{\frac{h-1}{2}}}{n}e^{2\pi i f_{\frac{h-1}{2}}}\right)\left(z-\frac{\beta_{\frac{h-1}{2}}}{n}e^{-2\pi i f_{\frac{h-1}{2}}}\right)$$

$$=z^h+a_1 z^{h-1}+\dots+a_{h-1}z+a_h$$

And this gives us a_k which is the prediction operator of unit time of τ/n. If it happens that β_0 is negative in the case of odd h, we introduce two roots $-\beta_0 e^{\pm i\pi}$ in place of β_0 and the rank h becomes $h+1$.

Following the above method, we take τ of 5.4 years and get from the correlogram

$$\rho'_1=0.1 \qquad \rho'_2=-0.3 \qquad \rho'_3=-0.3$$

then we obtain from the formula (14)

$$a'_1=-0.01 \qquad a'_2=0.28 \qquad a'_3=0.25$$

and the prediction operator of the unit time of ten months is given as follows,

$$a_1=-3.41,\ a_2=4.68,\ a_3=-2.92,\ a_4=0.75$$

The error of prediction, i. e. the standard deviation of expected value, for the first step is 2.1, and that for the second is 3.1.

The result of prediction for the long period variation is shown in fig. 10. The curve in the figure shows an unexpected steep descent, for $n(t)$ is from its definition a monotonous increasing function and the gradient of $n(t)-E(n(t))$ must be larger than $-\alpha$ where α is such that $E(n(t))=\alpha t$. But here ignoring such somewhat unreasonable fact that

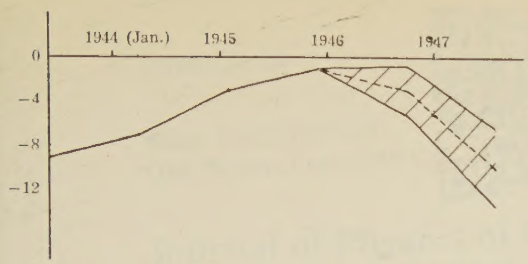

Fig. 10. Predicted curve of the long period variation

the gradient of predicted curve is less than $-\alpha$, the predicted cuves of long and short period variation is put together and shown in Fig. 11. And for comparison, the actual curve is given in the same figure.

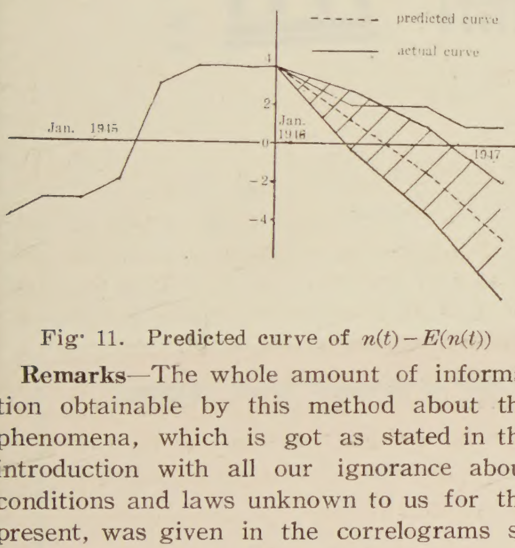

Fig. 11. Predicted curve of $n(t)-E(n(t))$

Remarks—The whole amount of information obtainable by this method about the phenomena, which is got as stated in the introduction with all our ignorance about conditions and laws unknown to us for the present, was given in the correlograms so far obtained. And the prediction was based on these correlograms. Though the prediction failed partly in the present case, the writer hopes that such a quantitative method for the study of occurrence of earthquake becomes a clue for a further approach to the problem. As far as the present case is concerned, the accuracy of prediction is damaged mainly by the relatively large variance of the long period variation, and the ambiguity in the choice of a correlogram from four ones in the case of short period variation. These difficulties may be overcome step by step in the future by considering the correlations which may exist between the occurrence of earthquake and other related observable phenomena.

References

(1) MATUZAWA, T. Seismology (in Japanese), Tokyo, 1950.

(2) WATANABE, S. The randomness, successive occurrence, and periodicity in the occurrence of earthquakes. (in Japanese) Bull. I.P.C.R? **15** (1936) p. 1083.

(3) KITAGAWA T. The weekly contagious discrete stochastic process. Mem. Fac. Sci. Kyushu Univ., Ser. A, 2, 1941, pp. 37-51.

(4) MATUZAWA, T., NAKAMATI, H., NISIKAWA, Y., und YOSIMURA, Y. Über die Jahresschwankung der Erdbenbahäufigkeit in Japan. Bull. Earthq. Res. Inst. **15** (1937) p. 711.

(5) The Central Meteorological Observatory, Tokyo, Japan. The Catalogue of Major Earthquakes which occurred in Japan (1885-1950) Seis. Bull. of C.M.O. 1950, pp. 99-183.

(6) OGAWARA, M. Theory of time series and its application (in Japanese). Chapter 7 of Applied Statistics 1947. (Collected papers compiled by the Society of Applied Mechanics.)

(7) WOLD, H. A study in the Analysis of Stationary Time Series, Uppsala, 1938.

(8) WIENER, N. Cybernetics, New York, 1947, pp. 74-112.